Mechanisms of Enhancing Solid Polymer Electrolytes using Nanofillers and Ionic Liquid for Applications in Flexible Lithium Ion Batteries

A Dissertation

Presented to

the Faculty of the Department of Mechanical Engineering

University of Houston

In Partial Fulfillment

of the Requirements for the Degree

Doctor of Philosophy

in Mechanical Engineering

by

Qin Li

May 2015

Mechanisms of Enhancing Solid Polymer Electrolytes using Nanofillers and Ionic Liquid for Applications in Flexible Lithium Ion Batteries

Qin Li

Approved:

Chair of the Committee
Haleh Ardebili, Assistant Professor
Mechanical Engineering

Committee Members:

Yashashree Kulkarni, Assistant Professor
Mechanical Engineering

Li Sun, Associate Professor
Mechanical Engineering

Jae-Hyun Ryou, Assistant Professor
Mechanical Engineering

Yan Yao, Assistant Professor
Electrical & Computer Engineering

Suresh K. Khator, Associate Dean
Cullen College of Engineering

Pradeep Sharma, Professor, Chair
Mechanical Engineering

Acknowledgements

I would like to express my sincere gratitude to all the people who have been involved in my doctoral study at the University of Houston during the past five years. Without their help, this dissertation could not have reached its present form.

My deepest gratitude goes first and foremost to Dr. Haleh Ardebili, my doctoral advisor, for her excellent guidance, caring, and providing a wonderful research environment for me. Her knowledge, persistence and enthusiasm for scientific research have always been admired. Her patience and support helped me overcome many difficulties I have encountered during my study. I have been amazingly fortunate to have the opportunity to work with her. She has always given me the chance to explore the research tasks on my own and guided me when I had problems. I could not remember how many times I was inspired by her. She walked me through all the stages while writing my dissertation. Without her consistent and illuminating instruction, I would never have been able to finish my dissertation.

Second, I would like to acknowledge my committee members, Dr. Yashashree Kulkarni, Dr. Yan Yao, Dr. Li Sun, and Dr. Jae-Hyun Ryou, for spending their valuable time to review my dissertation. All the efforts, insightful comments and constructive criticisms have been much appreciated. I am also indebted to Dr. Sharma who gave me a lot of help when I first came to University of Houston.

I am grateful to all the past and current members in Dr. Ardebili's research group. Sridharreddy Appanapalli and Eric Wood shared their experiences of fabricating solid polymer electrolytes with me. Mengying Yuan helped me in taking SEM images and conducting the TGA experiments. Taylor Dizon inspired me to explore the gel polymer electrolytes. I had very productive discussions with Mejdi Kammoun regarding the manufacturing and characterization of lithium ion batteries. Also, other members, Bahar Moradi, William Walker, Sean Berg, Abigail Zinecker, and Tam Nguyen, I wish you all tremendous success in your future study.

Most importantly, none of this would have been possible without the love and concern of my parents, to whom this dissertation is dedicated. They have always been there to give me the support and strength not only for the five-year doctoral study but also for my entire life. I would like to express my heartfelt gratitude to them.

Last but not least, I appreciate the financial support from NSF, TcSUH, and IIMEC that funded the research discussed in my dissertation.

Mechanisms of Enhancing Solid Polymer Electrolytes using Nanofillers and Ionic Liquid for Applications in Flexible Lithium Ion Batteries

An Abstract

of a

Dissertation

Presented to

the Faculty of the Department of Mechanical Engineering

University of Houston

In Partial Fulfillment

of the Requirements for the Degree

Doctor of Philosophy

in Mechanical Engineering

by

Qin Li

May 2015

Abstract

Polymer-based electrolytes have gained much attention in recent decades due to their many advantages including high thermal and chemical stability, and the consequent enhanced safety in lithium ion batteries. Also, thin-film manufacturability and mechanical strength make the polymer-based electrolyte excellent candidate for the development of thin, flexible lithium ion battery. One main issue with polymer electrolytes is their lower ion conductivity compared to that of conventional liquid electrolytes. In this dissertation, the properties of polymer-based solid and gel electrolytes and their applications for lithium ion batteries have been investigated. The focus of this dissertation is the influence of selected additives including nanofillers, and ionic liquids on the performance of the polymer electrolytes and flexible lithium ion batteries.

The effect of nanofillers on ion conductivity of polymer electrolytes is investigated using a continuum, bulk level approach. Based on the free volume theory, a model of the ion conductivity enhancement of polymer electrolyte as a function of nanofiller content is proposed. The model could fit to various experimental results of ionic conductivity enhancement and degradation. It could also be used to fit the temperature dependency of the ionic conductivity. The influence of the nanofiller is also studied at the molecular, discrete level using the molecular dynamics simulations of a polymer nanocomposite electrolyte. It is found that the embedded nanofiller can affect the salt dissociation, lithium-ion mobility, and the dynamics of polymer chains. Those effects can depend on the surface functionality and size of the nanofiller.

Furthermore, the effect of ionic liquid on polymer electrolyte performance is investigated. A highly conductive ionic liquid (IL), 1-Ethyl-3-methylimidazolium dicyanamide (EMIMDCA), with ionic conductivity as high as 27 S/cm, is incorporated in poly(vinylidene fluoride-co-hexafluoropropene) (PVDF-HFP) polymer matrix and lithium salt (i.e., lithium perchlorate) to form the polymer-IL electrolyte. The obtained electrolyte is a freestanding thin-film and exhibits solid-like appearance. Due to its high stability, the polymer-IL electrolyte film is used for a low-cost, simple lamination method to fabricate high performance flexible lithium ion batteries. The battery shows relatively stable energy delivery capability and can function in both flat and bent configurations.

Table of Contents

List of Figures

List of Tables

Chapter I Introduction

1. Motivation and objectives

Our daily lives have been significantly transformed with the emergence of portable electronics, including cell phones, laptops and tablets. The prevalence of these portable devices, has led to higher requirements for the sustainable power sources including smaller size, lighter weight, enhanced safety and stability to meet the ever-increasing and multi-faceted demands of the modern consumers [1-3]. Among the competing storage devices, lithium-ion batteries (LIBs) have gradually dominated the market due to their superior merits including high energy density, high output voltage, long life and environmentally friendly operation. Nowadays, billions of lithium-ion batteries are produced each year for the consumers to power their cell phones, tablets, laptops and other [4]. This huge market promotes scientists and engineers to seek new materials and structures for designing advanced lithium ion batteries. Besides the general requirements from the energy storage perspective, the mechanical flexibility of LIBs has also attracted increasing attention. The main objective of this research is to investigate suitable materials and structures for high performance flexible lithium ion batteries with an underlying focus on the polymer electrolytes.

2. Energy storage

2.1 Overview

In today's world, the demand for energy is ever increasing. From individuals to industries, all require higher amount of energy or power that is confined to less space, area or thickness or smaller weight. Over the past centuries, fossil fuels have been the major source of energy, however, environmental issues associated with this type of energy production, has raised many concerns. In addition to the pollution caused by fossil fuel consumption, another problem is that fossil fuels are not renewable. In the absence of suitable replacements, the energy crisis could lead to severe global, economical and social adverse effects. To solve the energy problem, it is urgent to develop new, “green” energy production methods that replace the old conventional ones. These types of renewable energy sources include wind power, solar power, and hydroelectricity [5]. In certain regions of the world, they are already in commercial use.

However, renewable energy sources are generally not as stable as the fossil fuels. Their energy outputs are sensitive to the weather or climate change. It is difficult to provide immediate response to the varying consumer demands, as these sources are not able to deliver regular supply that is easily adjustable to consumption needs. Therefore, the energy storage becomes a crucial element in the management of energy from renewable sources, allowing excess energy to be stored during the productive periods and to be released into the grid during peak hours (high consumption) when it is more valuable [6]. In addition to the large-scale industrial-level needs, there is a great need of

energy storage for individual consumer devices, and in particular, electrical energy storage for powering high population of mobile electronic devices, such as cell phones, laptops, and tablets.

Energy storage has been a long-standing issue for human societies. Historically, many technologies have been developed to address energy issues. Some of them are categorized in Figure 1.1. Since most other types of energy will be converted to electricity power in our modern society, electrical energy storage (EES) is of most importance [7]. In the field of EES, most efforts have been focused on batteries and capacitors.

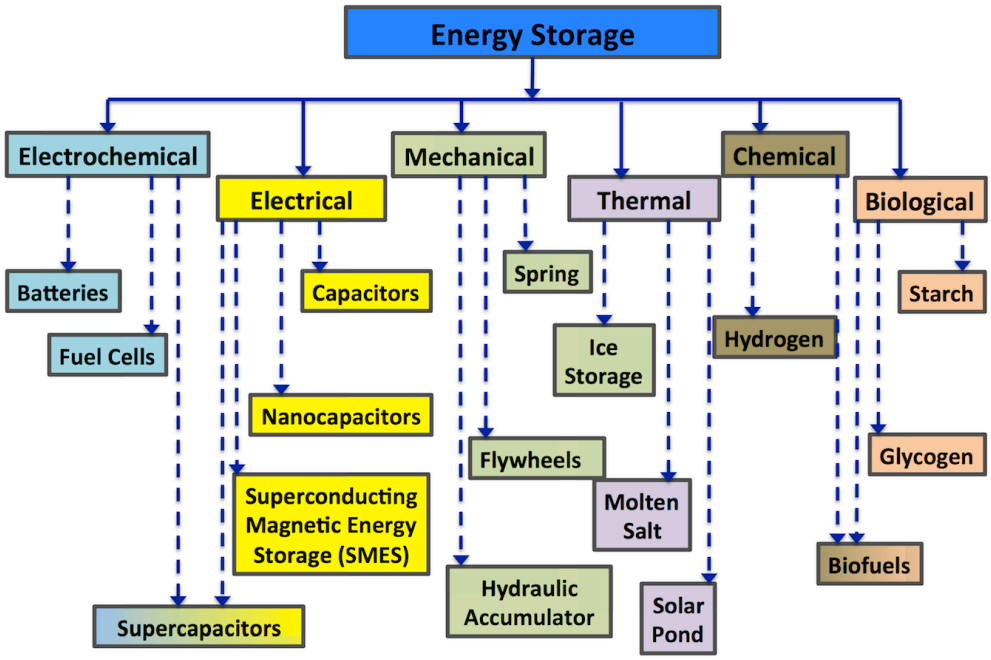

Figure 1.1. General categories of energy storage technologies (Courtesy of H. Ardebili).

2.2 Batteries

Batteries are electrochemical storage devices that can carry out conversions between electrical energy and chemical energy. There are three categories of batteries, i.e., primary batteries, secondary (rechargeable) batteries and specialty batteries for specific purposes. Most batteries that we can find in the market belong to the first two categories. The latter are mainly military and medical batteries. They have almost no commercial use for various reasons including cost, environmental issues, and limited market application [8]. All batteries, whether rechargeable or not, consist of two opposite electrodes and an ion conducting material (an electrolyte) between them. In case of liquid electrolyte, generally a separator membrane must also be used. Driven by the chemical potential difference between the two different electrode materials reduction and oxidation reactions would occur on the two electrode-electrolyte interfaces, respectively. Meanwhile the electrons will flow from the more negative to the more positive potential and the ions move through the electrolyte to keep the reactions going until all reactive materials are consumed. This is how primary batteries work and for rechargeable batteries, the above discharge process could be reversed by applying a larger voltage in the opposite direction and cause the battery to recharge.

There are many important performance features of batteries. First of all is the energy density i.e., the amount of electrical energy per mass or volume that a battery can deliver. The electrical energy of a battery can be measured by discharging the battery at constant current and calculated by the following equation,

$$E = \int_0^T U(t) I dt, \qquad (1.1)$$

where T is the total discharge time, U(t) is the voltage of the battery and I is the discharge current. Other properties include the power (high current discharge), working voltage, flatness of the discharge curve, rapid recharging, cyclability, safety and discharge capability at low temperature [9]. All the criteria above pose many challenges for a battery to be successful in the market. During the nineteenth and early twentieth centuries hundreds of electrochemical couples were proposed, but only Zn–MnO_2 (primary), lead–acid (secondary), and Ni–Cd (secondary) have been widely used in the market [10]. However, those batteries do not meet the increasing energy requirements for either consumer electronics or electric vehicles. Therefore, in the new century research has focused on the alkali metals, particularly lithium, as the lightest and most electronegative element in the family [11].

2.3 Supercapacitors

Capacitors are very common electrical energy storage devices. A simplest capacitor consists of two parallel conductive plates separated by a dielectric with permittivity ε. The capacitance can be expressed as

$$C = \frac{\varepsilon A}{d}, \qquad (1.2)$$

where A is the surface area and d is the distance between the two plates [12]. The equation indicates that reducing the distance between the two charged surfaces would result in larger capacitance. This is the starting point of the so-called supercapacitors. In

supercapacitors energy is stored by either ion adsorption (electrochemical double layer capacitors i.e., EDLCs) or fast surface redox reactions (pseudo-capacitors). They can be employed together with batteries or even as replacements of them in electrical energy storage and harvesting applications, when high power delivery or uptake is needed [13]. Figure 1.2 shows the general structure of an electrochemical double layer capacitor. Due to the very small spacing (in nanometers) of the double layer, the capacitance would be significantly increased.

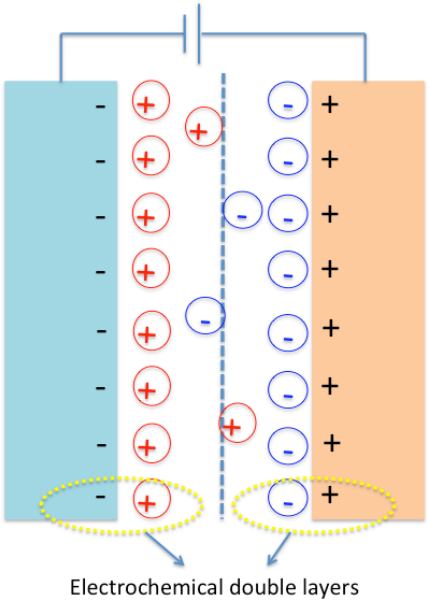

Figure 1.2. Representation of an electrochemical double layer capacitor.

Different from the EDLCs, in the pseudo-capacitors additional capacitance could be obtained by fast and reversible redox reactions between the electrolyte and some electro-active species on the electrode surface. However, this enhancement results in a lower power density and the lack of stability during cycling [14].

Although from Figure 1.2 we can see that the structure of a supercapacitor is very similar to a battery, there are also some differences between them. Unlike the batteries where the energy is stored inside the electrodes, supercapacitors store electrical charge only at the electrode surface. This different energy storage mechanism results in lower energy densities of supercapacitors compared to batteries. On the other hand, since charge-discharge process is limited on the surface rather than into the electrode bulk, the supercapacitors can run at high rates and provide high specific power. In addition, only a small fraction of the electrode materials participate in redox reactions. Therefore, the deterioration of the electrodes is negligible and a much longer cycle life can be reached for supercapacitors (i.e., above million cycles) [15].

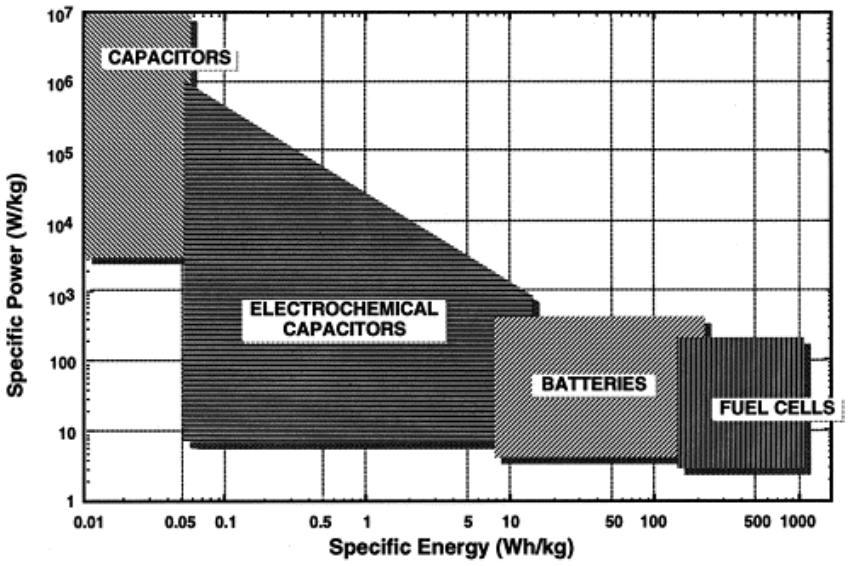

Figure 1.3. Representation of an electrochemical double layer capacitor.

Figure 1.3 [16] shows a typical Ragone plot (energy density *vs.* power density) for different energy storage systems. This plot also implies that batteries and EDLCs are

associated with different types of application, since they have high energy/low power and low energy/high power, respectively. Thus, using a hybrid system, which can combine these two devices, can lead to a better optimization of energy output.

2.4 Nanocapacitors

It is well known that the capacitance of a capacitor is inversely proportional to the thickness of the dielectric material. With the development of nanotechnology, the dielectric thickness can now reach nanoscale. Capacitors based on this extremely thin layer of dielectric are generally called "nanocapacitors" [17-19]. Similar to supercapacitors, the high capacitance of nanocapacitors also originates from the decreasing distance between the two conductive layers. On the other hand, their difference mainly lies in the structural aspect. The supercapacitors usually have normal overall size of traditional capacitors and only the thickness of the double-layer generated at the electrode-electrolyte interface is in nanoscale. The nanocapacitors maintain the metal-insulator-metal configuration but with a nanosized insulator layer and the absence of double-layer.

In addition, by using high dielectric constant materials the capacitance could reach even higher value [20]. However, there is a so-called "dead layer" effect that can lower the capacitance of nanocapaciotrs compared to the theoretical predication. For example, the expected capacitance based on classical electrostatics of a 2.7 nm SrTiO3 thin film is 1600fF μm^{-2}. But the *Ab initio* simulations of same-dimension capacitor system only shows 285fF μm^{-2} [21]. The dead layer is a low-permittivity thin layer existing at the metal/dielectric interface. It is like a low capacitance capacitor that is connected in series

with the dielectric film such that the overall capacitance becomes lower. It has been shown in our previous study [22] that this dead-layer effect can be suppressed by using graded dielectric films. We have calculated the enhancements of capacitance due to grading of selected properties of the dielectric films in parallel-plate nanocapacitor model, and up to 27% enhancement on capacitance has been found (more details regarding this study is in Appendix A).

3. Lithium ion batteries

3.1 Overview

The idea of using Li as the anode in a battery is based on the fact that Li is the most electropositive and the lightest metal [23]. In early 1960s, primary cells with metallic lithium negative electrodes and non-aqueous electrolytes were introduced into the market. Compared to the conventional batteries with aqueous electrolytes, they possess many outstanding features including

a) high operating voltage,
b) high energy density (both per mass and per volume),
c) low self-discharge rate, and
d) wide operation temperature window [24].

However, using lithium metal has some drawbacks. Its high reactivity and more importantly, the dendrite growth on the surface due to lithium deposition during charge-discharge cycles, cause severe safety issues. To overcome these problems, the so-called "intercalation"-type electrodes were considered. Instead of depositing on the surface

lithium ions could insert into those electrodes. The general intercalation electrode reaction could be expressed as

$$yM^{+} + ye^{-} + \langle H \rangle \rightleftharpoons M_y\langle H \rangle, \qquad (1.3)$$

where M is the cation in electrolyte (Li^{+} for lithium ion batteries) and <H> is the "host" material, and the coefficient *y* represents the ability of the host to accommodate the cation [25].

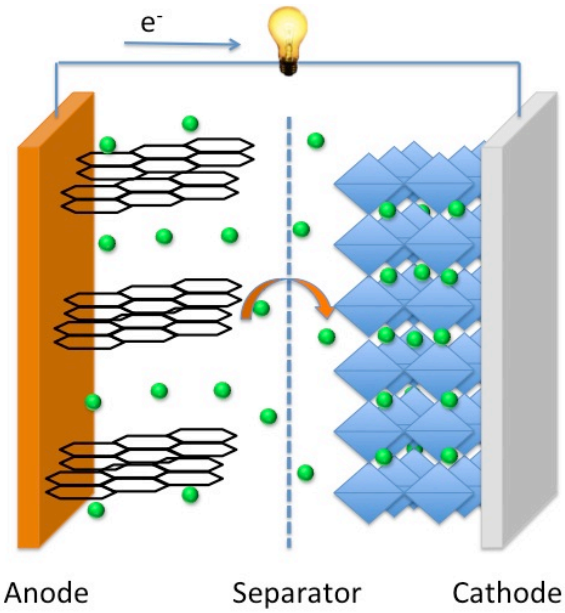

Figure 1.4. Schematic representation of a lithium-ion battery, the arrows indicate the transport directions of lithium ions and electronics while the battery is discharging.

In the field of lithium batteries, a breakthrough is the use of carbon-based materials as the replacement of Li metal as the anode. Indeed the first commercial lithium-ion battery has adopted the $LiCoO_2$/C system. Since carbon/graphite anodes could eliminate the dendrite growth problem, the safety issue associated with pervious lithium batteries was

resolved. A modern lithium-ion battery usually has a configuration as shown in Figure 1.4. In such a battery, both cathode and anode materials are able to accommodate lithium ions. During charge and discharge lithium ions move back and force between two electrodes while electrons are flowing through the external circuit to power the electronic devices. Because of this feature, lithium-ion batteries are also called the "rocking chair" batteries.

3.2 Cathode materials

For most current lithium ion batteries, cathode materials are the sources of the lithium ions and they govern the capacity of the batteries. Therefore, the cathode materials have been intensively studied. Key expectations for good cathode materials are as follows [26].

a) The materials contain large fraction of lithium ions and they are accessible for fast insertion and removal. This ensures high energy and power density.
b) The materials react with lithium with a high free energy of reaction.
c) The materials should have a high mixed conductivity (both ionic and electronic).
d) There should be limited or no degradation of the materials during charge and discharge to improve the cyclic performance.
e) The materials have to be relatively low cost and environmental benign.

Many cathode materials have been investigated. Among them lithium cobalt oxide ($LiCoO_2$) and lithium iron phosphate ($LiFePO_4$) are most commonly used in laboratory

research and commercial products [27]. LiCoO2 has a layered structure where lithium ions can be reversibly extracted from the structure with a corresponding change of cobalt oxidation. The chemical reaction of $LiCoO_2$ is

$$\mathrm{LiCoO_2} \rightleftharpoons \mathrm{Li_{1-x}CoO_2} + x\mathrm{Li^+} + x\mathrm{e^-}, \qquad (1.4)$$

where $0 \leq x \leq 0.5$ to keep the structure of $LiCoO_2$ stable [28]. In comparison to $LiCoO_2$, $LiFePO_4$ is superior in terms of cost, natural abundance, and safety [29]. It has an ordered olivine structure. The extraction of lithium from of $LiFePO_4$ can be written as

$$\mathrm{LiFePO_4} - x\mathrm{Li^+} - x\mathrm{e^-} \rightleftharpoons x\mathrm{FePO_4} + (1-x)\mathrm{LiFePO_4}. \qquad (1.5)$$

It shows that there is a second phase, $FePO_4$, during the extraction of lithium [30].

3.3 Anode materials

As mentioned before, replacing the unsafe lithium metal by carbon-based materials as the anode is a milestone in the development of lithium ion batteries. Since then the carbonaceous compounds, either graphite or coke (i.e., high carbon content), have become the "standard" anode materials for lithium ion batteries [31]. There are two main reasons: low cost and low operational potential. The mechanism of lithium intercalation in those anodes is well known as lithium ions reversibly insert into the space between discrete graphene layers, to reach the formation of LiC_6 with a maximum theoretical capacity of 372 mAh/g [32]. The reaction is

$$Li^+ + 6C \rightleftharpoons LiC_6. \qquad (1.6)$$

This process occurs at voltages below the decomposition limit of the most common electrolytes. Thus, over the first several charge-discharge cycles, a thin protective layer is generally formed at the surface of the anode. The formation of this so-called solid electrolyte interphase (SEI) will consume lithium ions resulting in irreversible capacity loss [33]. Furthermore, the gas generated during the formation of SEI can be a safety hazard.

Although the carbon-based materials are dominating this field, some alternative anode materials have also been investigated. For example, the Li_yM (M=Sn, Pb, Si, In, etc.) type alloy anodes have much higher capacity about 800-3000 mAh/g. However, it is difficult to reach long cycle life due to the volume expansion of those electrodes [34]. Transition-metal oxides (MO, where M is Co, Ni, Cu or Fe) are another promising type of anode materials. It has been reported that electrodes made of nanoparticles of transition-metal oxides demonstrate electrochemical capacities of 700 mAh/g, with 100% capacity retention for up to 100 cycles and high recharging rates [35].

The volume change induced structural degradation of the anode materials is always an obstacle for the goal of long cycle life. However, there is an anode material $Li_4Ti_5O_{12}$ that is promising to solve this problem. The lithium intercalation/de-intercalation process is

$$Li_4Ti_5O_{12} + 3Li^+ + 3e^- \leftrightharpoons Li_7Ti_5O_{12}. \qquad (1.7)$$

This material generally undergoes very little change in lattice dimensions, thus it is considered as an almost “zero-strain” electrode material [36]. Lithium batteries using this

material are expected to have good cycle performance and enhanced safety. However, the intercalation potential of $Li_4Ti_5O_{12}$ is high (~1.5 v.s. lithium metal) therefore, making the output voltage of the full batteries lower than that of the current ones using graphite anode [37]. This may be of less concern in the future, since the voltage required by the electronics tends to be progressively reduced with time and new technologies. Under this condition, $Li_4Ti_5O_{12}$ would be considered as a better choice for anode materials because of its improved cyclability and safety [32].

3.4 Electrolytes

Electrolyte is the basic component of many electrochemical devices including batteries, supercapacitors, and fuel cells. Despite the difference in their applications, electrolytes can be generally considered as materials that contain "free" mobile ions that transfer electrical charge from one electrode to another. On the other hand, electrolytes have to be perfect insulators for electrons, otherwise leading to short circuit inside the device. In the design of lithium-ion batteries, the electrolyte plays a very important role. Serving as the medium for Li ions transport, the electrolyte usually defines the rate of energy output of the battery while the nature of electrodes (usually the cathode) decides the capacity. The following are some requirements that a preferred electrolyte should meet:

a) high ionic conductivity and low electronic conductivity to facilitate ion transport and prevent self-discharge,
b) a wide electrochemical window to match the high working voltage of lithium-ion batteries,

c) low reactivity towards other components in the battery, and

d) it should be environmental friendly [38].

Inside the batteries, electrolytes are in intimate contact with both cathode and anode. Thus, their electrochemical stability is of great concern. Figure 1.5 shows the different energy levels of electrodes and electrolytes. For the electrolyte, the operational "window" is the energy difference Eg between its lowest unoccupied molecular orbital (LUMO) and its highest occupied molecular orbital (HOMO). The two electrodes have different electrochemical potentials (their Fermi energies ε_F) μ_A of the anode and μ_C of the cathode. In a battery, if the μ_A is above the LUMO of the electrolyte, then the electrolyte will be reduced, unless a passivation layer (SEI) creates a barrier to electron transfer from the anode to the electrolyte LUMO. That is the case for the graphite anode. Similarly, the electrolyte will be oxidized in contact with a cathode having a μC below the HOMO unless a passivation layer blocks the electron transfer. Therefore, the electrolyte should either have a wide window-Eg or be able to generate a stable SEI layer at the surface of the electrodes.

For lithium ion batteries, liquid type electrolytes are the most widely used conventional electrolytes due to their fast ionic conductivities. From safety point of view, solid electrolytes and gel electrolytes are more advantageous.

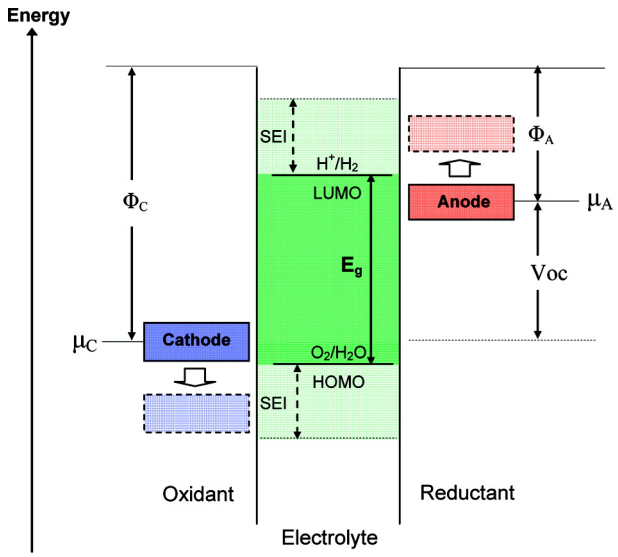

Figure 1.5. Schematic of the relative electron energies of electrodes and the electrolyte [39].

3.5 Other components

From electrochemical point of view, cathode, anode, and the electrolyte construct the core of an LIB. However, LIB also requires additional components to function properly. For example, to avoid direct contact between cathode and anode in liquid electrolyte, a separator is required. Other components like current collectors for electrodes and the encapsulation are also important in practical batteries.

A separator used in an LIB is usually a porous membrane that is permeable to ionic flow but is an electrical insulator and must also prevent physical contact between the two electrodes. The general requirements of separators are often associated with their thickness, permeability, porosity, wettability, stability, mechanical strength, and pore size. There are many commercial separators available in the market from cellulosic papers and cellophane to nonwoven fabrics, foams, ion exchange membranes, and

microporous flat sheet membranes made from polymeric materials. Figure 1.6 shows the microscopic of a commercial LIB separator [40].

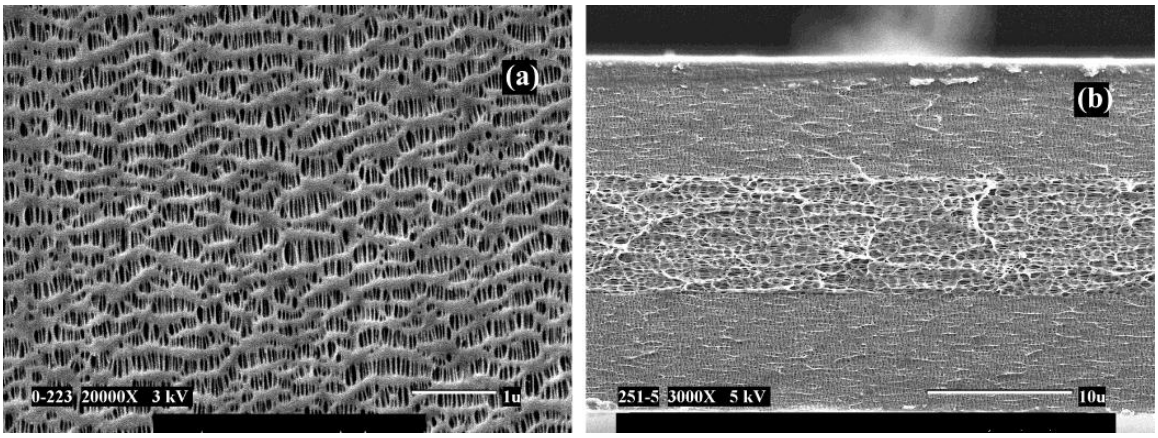

Figure 1.6. Scanning electron micrographs of Celgard 2325 (PP/PE/PP) separator used in lithium-ion batteries: (a) surface SEM and (b) cross-section SEM [41].

Regarding current collectors, low cost, high electrical conductivity and resistance to corrosion are the basic requirements. Copper (for anode) and aluminum (for cathode) are most commonly used current collectors. In addition, some other materials like graphene papers [41], nickel mesh [42] have also been investigated.

4. Liquid electrolytes

4.1 Organic solvents

The simplest way to generate free ions is to dissolve the corresponding salts in the liquids. Water, the most common solvent, presents many advantages including low cost, high polarization, and high ionic conductivity and the aqueous electrolytes have been used in traditional (i.e., non-lithium) batteries. However, the low decomposition potential,

theoretically only 1.23 V, and the reactivity with lithium make it almost impossible to be used in lithium ion batteries with a general voltage higher than 3 V [43].

Organic solvents, in particular, the carbonates, are good replacements for water. Currently, the most commonly used electrolytes are carbonates or carbonate blends consisting of one or more of the following: propylene carbonate (PC), ethylene carbonate (EC), diethyl carbonate (DEC), dimethyl carbonate (DMC), or ethylmethyl carbonate (EMC) [44]. Some properties of the common carbonates are summarized in Table 1.1.

Table 1.1. Some properties of common carbonates [38].

Solvent	T_m/°C	η/cP, 25 °C	ε, 25 °C	ρ/gcm^{-3}, 25 °C
EC	36.4	1.9	89.78	1.321
PC	-48.8	2.53	64.92	1.2
DMC	4.6	0.59	3.107	1.063
DEC	-74.3	0.75	2.805	0.969

A desirable solvent should dissolve lithium salts effectively in proper conditions and also have a low viscosity (η) to facilitate ion transport. In addition, safety and stability must be addressed. However, electrolytes using single solvent can hardly meet those requirements, so a mixture of two or more types of solvents is usually employed to make an optimized liquid electrolyte. A commercial liquid electrolyte used commonly in our lab consists of 1 mol/L $LiPF_6$ in a mixture of EC, DMC, and DEC (2:1:2 in volume), where the ionic conductivity could reach 10^{-2} S/cm.

Recently, room-temperature ionic liquids (RTILs) have been considered as alternative electrolytes for Li-ion batteries. This consideration is mainly form safety and stability point of view. Unfortunately, they have a relatively higher viscosity, which reduces their Li-ion conductivity.

4.2 Lithium salts

Another important component of liquid electrolytes are the lithium salts. Unlike their liquid partners (organic solvents) the combination of two or more types of lithium salt in the formulation of liquid electrolytes is very rare. The reason is that different lithium salts may not necessarily complement each other to enhance the final performance of the liquid electrolytes and can counteract individual benefits. The requirements of lithium salts lie in two aspects. First is the solubility, which ensures the concentration of lithium ions to be sufficient for fast electrode reactions. The second is the stability of the anions. In order to increase the solubility, the anions of the lithium salts are usually much larger than the lithium ions and have complex structures. Those anions might undergo decomposition in the potential range of a working LIB [45, 46].

Lithium hexafluorophosphate ($LiPF_6$) and lithium perchlorate ($LiClO_4$) are two commonly used lithium salts. $LiPF_6$ is the only lithium salt that has been commercialized as the solute in liquid electrolytes used for almost all the LIBs in the market. It has relatively high ionic conductivity in non-aqueous solvents based on mixed carbonates. For example, in EC/DMC (1:1) the conductivity is 10.7 mS/cm [47]. The major problem of $LiPF_6$ is the sensitivity toward moisture and high temperature, causing tremendous difficulty in preparation, storage and purification.

Unlike the success of $LiPF_6$ in the market, $LiClO_4$ has been a popular lithium salt in laboratories for research purpose because it is inexpensive and easy to handle compared to $LiPF_6$ [48]. It has satisfactory solubility and good conductivity (~9.0 mS cm^{-1} in EC/DMC at 20 °C) [49]. However, the high oxidation perchlorate anion makes $LiClO_4$ impractical as an electrolyte solute for large scale industry purposes [50].

5. Solid polymer electrolytes

Although liquid electrolytes are widely used for most commercial lithium-ion batteries, the safety is always a concern. Leakage of those flammable organic solvents is the major problem associated with conventional liquid electrolytes. In addition, the fluidity of the liquid electrolyte usually requires a rigid container thus increasing the overall weight of the battery. To make a safer lithium-ion battery, solid (solvent-free) electrolytes have gained much attention. Currently, there are two types of solid electrolytes. One is based on polymers and the other is inorganic ceramics.

While the ceramic solid electrolyte family has a long list of members, in the field of solid polymer electrolytes most attentions have been focused on polyethylene oxide (PEO)-based materials, owing to their excellent salt-dissolving ability, availability at various molecular weights, and attractive mechanical properties [51]. Ion conduction in ceramics is based on the general diffusion mechanism by which ions move through vacancy and interstitial sites inside the materials [52]. On the other hand, the transport of lithium ions in polymers relies on the so-called ion hopping mechanism. For PEO-based materials the positive charged lithium ions are coordinating with the negatively charged

ether oxygen atoms. With the motion of the PEO chains lithium ions could hop from one available site to another. Therefore, the movement of ions is coupled with the motion of polymer chains [53]. Figure 1.7 illustrates these two different mechanisms [Ref]. Another major difference between ceramic electrolytes and polymer electrolytes lies on the mechanical properties. Ceramic electrolytes usually have high elastic moduli (i.e., stiffness) that make them more suitable for rigid battery designs. Also, ceramics are more stable in aggressive environments like high temperature working conditions. Polymer electrolytes, on the other hand, are soft and able to comply to shape change of the battery so they are favored in the designs of flexible batteries. In addition, it is easier to process polymers than ceramics, which reduces the fabrication costs [54]. In our lab, we focus on polymer electrolytes.

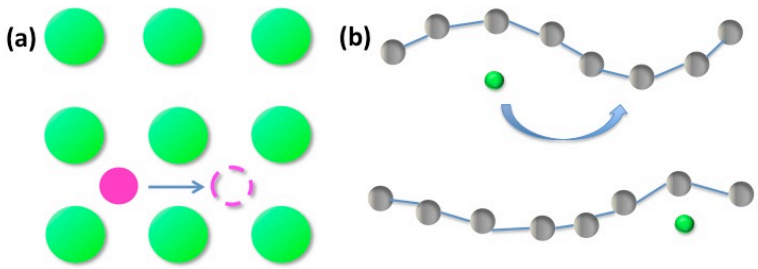

Figure 1.7. Comparison of ion conduction in (a) ceramics and (b) polymer matrix.

Despite all their advantages, the application of solid electrolytes is still restricted by their low ionic conductivity compared to that of their liquid counterparts. Figure 1.8 shows the comparison of ionic conductivity of several solid and liquid electrolytes. How to increase the ionic conductivity of solid electrolytes, therefore, has become a focused research subject, and several methods have been proposed. Based on the conduction

mechanism of polymer electrolytes as shown in Figure 1.7, the motion of polymer chains largely governs the transport of ions. The most common approach to promote that motion is adding liquid plasticizers like organic solvents [55], low molecular weight polymer [56], and ionic liquids [57]. Experimental results show that the room temperature ionic conductivity of those plasticized solid polymer electrolyte could reach the level of 10^{-4}-10^{-3} S/cm. However, this approach introduces liquid phase into the solid polymer electrolyte, so the mechanical properties electrolyte are compromised.

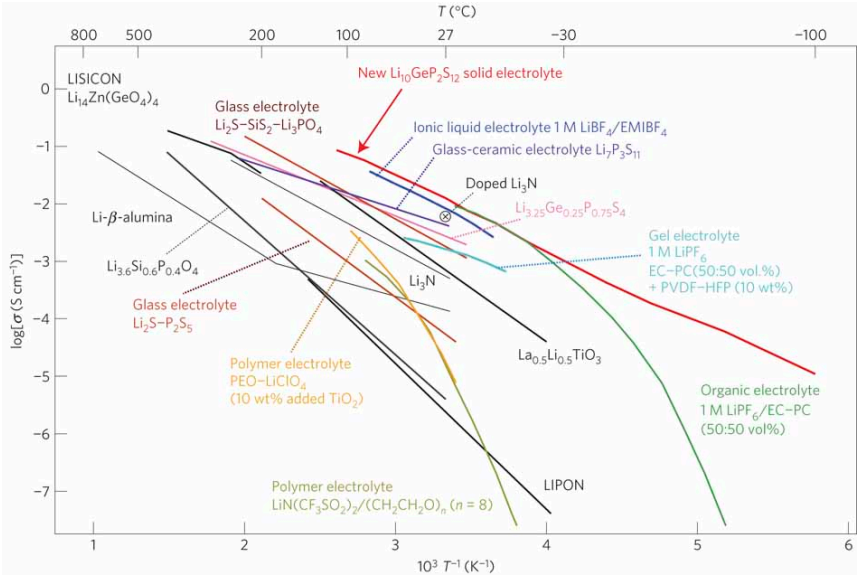

Figure 1.8. Ionic conductivity comparison of various electrolytes.

In the year of 1998, F. Croce and coworkers found that adding nano-sized ceramic fillers to the solid polymer electrolyte could enhance the ionic conductivity [58]. They prepared their electrolytes by dispersing nanofillers into the solution of PEO and lithium perchlorate. The obtained electrolytes had ionic conductivity of about 10^{-5} S/cm at 31°C versus 10^{-8} S/cm of the filler-free ones. This new class of solid polymer electrolytes,

usually referred to as polymer nanocomposite electrolyte (PNCE), also had improved mechanical properties. This discovery attracted intensive attentions and various nanofillers were studied [59-62]. Although the enhanced ionic conductivity has been confirmed, it is still insufficient for practical applications in high performance lithium-ion batteries.

6. Gel electrolytes

Since both the liquid electrolyte and the solid polymer electrolyte (including polymer nanocomposite electrolytes) have their own advantages and drawbacks, a combination of them — gel polymer electrolytes (GPEs) have gained attentions [63]. As shown in Figure 1.9, GPEs are comprised of liquid electrolyte and a polymer network where those liquid electrolytes are trapped. The polymer matrix could provide mechanical support while the lithium ions are moving in the liquid phases. Thus the ionic conductivity essentially is in the same level as that of the liquid electrolyte if sufficient amount of liquid electrolyte is retained. They differ from the above plasticized solid polymer electrolytes in the way that the ion conduction is no longer associated with the motion of polymer chains so that other polymers rather than PEO could be used. Indeed, polyacrylonitrile, Polyacrylonitrile, PAN, poly(methyl methacrylate), PMMA, and Poly(vinylidene fluoride-*co*-hexafluoropropylene), PVDF-HFP have been intensively studied as the polymer hosts for gel polymer electrolytes [64-68]. GPEs usually show higher conductivity (compared to solid polymer electrolytes) and higher stability (compared to liquid electrolytes). These are expected results since GPEs are actually comprised of those two kinds of electrolytes.

Gel polymer electrolytes are usually made with the general solution-casting method. Depending on the different polymer matrix, the obtained gel electrolytes could be either paste-like (e.g., PMMA-based gel electrolytes) or solid-like (PVDF-based gel electrolyte). For the PVDF-HFP gel electrolytes, beside the general solution-casting method, there is another route to make a free-standing thin film proposed by Tarascon and coworkers [69]. In their approach, a lithium-free gel polymer electrolyte was first obtained by casting a PVDF-HFP/solvent solution. Then, the solvent in the GPE was removed to leave plentiful micro-pores inside the PVDF-HFP. This microporous solid membrane could re-swell in general liquid electrolytes to form the final gel polymer electrolyte. The significant benefit of this method is that only the last re-swelling step requires controlled environment (inside the glove box) and other steps could be done under general conditions, so that the processing cost would be reduced.

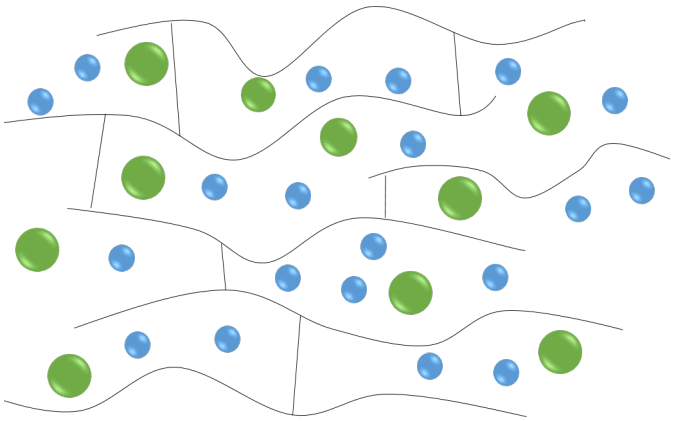

Figure 1.9. Schematic of a gel electrolyte.

In summary, the electrolyte is an essential component in any lithium-ion battery. Its formulation profoundly affects the performance of a battery in many aspects. Compared to the research in electrodes, study in electrolytes is relatively divergent owing to

diversity of the available materials. This situation is even more complex after introducing polymer to the picture. Although numerous electrolytes have been investigated, the development of lithium-ion batteries always raises new challenges. For example, to support the high voltage (~5 V) lithium-ion battery, electrolytes with corresponding wide electrochemical widow are essential [70]. Such demands would screen out many currently using electrolyte materials and provoke new discoveries in this area.

7. Molecular dynamics simulation in materials science

7.1 Overview

In the past, scientific studies usually have been carried out either theoretically or experimentally. In experiments, a sample of the material is prepared and is subjected to various measurements. By changing the experimental conditions, we can discover the relations behind the obtained results. In theoretical research, a model of the system is constructed based on several assumptions to describe the behavior of interested properties. The validation of the model could be accomplished by comparing the modeling results to the experimental results. To reach new findings in materials science, experiments are often very costly and time consuming especially for some "extreme" conditions. On the other hand, the models are usually in the form of complex mathematic equations that are difficult to solve theoretically. The advent of high-speed computers has altered this scenario and brought a third approach, computer simulation, to investigate the research problems. Computer simulation also called computer experiment has been developed rapidly and now it plays an important role in material science. It can shorten

the time period of a discovery going from laboratory to industrial level by avoiding some time consuming and labor-intensive experiments. It can help researchers to better understand the strengths and weaknesses of potential material candidates at early stage of materials design [71].

In a computer experiment, a "sample" is constructed according to the model of the material. Then the "sample" is tested by applying certain conditions. Under different conditions the "sample" will respond according to the equations based on the model. All the processes are carried out by computer calculation using high efficiency algorithm. Molecular dynamics is one of those computer simulations. It is a powerful tool to understand the problem at molecular level. It assumes that the atoms are rigid points and their motions follow the Newton's equations of motion. After setting the initial status of the system, it will evolve with time based on the interactions between all the atoms. The information of the system (e.g., temperature, pressure, volume) could then be extracted.

7.2 Fundamental and methods

In molecular dynamics, the motion of all atoms are obtained by integrating the Newton's equations of motion given by [72]:

$$m_i \frac{dv_i}{dt} = \sum_j F_2(r_i, r_j) + \sum_j \sum_k F_3(r_i, r_j, r_k) \ldots$$

$$\frac{dr_i}{dt} = v_i \,, \qquad (1.8)$$

where m_i, v_i, r_i, are the mass velocity, position of the atom i, respectively. F_2 is the force function for pairwise interactions between any two atoms i and j while F_3 is the force

function for three-body interactions. Items for interactions between more than three atoms could be added after F_2 and F_3. In Equation 1.8, the positions are decided by the initial structure of the system and the velocity could be set according to the temperature. However, the interactions between atoms (F_2, F_3, and more), also called force field, are not easy to determine. It could be very simple like in Lennard-Jones liquids or very complex as in polymer and biomolecules.

The results from molecular dynamics simulations are essentially the trajectories of all the atoms in the system at different times. Those "raw" data provide the microscopic information of the system that may not be of interest. Macroscopic properties are often those that we want to investigate. Statistical mechanics is the link between the microscopic world and reality. According to statistical mechanics, physical quantities are the averages over the system's microscopic configurations distribution according to a certain statistical ensemble i.e., the ensemble averages. Therefore, the extraction of a physical quantity from the simulation results could be considered as simply, averaging it over all microscopic states.

7.3 Applications and limits

The first published application of molecular dynamics simulation dates back to 1957 [73]. Alder and Wainwright investigated the phase transition for a system of hard spheres. Hard spheres represent the molecules in the system, they move at constant velocity between perfectly elastic collisions. This interaction is pretty simple so the simulation could be handled with those "old" (from modern point of view) computers. Today, molecular dynamics simulation has been applied to the research on various

materials spanning from crystals to proteins; and different phenomena including transport processes and phase transitions. In addition, some new technologies have been developed like *ab inito* molecular dynamics [74] and steered molecular dynamics [75].

However, there are some limits associated with molecular dynamics simulation. Although the capabilities of current computers have dramatically increased compared to before, they are still not realistically compatible for using molecular dynamics and to study macromolecules in details, because of the long relaxation times. Also, limited by the computational power, simulations of long time (~ms) behavior are expensive. Another limit comes form the force field. Unlike the first principle, the simulation is often based on some basic physical constants, and the choice of force filed is more empirical, therefore, it may introduce some inaccuracy.

8. Flexible lithium ion batteries

8.1 Overview

Consumer electronics are becoming thinner, lighter, flexible, and even wearable. The flexible electronics may undergo bending, twisting, and folding while maintaining their functionalities. Some conceptual products, like the fluid smartphone from Philips, Nokia Morph Concept, have already been introduced to the public. Flexible electronics are leading a revolution in relevant industry fields and will influence our future lifestyles. For flexible electronic devices, a key requirement would be the corresponding flexible power source. Unfortunately, most power devices (e.g., batteries) currently used for portable electronics, are too rigid, thick, and bulky. Therefore, developing flexible power sources,

such as flexible LIBs, capable of conforming to the device shape change are urgently required to integrate with flexible electronic products [76]. A paramount requirement for flexible LIBs is that they should be able to work as well as the ordinary batteries especially when they are under common mechanical strains, such as under bending, twisting or other deformation modes for long-term use. Moreover, safety is always a priority and it is even more critical for flexible LIBs due to the possible shape change. This should be considered with great care [77]. However, profound challenges are present in both material science and assembly technology, to meet those requirements. First, all the materials used in such batteries, including the electrode-active materials, ionic conducting materials (electrolytes), current collectors, and the encapsulation materials are essentially required to possess robust flexibility. Meanwhile, the general requirements, i.e., high capacity, cycling stability, good conductivity should not be compromised. On the other hand, since the rigid cases are eliminated for flexibility, compact packing is necessary to guarantee the integrity of the flexible battery especially during deformation.

8.2 Progress

During the past several decades, many structural and material designs have been proposed to fabricate a flexible LIBs [78-86] *Min Koo* and coworkers developed an all-solid-state bendable lithium-ion battery and integrated it with a flexible light-emitting diode (LED) [78]. *Liangbing Hu* et al., designed a paper-based lithium-ion battery which employed carbon nanotube instead of the traditional metals as the current collector to enhance the flexibility [79]. *Sheng Xu* and others proposed self-similar interconnects to

pack a set of cells to form a highly stretchable battery [80]. More comprehensive survey in this research area can be found in two recent reviews [77, 87].

9. Outline of the dissertation

This dissertation aims to investigate the properties of polymer electrolytes and explore the potential applications in flexible lithium ion batteries. Related research approaches and experimental results will be discussed.

Chapter I presents the motivation and objectives of this study. Relevant background is introduced including energy storage, lithium ion battery, and molecular dynamics simulation. The focus here is on polymer electrolytes.

Chapter II proposes a theoretical model for the mechanism of ionic conductivity enhancement by incorporating nano-sized filler to polyethylene oxide (PEO)-based solid polymer electrolyte. The details of the modeling and the comparison with some published experimental data are provided.

Chapter III describes an atomistic and molecular dynamics simulation of nanocomposite solid polymer electrolyte. The model, force field, simulation details and results are discussed.

Chapter IV investigates the application of the above solid polymer electrolyte in flexible lithium ion batteries. The fabrication methods of the electrolyte and the battery as well as their performance are described. Solid electrolyte based on Poly(vinylidene fluoride-*co*-hexafluoropropylene) (PVDF-HFP) is introduced and tested.

Chapter V shifts to PVDF-HFP based gel polymer electrolyte because of the expected high ionic conductivity. Its composition, ionic conductivity, and the performance of coin cell made with this type of gel electrolyte are discussed.

Chapter VI introduces a type of ionic liquid to fabricate stable solid-like gel polymer electrolyte for flexible lithium batteries. The motivations of using ionic liquids, fabrication of the flexible battery and the enhancement of battery performance are explained.

Chapter VII concludes all the results of this dissertation. The limitations and future work are discussed.

Chapter II Ionic Conductivity Enhancement Model for Polymer Nanocomposite Electrolytes

1. Introduction

1.1 Ionic conductivity enhancement of polymer nanocomposite electrolyte

As the demand on lithium ion batteries has increased significantly during the past decades, their safety issue has gained more and more attention. Among all the materials used in LIBs the volatile, flammable organics solvents in liquid electrolytes are considered hazardous. Their poor thermal stabilities make them vulnerable to any abuse, including disposing in fire, overcharging, and external short-circuiting or -crushing. In those situations spontaneous heat-evolving reactions would occur and eventually might lead to fire and explosion [88, 89].

Solid polymer electrolytes (SPEs), usually consist of polyethylene oxide (PEO) and lithium salts, due to their advantages like safety, suppression of dendrite growth, and thin membrane manufacturability have attracted great attention in the past few decades [51, 54, 90-97]. However, the major disadvantage of poor ion conductivity especially at room temperature still presents a challenge. Liquid plasticizers can significantly improve room temperature ion conductivity in SPEs [57, 98-101], but they also lead to mechanical instability. Another approach is to add nanosized fillers into SPEs that can increase ion conductivity up to three orders of magnitude without compromising the mechanical properties [58, 102-110]. Figure 2.1 shows some published ionic conductivity data of

solid polymer electrolytes with different nanofillers [111]. It is clear that nanofillers could enhance the ionic conductivity of solid polymer electrolytes. The origins of such ion conductivity enhancement in polymer nanocomposite electrolytes (PNCEs) are postulated as:

a) nanofillers facilitate salt dissociation [61, 112, 113];
b) nanofillers embedded in the polymer matrix disrupt its crystallization and enlarge the amorphous regions where fast ion transportation can occur [58, 114];
c) nanofillers stabilize the highly ion conductive channel-like crystalline structure [59, 115];
d) a highly conductive layer (i.e., liquid) is present on the nanofiller surface (effective medium theory) [116, 117].

However, the precise mechanisms of ion transportation in PNCEs still remain unclear.

In this chapter, we investigate the mechanisms of lithium ion conductivity enhancement and degradation in polymer nanocomposite electrolytes. The study aims to reveal the microscopic mechanisms of ion conductivity enhancement in semi-crystalline PNEs. We explore the role of nanofillers in increasing ion conductivity (as well as decreasing) from several aspects like dissociation of lithium salts and local structural changes in the polymer matrix and present an equation of ion conductivity enhancement as a function of nanofiller loading. Our modeling of ion conductivity is based on free volume and the local interactions between polymer, salt ions, and nanofillers. Agreement

between our model predictions and experiments confirm that our postulated mechanisms can explain the dependence of ion conductivity on nanofillers.

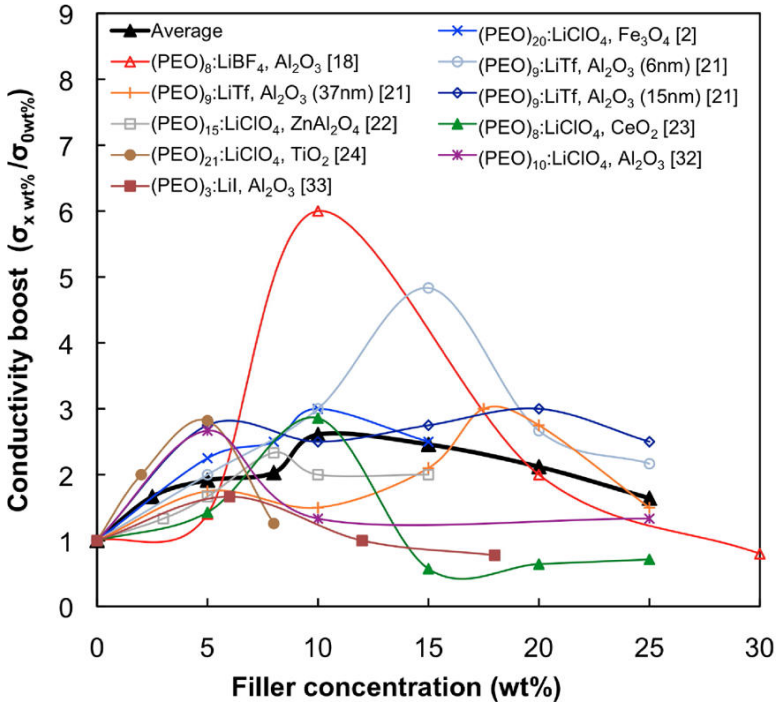

Figure 2.1. Ionic conductivity enhancement for different polymer nanocomposite electrolytes.

1.2 Fundamental of ionic conductivity

There are two different ways for materials to conduct electrical current corresponding to different charge carriers. One is through electrons. Metals are the most common representatives for this family. In the other type of conductors, ions are the majority of the charge carriers. The typical examples for those materials are the electrolytes in various electrochemical devices. In batteries, redox reactions occur at the two electrode-electrolyte interfaces and ions are generated and consumed on each electrode, respectively. In order to maintain the reactions, the electrolyte should be able to transport

the new generated ions to the other electrode where the ions would be consumed. Ionic conductivity is a measure for such ability of the electrolytes. Electrolytes with high ionic conductivity could transport the ions effectively so that there would be no excess or insufficiency of the ions for the reactions and the battery could provide a stable power.

Ionic conductivity is defined in the same way as for the general electrical conductivity which is the inverse of the resistivity:

$$\sigma = \frac{1}{\rho} = \frac{J}{E}, \qquad (2.1)$$

where J (A/m^2) is the area density of the generated current in a conductor and E (V/m) is the applied electrical field. Thus the SI unites of ionic conductivity are Siemens per meter (S/m). From microscopic point of view, the ionic conductivity could also be expressed as

$$\sigma = q\, n\, \mu\,, \qquad (2.2)$$

where q is the charge carried by the ion, n is the concentration, and μ represents the mobility [118] which is related to diffusion constant D by the following so called Nernst-Einstein equation

$$\mu = \frac{q}{k_B T} D, \qquad (2.3)$$

where k_B is the Boltzmann constant and T is the temperature [119].

1.3 Diffusion in polymeric materials

In solid polymer electrolytes, the conduction/diffusion of the ions is coupled with the motion of polymer chains. Figure 2.2 shows the "ion hopping" mechanism in a PEO-Li salt type electrolyte. The positive charged lithium ion is coordinated with the negative

charged oxygen atoms in the polymer chain. Accompanied with the movement of the chain the lithium ion could jump from one coordination site to another available location. After continuous jumps the macroscopic diffusion can be observed.

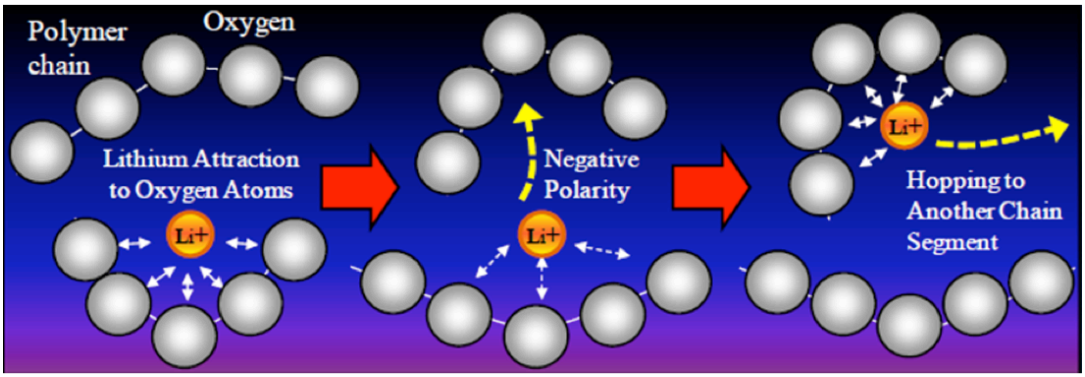

Figure 2.2 Ion hopping mechanism in polymer electrolyte.

For many years, the free volume theory has been widely used to investigate the diffusion process in the polymeric materials [120-125]. Inside the materials, the molecules do not occupy all the volume and some void space/free volume exists between molecules (Figure 2.3) [Ref] due to irregular packing in amorphous regions. The average free volume per molecule v_f is defined by

$$v_f = v_m - v_0 \,, \qquad (2.4)$$

where v_m is the average volume per molecule and v_0 is the van der Waals volume of the molecule. According to the free volume theory, the diffusion of the molecule is dependent on the size of free volume in its vicinity. This theory was first applied on a hard sphere liquid model by *Morrel H. Cohen* and *David Turnbull* [126]. They proposed that the molecule might "jump" to other location if there was enough free volume

adjacent to the molecule to accommodate it. Statistically, the possibility of the jump to occur will be higher if the size of the free volume is larger. They also suggested that the diffusion should be considered as a result of redistribution of the free volume within the material rather than as a result of activation process in the ordinary sense. Based on the above discussion *Cohen* and *Turnbull* developed the following relation between the diffusion coefficient and the free volume

$$D = C_0 exp\left(-\frac{\gamma v^*}{v_f}\right), \qquad (2.5)$$

where D is the diffusion coefficient of the molecule, V^* is the minimum free volume for a molecule jump to occur, and γ is the overlap correction factor accounting for free volume being shared by the neighboring molecules. V_f is the average free volume per molecule and C_0 is pre-exponential constant which is related to the gas kinetic velocities according to *Cohen* and *Turnbull*.

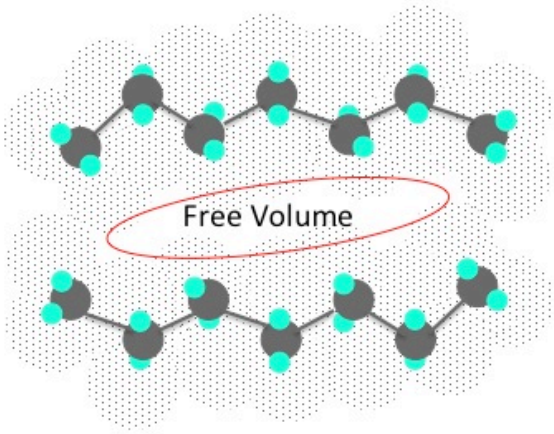

Figure 2.3. Free volume in a polymer matrix.

2. Influence of nanofillers on solid polymer electrolytes

The ionic conductivity enhancement in solid polymer electrolytes upon adding nanofillers has been observed by many groups. Some possible general reasons were also provided in the previous section. In this section the influence of nanofillers on the salt and the polymer would be discussed in details.

2.1 Dissociation of lithium salts

In the electrolyte of a lithium ion battery, the Li-ions are formed through the dissociation of the Li salt where the cations (Li^+) and the anions (e.g., ClO_4^{-1}) are separated as a result of the interaction between the salt molecules and the solvent molecules. In order to ensure sufficient concentration of lithium ions, the solvent should be able to dissolve the lithium salt effectively. It is well known that the salts would be easily dissolved in the organic solvents owing to the latter's polar molecules. However, one could predict that for solid polymer electrolyte this process would experience some difficulties. The typical method to produce a solid polymer electrolyte has been to dissolve the polymer (e.g., PEO) and the lithium salt in a common solvent (e.g., acetonitrile) and then remove the solvent. In the product — polymer lithium salt mixture — complexes of lithium ions and the polymer host would be formed because of the following reaction

$$m(LiX) + (CH_2CH_2O)_n \rightarrow mLi \cdot (CH_2CH_2O)_n \cdot mX\ , \qquad (2.6)$$

where X represents the anion and (CH_2CH_2O) is the repeat unit of PEO [97, 127]. The formation of such complexes prevents the recombination of lithium ions and the anions.

Thus, the relatively free lithium ions (attached on the polymer chains) are generated in this manner for future conduction. The above reaction requires that the Gibbs free energy of solvation is larger than the lattice energy of the salt. So, for a given polymer, only salts with low lattice energy will form complexes and such salts generally have large anions with a dispersed charge [51]. In addition to the consideration of lattice energy of the salt, there are some other criteria for the polymer host in order to form the complexes that include: a) sufficient number of polar (basic) atoms/groups on the polymer chain to solvate the salt effectively; b) low cohesive energy of the polymer; and c) high flexibility of the polymer chain so that the reorientation of the local coordination geometry is easily achievable. Most qualified polymer electrolytes are based on oxygen-containing monomers, including ethers in PEO and poly(propy1ene oxide) and polysiloxanes. In general, a good polymer host should have enough Lewis base atoms/groups on the polymer chain so that the acidic lithium ions could coordinate with them to form the complex structure [127].

Fourier transform infrared (FTIR) and nuclear magnetic resonance (NMR) results have shown that adding nanofillers to polymer electrolytes can increase the free ion fraction [128, 129]. Researchers usually attribute this to the Lewis acid-base interaction between nanofillers and lithium salts [130]. In addition, high dielectric constant nanofillers can further facilitate salt dissociation [131]. At higher filler contents, however, the free ion fraction can decrease due to ion pairing and trapping [132, 133]. The adverse effects of high filler content will be addressed later. Thus, we present a linear expression of ion concentration as

$$n(w) = n + k_1 w \ , \qquad (2.7)$$

where parameter k_1 is the "salt dissociation efficiency" which depends on the lattice energy of the salt and nanofiller properties (i.e., dielectric constant and surface coating). Basically, we assume each single nanofiller could contribute to the dissociation of the lithium salt and there is no overlap of those contributions. Therefore, the total ion concentration *n* would be a linear function of the content of the nanofiller (*w*).

2.2 Recrystallization and free volume of polymer matrix

We know from Equation 2.4 that the diffusion coefficient will increase with the increased fraction of free volume in the polymer matrix. In polymer nanocomposite electrolytes, the dispersed nanofiller can impair the recrystallization kinetics of the PEO polymer chains and create more amorphous and associated free volume [58, 106, 134, 135]. This conclusion could be confirmed by the positron annihilation lifetime (PAL) spectroscopy results. Both the density and the average size of the free volume "holes" are increased because of the nanofillers [136, 137]. In addition, some molecular dynamics studies suggested that not only the fraction of free volume but also its distribution in the polymer matrix would contribute to ion diffusion [138-140]. This conclusion implies a percolation mechanism for ion transportation [111]. A figure 2.4 demonstrates that the embedded nanofillers could disrupt the organization of the polymer chain and enlarge the free volume.

We assume that the free volume fraction will increase with nanofiller content until it reaches a limit and propose an expression for free volume fraction $v_f(w)$ as

$$v_f(w) = k_3[1 - exp(-k_4 w)] + v_{f0}\ , \qquad (2.8)$$

where v_{f0} is the free volume fraction of unfilled polymer electrolyte, k_3 is the "free volume enhancement ratio" and k_4 is the "free volume expansion coefficient".

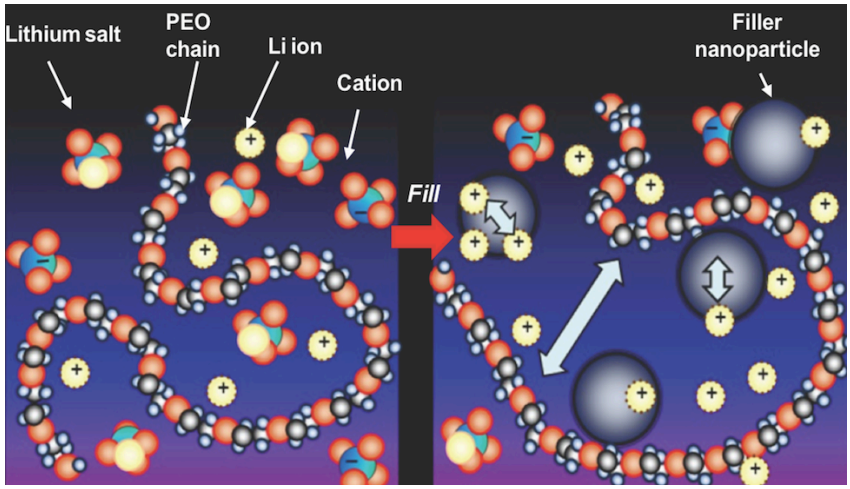

Figure 2.4. The free volume has been increased by the nanofiller.

2.3 Adverse effects of nanofillers

The relation between the ionic conductivity enhancement and the loading of the filler is not straightforward as indicated by the variety of the curves in Figure 2.1. However, we can still notice a trend that when the filler concentration is increasing the ionic conductivity will increase slowly at the beginning and then suddenly jump up to a maximum and then drop down. This behavior might indicate that there are two types of results induced by the nanofiller competing with each other. One is causing the increase of ionic conductivity (including enhanced dissociation of salts and expansion of free volume) which is dominating at lower filler content. The other one only has little

influence when the amount of nanofiller is small but it controls the ionic conductivity to drop down at high filler loading.

One of the latter type results is blocking where the presence of solid nanofillers can cause the ion diffusion paths to deviate from straight lines as shown in Figure 2.5. This effect will impair the diffusion process because of the elongated diffusion path. Tortuosity τ, as defined by the ratio between the deviated and original diffusion paths, is a characterization of this effect and can be related with the content of the nanofiller (w) by the following equation

$$\tau = \frac{\Delta l}{\Delta x} \approx \frac{\Delta x + N(\pi r - 2r)}{\Delta x} = 1 + N(\pi - 2)\frac{r}{\Delta x} \approx 1 + k_5 w \,, \qquad (2.9)$$

where r is the radius of a spherical nanofiller, N is the number of such nanofillers in the travelling path and k_5 is the "blocking factor" which depends on the shape and porosity of nanofillers [141]. Taking the tortuosity into account the diffusivity should be scaled following the equation:

$$D' = \frac{D}{\tau^2}, \qquad (2.10)$$

where D' and D are diffusivities with and without nanofillers, respectively [142].

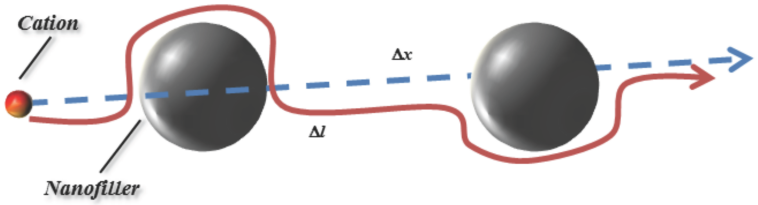

Figure 2.5. Modified travelling path of an ion due to blocking by solid fillers.

At high nanofiller content some other adverse effects for ion transport could be triggered. Figure 2.6 illustrates the ion trapping effect. A large amount of nanofillers close to one another will result in a region of less polymer chains. Ions in those regions are difficult to form the complexes with polymer host and the chance of those ions to re-form the salt molecules is increased [143]. Thus the ions are considered as being trapped in "nanofiller cages" and they could not contribute to the ionic conductivity.

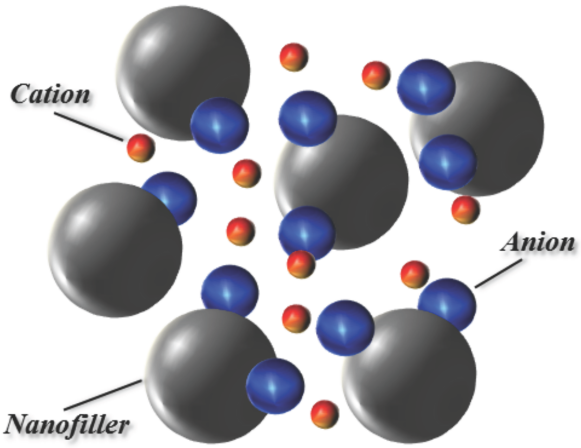

Figure 2.6. Ions are trapped in the region of crowd nanofillers.

In addition, it has been shown that the polymer chain dynamics under confinements would be impacted [144, 145]. In polymer nanocomposite electrolytes the relatively heavy nanofillers would act as anchoring points embedded in the polymer matrix. With more and more nanofiller they will constrict the motion of polymer chains between them. Therefore, the ion transport will be impaired also as it is coupled with the motion of polymer chains.

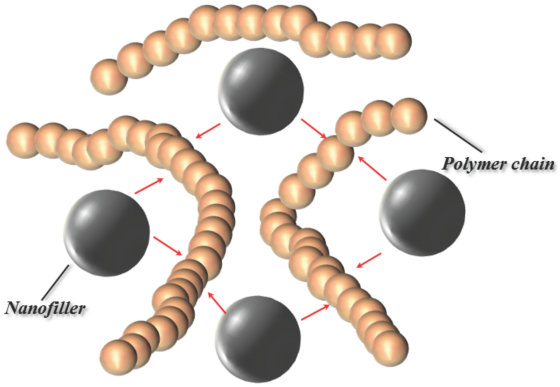

Figure 2.7. The motion of polymer chains is constricted by the anchoring nanofillers.

Large specific surface area is the outstanding characteristics of the nano-sized filler. In the above discussion we have ignored the interactions between each nanofiller. However, nanofillers exhibit strong tendency to aggregate due to their high surface energy and aggregation in polymer matrix is more likely to occur at higher filler content [146-148]. Nanofiller aggregation will lead to the reduction of the effective surface area of nanofillers and make them lost their functions.

The common point of the above adverse effects is that they would become more and more significant when the content of nanofiller is increasing. However, at very low concentration of nanofiller the adverse effects are almost negligible. Thus, we use an exponential function as

$$F_{ad} = exp(k_6 w) , \qquad (2.11)$$

to represent the combination of the adverse effects except for the tortuosity effect.

3. Results and discussion

3.1 Model for ionic conductivity enhancement

We first define the ionic conductivity enhancement as the ratio between the ionic conductivity of filled solid polymer electrolytes and the ionic conductivity of the unfilled solid polymer electrolytes. This enhancement is a function of the filler content. The ionic conductivity of the unfilled solid polymer follows the general form:

$$\sigma = \frac{q^2 n}{k_B T} D \ . \qquad (2.12)$$

Equation 2.12 is the combination of Equation 2.2 and 2.3. In addition, we know from Equation 2.5 that in polymeric materials the diffusion coefficient is related to the free volume. Plugging Equation 2.5 into Equation 2.12, we obtain

$$\sigma = \frac{q^2 n}{k_B T} C_0 exp\left(-\frac{\gamma v^*}{v_f}\right). \qquad (2.13)$$

Based on our discussions in previous section, the ion concentration *n* and the diffusion coefficient *D* in Equation 2.13 should both be functions of the nanofiller content *w*. Furthermore, the adverse effects need to be taken into consideration. Based on Equation 2.7-2.11 and Equation 2.13, the ionic conductivity of filled solid polymer electrolytes could be expressed as

$$\sigma(w) = \frac{C_1 n(w) C_0 exp\left[-\frac{\gamma v^*}{v_f(w)}\right]}{(1+k_5 w)^2 exp^{(k_6 w)}}, \qquad (2.14)$$

where $C_1 = q^2/k_B T$ is another constant if T is fixed. Next, we obtain the ionic conductivity enhancement

$$E_w = \frac{\sigma(w)}{\sigma} = \frac{1+K_1 w}{(1+K_5 w)^2} exp\left[\frac{-K_2}{K_3(1-e^{-K_4 w})+1} + K_2\right] exp(-K_6 w)\ , \qquad (2.15)$$

where E_w is the enhancement of ion conductivity, w is the nanofiller content, $K_1=k_1/n$, $K_2=\gamma v^*/v_{f0}$ is the "free volume factor", $K_3=k_3/v_{f0}$, $K_4=k_4$, $K_5=k_5$ *and* $K_6=k_6$ are parameters to be determined by fitting to experimental results.

3.2 Comparison to experimental results

Equation 2.15 describes how the ionic conductivity enhancement changes as filler content increases. We can fit the equation to some experimental data to check its applicability. We first fit our model (Equation 2.15) to the ion conductivity data from our previous study on hybrid clay-carbon nanotube filled polymer electrolyte [149]. The fitting curve is shown in Figure 2.8 as dashed line. To simplify the fitting process we use the logarithm of the enhancement.

It is clear that the fitting curve deviates largely from the experimental data at the beginning and it is more consistent with the experiment at high nanofiller contents. It seems that the nanofillers promote the ionic conductivity more effectively predicted by our model than they actually exhibit in the experiments. A plausible explanation is related to the concept of "free volume distribution" and the percolation mechanism in ion transport. Based on the previous discussion, the free volume in the matrix governs the ion transport. However, to conduct the ions effectively a continuous network of the free

volume is required. So far our model only considered the increased amount of the free volume by the nanofillers. At lower nanofiller contents, the dispersed nanofillers can increase the local free volume. But since the amount of nanofillers is relatively small, those additional free volume sites might be isolated in the electrolyte and are hardly connected together to form an effective ion transport network. So, we modify the expression of free volume (Equation 2.8) to

$$v_f(w) = k_3\{1 - exp[-k_4 w(1 - e^{-K_7 w})]\} + v_{f0}\ , \qquad (2.16)$$

by taking into account the formation of free volume network.

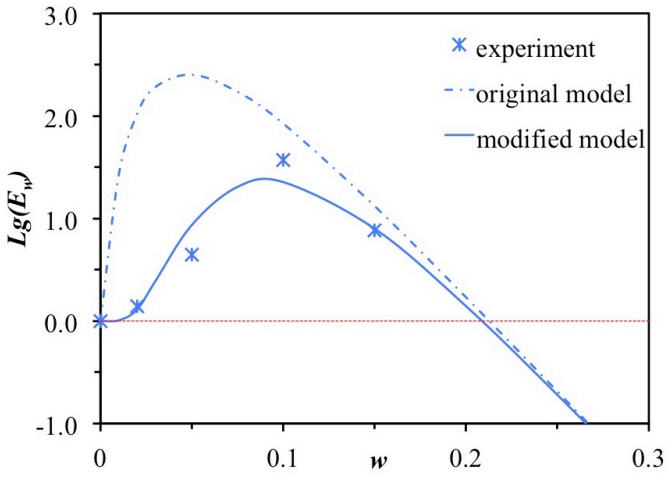

Figure 2.8. Fitting our original (Equation, 2.15 dashed line) and modified (Equation 2.17, solid line) models to the experimental data of ionic conductivity of solid polymer electrolyte with hybrid nanofillers (cross).

Equation 2.16 indicates that an initial portion of nanofillers may be utilized to overcome the barrier of forming the percolation network and until that is complete, the ionic conductivity enhancement will not be realized. Consequently, our original model for ionic conductivity enhancement could be defined as

$$E_w = \frac{\sigma(w)}{\sigma} = \frac{1+K_1 w}{(1+K_5 w)^2} exp\left\{\frac{-K_2}{K_3\left[1-e^{-K_4 w(1-e^{-K_7 w})}\right]+1} + K_2\right\} exp(-K_6 w)\,, \qquad (2.17)$$

where K_7 is the "percolation factor". Then, we fit this modified model to the same ionic conductivity experimental data. The fitting curve (solid line in Figure 2.8) shows much better consistency with the experimental data.

We also fitted the new model (Equation 2.17) to two more sets of ionic conductivity experimental data obtained for two widely used nanofillers investigated in literature, Al_2O_3 [150] and SiO_2 [151]. Figure 2.9 compares the fitting curves and the experimental data. The value of each "K parameter" is listed in Table 2.1. It can be seen that our revised model agrees very well with the experimental results and predicts both enhancement and degradation of ion conductivity with the addition of nanofillers.

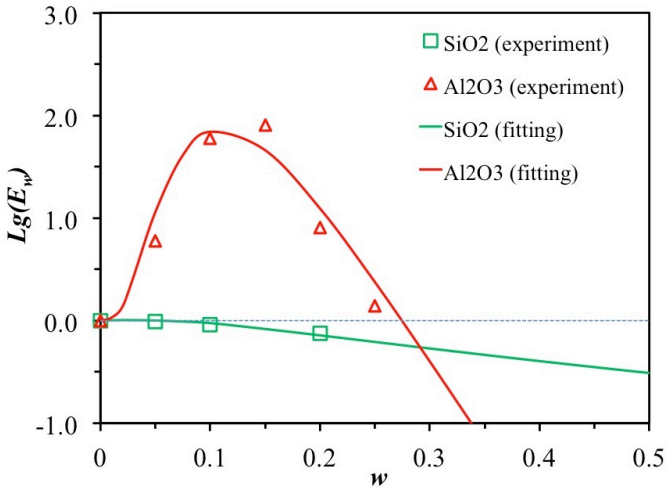

Figure 2.9. Fitting our modified model to the experimental data of ion conductivity of polymer electrolyte with two more different nanofillers.

In the study of polymer nanocomposite electrolyte, using SiO_2 nanofiller by Walls et al. [151], no enhancement of ion conductivity was observed in the experiments. On the contrary, the ion conductivity actually was found to decrease with the addition of nanofillers as the plot shows in Figure 2.9. According to our proposed mechanisms, it indicates that the positive influences of the nanofiller have been suppressed. Thus, adding nanofiller could not trigger the enhancement of ionic conductivity. In that polymer nanocomposite electrolyte, low molecular weight (250 and 500) poly (ethylene glycol) dimethylether has been used instead of the PEO. Thus, the expansion of free volume and the increase of the dynamics of the polymer chains might not be that significant as in the PEO matrix because the polymer may have been already in the state of high free volume. Correspondingly, the value of K_3 would be very small as listed in Table 2.1 since we know from Equation 2.16 that vanished K_3 leads to invariant $v_f(w)$. Consequently, the adverse effects dominate from the onset of nanofiller addition, which will lead to ionic conductivity degradation.

Table 2.1. The parameters used to calculate the ion conductivity enhancement in Figure 2.8 and 2.9 (unitless).

	K_1 *(Salt dissociation efficiency)*	K_2 *(Free volume factor)*	K_3 *(Free volume enhancement ratio)*	K_4 *(Free volume expansion coefficient)*	K_5 *(Blocking factor)*	K_6 *(Aggregation, trapping & confinement factor)*	K_7 *(Percolation factor)*
Hybrid	*1*	*5.5*	*3*	*15*	*3*	*40*	*6*
Al_2O_3	*1*	*7.6*	*1.5*	*15*	*2*	*35*	*8*
SiO_2	*1*	*2*	*0.01*	*10*	*2*	*0.6*	*N/A*

We also investigated the temperature dependency of ion conductivity in our model. We assumed that the free volume fraction v_{f0} is linearly dependent on temperature and other effects of temperature on the system are relatively negligible. Thus, among the parameters in Equation 2.17 only K_2 and K_3 are mainly changing with varying temperature (they are proportional to the reciprocal of temperature). We calculate the enhancement of ion conductivity as an exponential function of temperature due to the relation between the free volume and ion conductivity in our model. The temperature dependency results show good agreement with the experimental data [149] (Figure 2.10). The well-known Vogel-Tamman-Fulcher (VTF) equation predicting temperature dependency of ion conductivity[51, 103] was also plotted in Figure 2.10 for comparison.

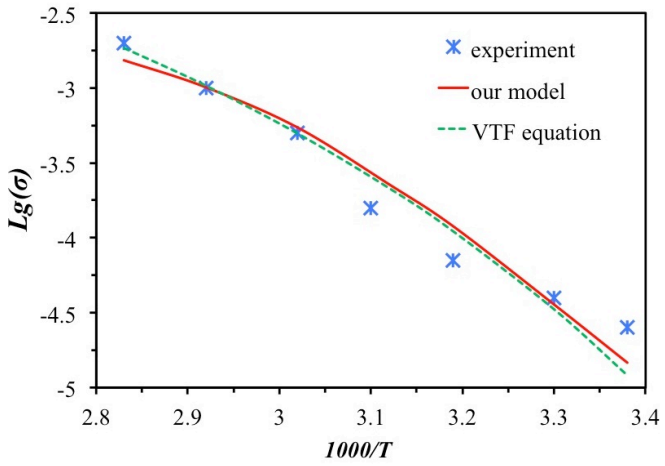

Figure 2.10. Fitting VTF equation (dashed line) and our model (solid line) to the experimental data (crosses) of ion conductivity of nanocomposite polymer electrolyte at varying temperatures and fixed filler content (w = 0.1).

In this model, many adjustable parameters are involved. We probed the role of each parameter by increasing its value by a factor of 2 while others were fixed. The results are plotted in Figure 2.11 where it can be seen that K_2, K_3, K_6 appear to have the most

dominant effects toward ion conductivity enhancement. All the parameters in Equation 2.17 along with their values used to plot the ion conductivity curves (Figure 2.9) are summarized in Table 2.1. Among these parameters, K_1 can be determined directly by FTIR experimental results. K_2, K_3, K_4 can be derived on the basis of assumed quantities like maximum free volume fraction. Other parameters are chosen empirically. For example, since the geometrical shape of the clay-CNT hybrid filler is more irregular, it is expected to correspond to a higher K_5 than that of the spherical Al_2O_3 nanofillers. However, this is a relatively complex multi-parameter model and fine-tuning all parameters can be time and labor intensive. To determine each K parameter, we must consider the experimental results as well as physical intuition for acceptable K value ranges. Another limitation of this model is that it does not address the potential coupling between various effects induced by the nanofillers. This aspect could be more influential at high filler contents. Future studies can address some of the above limitations and further enhance the ion conductivity model for polymer nanocomposite electrolytes.

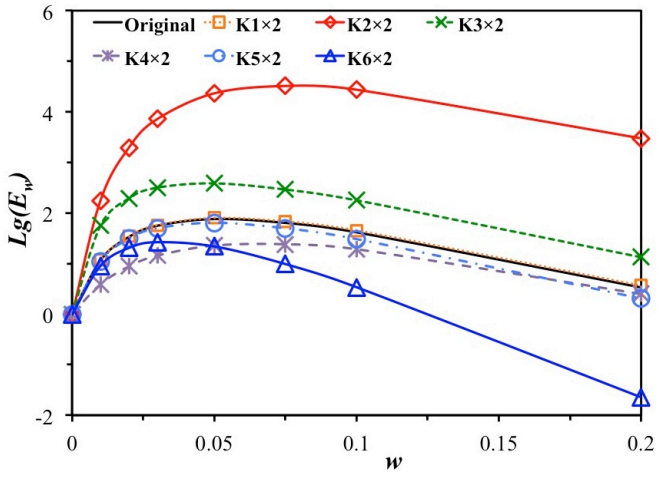

Figure 2.11. Influence of each parameter (K_1, K_2, K_3, K_4, K_5, and K_6) on ion conductivity in our model.

4. Conclusions

In summary, we investigated the role of nanofillers in enhancing ion conductivity of polymer electrolytes for lithium ion batteries. Based on the free volume theory and the interaction between polymer, nanofillers and lithium salt, we proposed a model of ion conductivity enhancement as a function of nanofiller content. Both enhancement and adverse effects of nanofillers on ion conductivity were considered including salt dissociation, free volume expansion and distribution, diffusion blocking, filler aggregation, ion trapping, and chain confinement using adjustable k-parameters. Our model agrees very well with the experimental results. It also predicts dependency of ion conductivity on temperature. This model can offer insight into the fundamental mechanisms of ion conductivity in the polymer-salt-filler system and facilitate a more effective design of polymer nanocomposite electrolytes.

Chapter III Molecular Dynamics Simulation of Polymer Nanocomposite Electrolyte

1. Introduction

Solid polymer electrolytes (SPEs) and gel polymer electrolytes (GPEs) have attracted intensive studies during the past decades due to their potential applications in various advanced devices including lithium ion batteries [2, 51, 90], supercapacitors [152], and stretchable actuators [153]. Compared to the traditional liquid electrolytes used in Li ion batteries, SPEs offer enhanced safety, stability and thin film manufacturability but their low ionic conductivity especially at room temperature has suppressed their development [54, 92]. One effective method to improve the ionic conductivity introduced by *Croce* et al., is adding nanosized fillers into SPE to form the polymer nanocomposite electrolyte (PNCE) which can produce up to three orders of magnitude enhancement [58]. Beside the common spherical shape, nanofillers with other shapes like rod [154], sheet [155], and hybrid [149], have also been utilized to obtain higher ionic conductivities. As we discussed in the last chapter, the reasons for the nanofiller-induced increase in the ionic conductivity of polymer electrolyte is still not fully understood. Ionic conductivity generally depends on the concentration and mobility of the conductive ions. Recent experiments have demonstrated that nanofillers can facilitate the Li salt dissociation [61, 112, 113] and therefore, increase Li ion concentration. Furthermore, experiments have shown that nanofillers disrupt the recrystallization of polymer matrix and consequently, increase the amorphous regions in the polymer matrix where the Li ion mobility is

relatively higher [58, 114]. However, at higher filler concentrations, adverse effects of nanofillers can dominate including aggregation, ion trapping, increased crystallinity, and constriction of polymer mobility [141, 147, 156] leading to decline in ion conductivity. Although a few studies have proposed models that provide interesting insights into the mechanisms of conductivity improvement in PNCEs [116, 117, 141], however the effects of nanofiller's shape and size remain unclear.

Molecular dynamics (MD) simulation is a powerful tool that can provide us insights at the molecular level on the phenomena of interest. MD simulations of polymer composites have traditionally focused on mechanical properties [157-163]. For example, some of the afore-mentioned works have shown that the nature of filler surface (attractive, repulsive or neutral) can play an important role in the composite mechanical properties. Also, the perturbed confinement of polymer chains near the solid surface has been investigated in the past [164-166]. Our interest is in the atomistic investigation of ionic conductivity in polymer electrolytes--which generally are comprised of the polymer host and the alkali metal salt. For example, *Siqneira and Ribeiro* performed united atom MD simulations of polyethylene oxide (PEO)/$LiClO_4$ system [167, 168] to reveal the temperature and salt concentration effects on both static and dynamic properties. Others works have targeted the same system but focused on ion pairing and lithium ion hopping process [169, 170]. PEO hosts doped with different salts have also been investigated [171-185]. MD simulations have also been used to analyze polymer nanocomposite electrolytes. These works concluded that incorporation of Titania and Alumina fillers did not show direct evidence of ionic conductivity enhancement. In fact, the dynamics of the

PEO chains and the charge carriers were found to be slowed down by the nanofillers [178, 186-189]. There are also other polymer-based electrolytes [140, 190-196] like the polymer/ionic liquid mixture[194] and copolymer single ion conductor[196] that have been investigated by MD simulations.

In this chapter, we focus on using molecular dynamics simulation to understand the shape and size effects of nanofillers on the ionic conductivity of solid polymer electrolytes. Specifically, we consider PEO/$LiClO_4$ solid electrolyte with EO:Li ratio of 10:1, with and without TiO_2 nanofillers.

2. Simulation details

2.1 Simulation model

We created a relatively long PEO chain with 200 CH_2CH_2O repeat units capped by methyl groups in both ends. 200 $LiClO_4$ molecules are doped into 10 such PEO chains in the form of disassociated ions corresponding to the ratio between ether oxygen (EO) atoms and lithium ions (EO:Li) at 10:1. All atoms were wrapped into a periodic simulation cell with the side length of about 50 Å. That was the case without nanofiller denoted by PEL. Based on the PEL case, we made a void in the center of the simulation box by pushing PEO and $LiClO_4$ atoms in the central region away and placed the TiO_2 nanofiller inside to form our desired nanocomposite. The position of the nanofiller was fixed during the simulations to approximate the behavior of solid polymer nanocomposites.

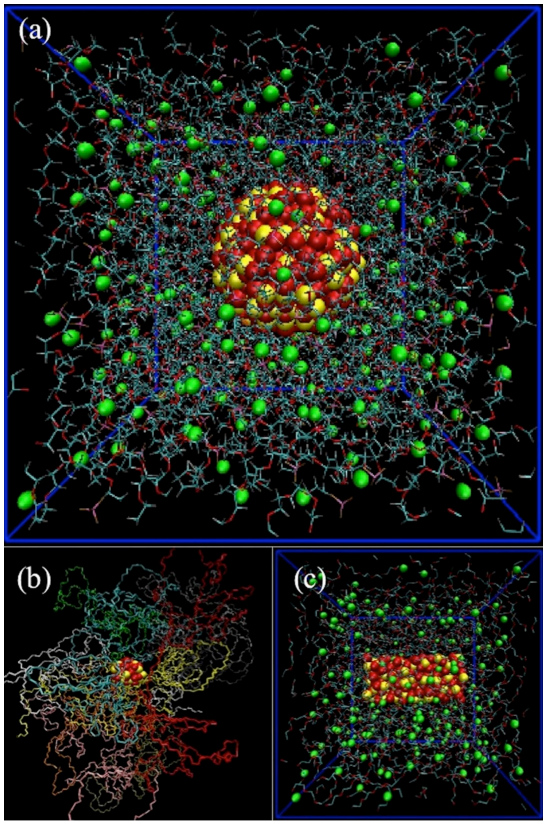

Figure 3.1. Simulation cases of PNC1(2.4) (a), PNC2(1.2) (b), and PNC3(rod) (c) visualized by VMD. Lithium ions and nanofiller atoms are shown in solid spheres.

In order to investigate the influence of nanofiller's shape and size we created 3 nanofillers. Two spherical TiO_2 nanofillers with diameters of about 2.4 nm and 1.2 nm and a rod-like nanofiller with diameter of 1.5 nm and height of 4 nm were cut from a bulk TiO_2 crystal (rutile). The dimensions of the rod-like nanofiller are chosen to ensure the same volume as that of the larger spherical nanofiller. Some surface atoms were removed to make the ratio Ti:O=1:2. For convenience, hereafter we name the simulation case with the larger spherical nanofiller PNC1(2.4), the simulation case with the smaller spherical nanofiller PNC2(1.2) and the one with the rod-like filler PNC3(rod). In addition, we created two other simulation cases by modifying the Li ion-nanofiller and PEO-nanofiller

interactions in PNC1(2.4) and PNC2(1.2) to purely repulsive by setting the attraction terms in the force field to zero (in experiments this could be done by chemical functionalization of the nanofiller's surface) and we call these new cases PNC1-SR and PNC2-SR, respectively. Such artificial filler surfaces have been used in a previous MD study [186]. Figure 3.1 shows three of our simulation cases PNC1(2.4) (a), PNC2(1.2) (b), and PNC3(rod) (c). The simulation cases are visualized using the Visual Molecular Dynamics (VMD) [197].

2.2 Discussion of the model

Due to the complexity of the atomistic models only one nanoparticle is included in each case. To investigate the effects of nanofiller concentration a much larger model including the desirable number of nanofillers and extremely intensive computation are required for atomic level molecular simulations. Therefore, the influence of nanofiller concentration is outside the scope of this study. Also, in an experimental case the TiO_2 filler particles may not have a strictly defined mono-dispersed size and shape. This mixed particle-size distribution could not be captured in our very idealized models. However, from our simplified models some insights for choosing nanofillers to achieve higher ionic conductivity could be offered. Also, the results in this study would be helpful to explain some observations from relevant experiments. In addition, the actual polymer nanocomposite electrolytes used in lithium-ion batteries can be highly complex and may involve high molecular weight polymer (i.e., >100,000) and other possible additives such as plasticizers. The molecular dynamics models created in this study were simplified to meet the computational demands involving shorter polymer chains lengths and excluding

the plasticizer. Since the polymer chains in our model are amorphous and one of the main roles of plasticizers is to reduce the crystallinity of the bulk polymer, our results can be applied to the case of polymer electrolyte with plasticizer. However, the addition of plasticizers can increase the complexity of the force field and the expected enhancement of lithium ion mobility would be attributed to multiple factors rather than the isolated properties of nanofillers.

Furthermore, nanofillers appear to play a significant role in the electrode/electrolyte interfacial properties in Li ion batteries. Experimental results show that nanofillers could stabilize the electrode/electrolyte interface and decrease the interfacial impedance during storage and cycling of lithium-ion batteries [198-201]. The models created in this study represent the "bulk" polymer electrolytes only and the interface of the electrolyte with the electrodes has not been considered. So the results obtained here are not expected to provide all the essential criteria for the formulation of the electrolyte materials, and nanofiller's role in the interfacial conductance of the electrolyte has been ignored. Future MD simulations may provide insight into the mechanisms of nanofiller effects on electrode/electrolyte interfacial transport.

2.3 Force field

The choice of an appropriate force field plays a critical role in MD simulations. In this work we adopted force fields from previous studies [164, 167, 186, 202, 203]. The assembled potential energy consists of bonded and non-bonded energy in the following forms

$$U^{bonded} = \sum_{ij} K_{ij}(r_{ij} - r_0)^2 + \sum_{ijk} K_{ijk}(\theta_{ijk} - \theta_0)^2 + \sum_{ijkl}\sum_{n=0}^{3} K_n cos(n\varphi_{ijkl}), \quad (3.1)$$

$$U^{nonbonded} = \sum_{ij}\{A_{ij}\exp(-B_{ij}r_{ij}) - \frac{C_{ij}}{r_{ij}^6} + \frac{q_i q_j}{4\pi\epsilon_0 r_{ij}},$$

or

$$U^{nonbonded} = \sum_{ij}\{\frac{A'_{ij}}{r_{ij}^{12}} - \frac{C_{ij}}{r_{ij}^6} + \frac{q_i q_j}{4\pi\epsilon_0 r_{ij}}\}, \quad (3.2)$$

where r_{ij} is the distance between atom *i* and atom *j*; θ_{ijk} is the angle formed by atoms *i, j* and *k;* φ_{ijkl} is the dihedral angle; q_i and q_j are partial charges of the atoms *i* and *j*. All the parameters are summarized in Table B1 in the Appendix B.

2.4 Simulation procedures

The molecular dynamics simulation software LAMMPS[72] was used for all the simulations. All simulation cases were first initialized at the temperature of 500K and constant pressure of 1 atm using small time step of 0.1 fs. Then the temperature was dropped to 300K during 100 ps of *NPT* (constant number of atoms, pressure and temperature) simulation. At the temperature of 300K, 100 ps of *NPT* simulation followed by 3 ns *NVT* (constant number of atoms, volume and temperature) simulation were carried out to equilibrate the systems. The system was determined to have reached a relative equilibrium when the total energy did not change too much for approximately 1ns. Then, 2 ns of *NVT* simulation was performed with a time step of 2 fs. System

information was collected during the last 2 ns at intervals of 10 ps resulting in 201 different system configurations for each simulation case.

3. Results and discussion

The simulation results of all the cases, PEL (without nanofiller), PNC1(2.4) (filled with a spherical nanofiller with diameter of 2.4 nm), PNC2(1.2) (filled with a spherical nanofiller with diameter of 1.2 nm), PNC3(rod) (filled with a rod-like nanofiller), PNC1-SR (filled with a spherical nanofiller with diameter of 2.4 nm and repulsive surface) and PNC2-SR (filled with a spherical nanofiller with diameter of 1.2 nm and repulsive surface), are compared in two major aspects, namely, the dissociation and the mobility of lithium salt ions ($LiClO_4$), since they both directly affect the ionic conductivity as discussed in the last chapter.

3.1 Dissociation of the $LiClO_4$

The MD results indicate that not all the salt molecules in the polymer electrolyte could be dissociated to generate free Li ions. A portion of the ions forms clusters of various sizes. Figure 3.2 shows the radial distribution functions *g(r)* and coordination numbers (CN) of Li-Cl for all the cases. We can see from Figure 3.2 that there is a sharp peak at the same location of *g(r)* for each case. This indicates that the first Cl coordination shells of most lithium ions are located about *3.5*Å away from the lithium ions and this radius does not change upon adding nanofillers. On the other hand, from the plateaus of CN curves, we notice that the number of Cl atoms in the first Cl-shell is between 1.1 and 1.4 of all the cases. This suggests formation of ion clusters in all cases

where lithium ions appear to coordinate with more than one anion. Furthermore, the CN numbers of Li-Cl in the filled cases are slightly smaller than that of the unfilled case. This may be attributed to the disturbance of the spatial structure of polymer-salt system due to the presence of nanofiller and the reduction in ion cluster formation.

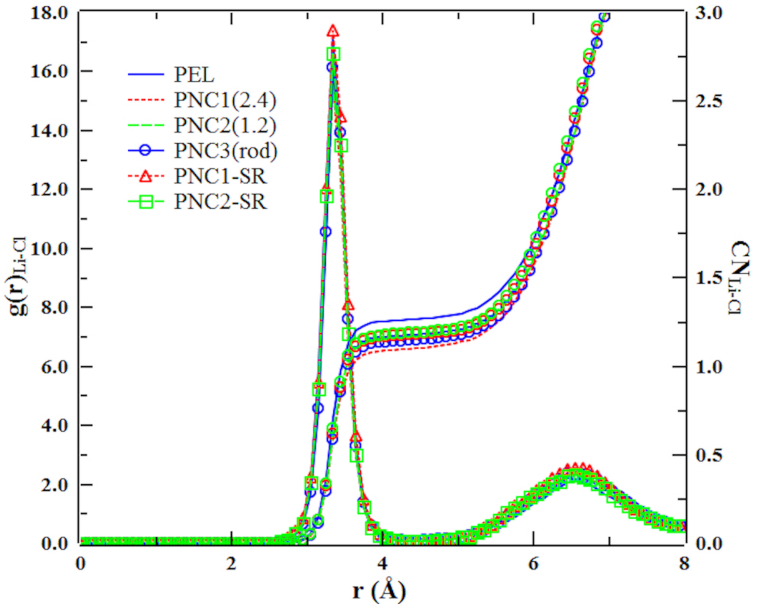

Figure 3.2. Radial distribution functions and coordination numbers of lithium ions with chlorine atoms in all the cases.

The lithium ions that are not associated with the nearby anions are considered "free" and "mobile" in our MD simulations. We chose *4.0*Å based on the g(r) in Figure 3.2 as the separation distance beyond which the pair of lithium cation and perchlorate anion is considered dissociated. In other words, if there are no anions around a lithium ion within the *4.0*Å distance then such a lithium ion is considered a "free ion". In addition, we observed in our MD simulations that a few lithium ions can be "trapped" in the vicinity of the nanofiller surface depicted in Figure 3.3a. Those lithium ions are usually

coordinated with some oxygen atoms on the nanofiller's surface and are therefore, not considered "free". Our simulation results show that this type of trapping can be eliminated by the applied repulsive surface as shown in Figure 3.3b.

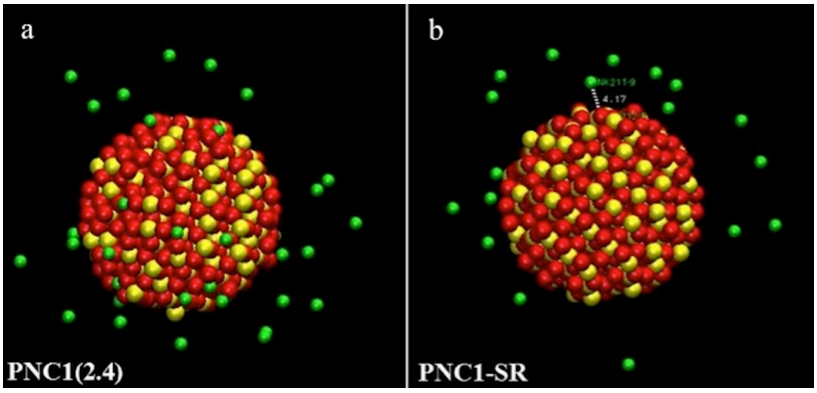

Figure 3.3. Comparison of lithium ions near nanofillers with normal surface (a) and repulsive surface (b). The dotted line and the number (4.17 Å) indicate the smallest distance between lithium ions and oxygen atoms in the nanofillers.

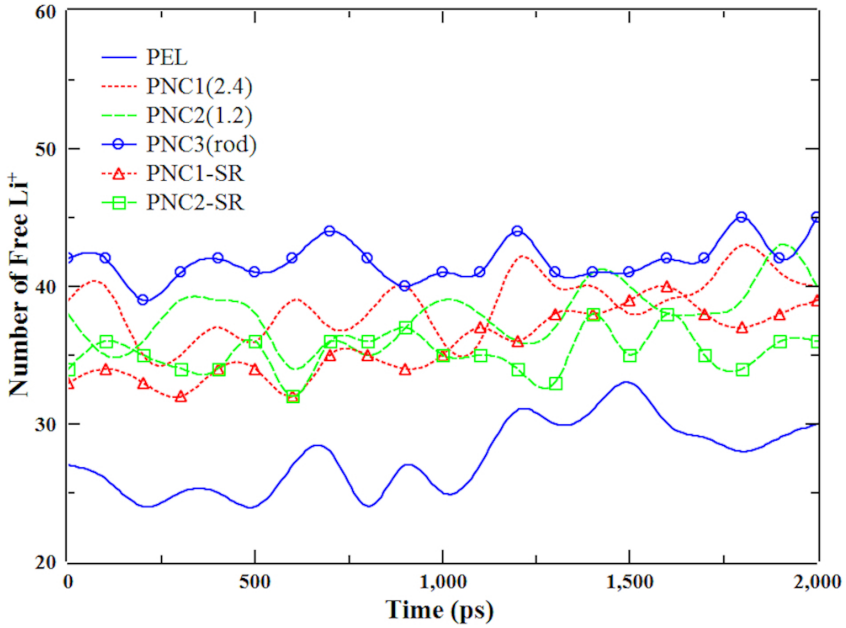

Figure 3.4. Numbers of free lithium ions varying with time in all the cases.

The plots of free Li ion number versus the simulation time for all the cases are shown in Figure 3.4. We can see that the nanofillers appear to increase the number of free ions with respect to the curve representing the pure polymer electrolyte (PEL) at the bottom. This confirms our above result regarding the ion cluster from the *g(r)* and CN plots that the nanofillers could prevent ions to form ion clusters. Consequently, more lithium ions are released as free ions.

3.2 Mobility of the Li ions

Another important aspect of the lithium ion transport is the mobility of lithium ions. Mobility is proportional to the diffusion coefficient *D*. In MD simulations, the latter can be calculated by the Einstein relation:

$$D = \lim_{t\to\infty} \frac{< MSD >}{6t}, \qquad (3.3)$$

where MSD is the mean-square-displacement of the interested atoms and it is averaged over the ensemble. The MSDs of lithium ions in all the cases are compared in Figure 3.5. It can be seen that PNC1-SR and PNC2-SR cases have higher lithium-MSD values than those of other cases. As we speculated, the repulsive surface could increase the mobility of lithium ions. On the other hand, among those nanofillers with normal or untreated surfaces, the one with the smaller size (PNC2(1.2)) shows a larger increase in lithium-MSD compared to the unfilled case. The larger nanofillers with untreated surfaces (PNC1(2.4), PNC3(rod)) exhibit limited impact on the MSD of lithium ions. Given the condition of equal volume, the difference in filler shapes (sphere to rod) does not result in a noticeable difference in the MSD of lithium ions. Overall, we can conclude that the

nanofillers with smaller sizes (lower volume fraction) and repulsive surfaces can increase the mobility of lithium ions.

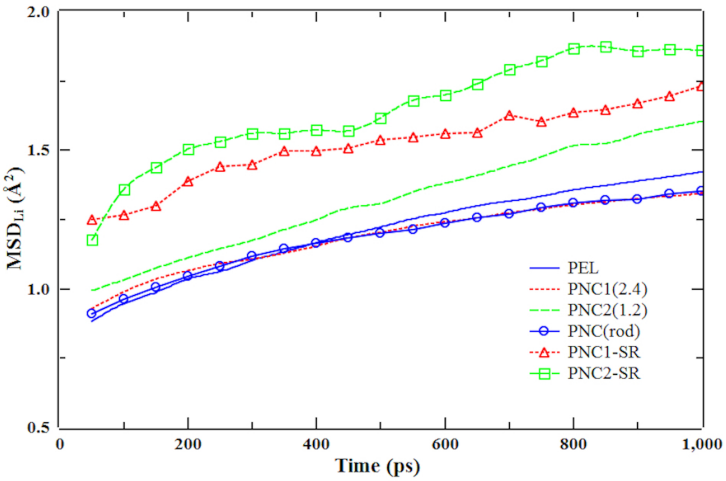

Figure 3.5. Mean-square-displacements of lithium ions.

In polymer electrolytes, the motion of lithium ions appears to be coupled with the dynamics of ether oxygen (EO) atoms in PEO chains. The MSDs of EO atoms are plotted in Figure 3.6. Compared to Figure 3.5 we can first see that the EO atoms are moving faster than the lithium ions in all the cases indicated by the larger MSD values. The similar relative positions of MSD curves in Figure 3.5 and Figure 3.6 confirm the coupled dynamics of lithium ions and EO atoms. Based on the MSD results, we calculated the diffusion coefficients of lithium ions and EO atoms and summarized them in Table 3.1. Compared to the results from experiments where the diffusion coefficients reached 10^{-7}cm^2/s, our values of diffusion coefficients are smaller. This is most likely due to the much longer PEO chains (25 repeat units vs. repeat 200 units per chain in our study) and lower temperature (373 K vs. 300 K in our study). On the other hand, from the

experiment data of ionic conductivity in Ref. 8, we calculated the Li diffusion coefficient in the system PEO_8-$LiClO_4$ at 300 K was in the level of $10^{-10}cm^2/s$ which is smaller than our simulation results due to the very long chain of common PEO used in experiments. From Table 3.1 we can see the diffusion coefficients of EO atoms are increased in all the nanofiller-filled cases. However such increase of the dynamics is not large enough to account for the significant enhancement (up to 3 orders in magnitude at room temperature) of ion conductivity caused by the addition of nanofillers observed in the experiments [58, 149]. The main reason for nanofiller-induced enhancement of ion conductivity may be attributed to the disturbance of polymer recrystallization and the enhanced amorphous regions [156]. Polyetheylene oxide (PEO) exhibits semi-crystallinity at room temperature and fast ion transport is believed to occur in the amorphous regions. The added nanofillers could suppress the recrystallization process of the neighboring PEO chains and thus increase the polymer amorphous regions.

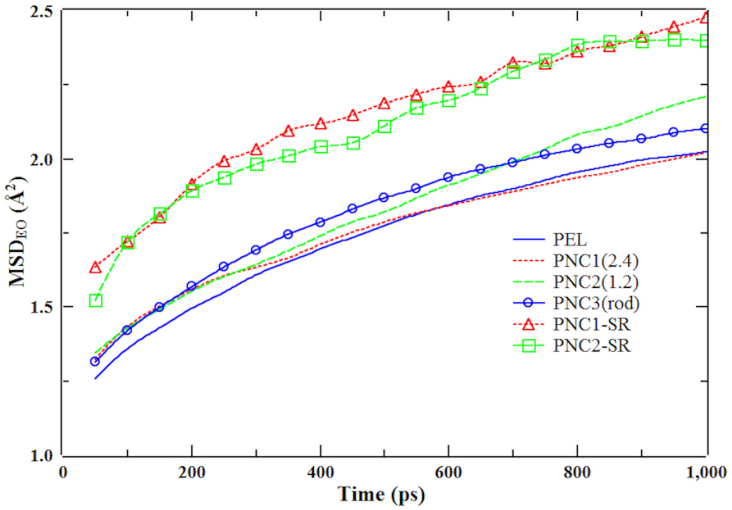

Figure 3.6. Mean-square-displacements of EO atoms.

Table 3.1. Diffusion coefficients D of the lithium ions and EO atoms.

	D (cm^2/s)	
Case	Li	EO
PEL	5.77e-09	3.01e-09
PNC1(2.4)	4.20e-09	3.01e-09
PNC2(1.2)	8.45e-09	1.05e-08
PNC3(rod)	4.20e-09	5.05e-09
PNC1-SR	8.52e-09	1.09e-08
PNC2-SR	1.01e-08	1.02e-08

3.3 Ion hopping

We also investigated the lithium ion transport by means of Li-EO coordination. In PEO-based polymer electrolytes the negative charged EO atoms attract the positive lithium ions. Some of these lithium ions are attached to and move along with the polymer chains as illustrated in Fig. 7a. We specifically traced a free ion in the PNC1(2.4) case for observation. Fig. 7b shows 2 snapshots of a lithium ion and a PEO segment consisting of 6 monomers at different times during the simulation. We clearly observe that the coordinated lithium ion can hop from its original site to a nearby site through the motion of the PEO chain. This is the so-called “ion hopping” mechanism. This process consists of two different stages. Because of the attraction between the lithium ions and EO atoms, a lithium ion might get trapped in a “cage” formed by EO atoms. After spending a small finite time in the cage, the lithium could jump to another cage formed by other EO atoms. The lithium ions hopping time appear to be generally much shorter than the time in the cages, also previously observed [171]. Relying on this successive trapping and jumping sequence, the dynamics of lithium ions and EO atoms are coupled as indicated by the

MSD plots. The positive lithium ion seems to associate with the polymer segment that has the highest local negative polarity and it moves along as the polymer segment propagates through the entire chain.

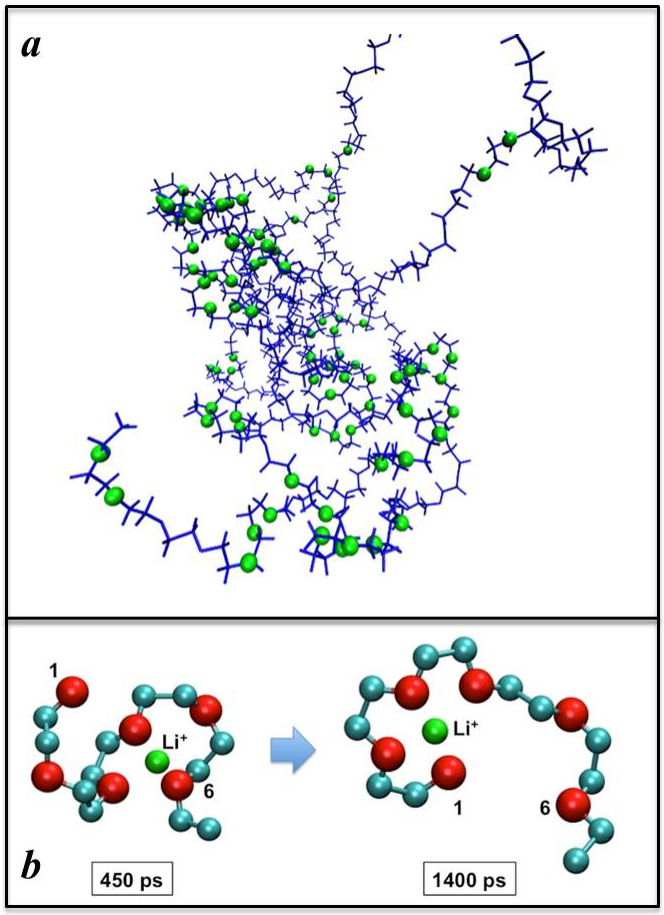

Figure 3.7. (a) Snapshot of a PEO chain with attached lithium ions (green spheres), (b) a lithium ion (green) "hopping" along the PEO chain where the numbers 1 and 6 indicate the first and last EO atoms in the segment, respectively.

4. Conclusions

MD simulations of TiO_2 nanofiller embedded in PEO/$LiClO_4$ electrolyte were performed using an assembled force field, 200 repeat units of each PEO chain and EO:Li

ratio of 10:1. Comparing the results of the structural and dynamic properties, we found that the addition of nanofillers can affect the salt dissociation, lithium-ion mobility, and the dynamics of PEO chains. Among the nanofillers, the repulsive nanofillers with different sizes showed good performance in both the suppression of ion-cluster formation and the enhancement of lithium ion mobility. This indicates that the surface property of nanofillers plays a crucial role in ionic conductivity of polymer nanocomposite electrolytes. Also, the smaller size (lower volume fraction) nanofiller is found to better increase the mobility of lithium ions. We could not observe significant effects induced by the shape of the nanofillers.

Chapter IV The Effect of Nanofillers on the Ion Conductivity of Solid Polymer Electrolytes for Flexible Lithium Ion Batteries

1. Overview

1.1 PEO-based solid polymer electrolytes for flexible lithium ion batteries

Flexible lithium ion batteries have gained attention recently because of the development of thinner, shape-flexible, and even wearable electronic devices. Those electronics devices are designed to satisfy the consumer's increasing demands of less weight, high portability, and tolerance of shape deformations. Flexible electronics require flexible power sources for effective integration.

Currently, lithium ion batteries are dominating the consumer electronics market. However, to power those flexible electronic devices new requirements for the design of lithium ion batteries are proposed. In general, they are required to work functionally when undergoing bending, twisting, folding and other mechanical deformations. In order to reach this goal, all the components including electrodes, electrolyte, and the encapsulation materials are expected to possess robust flexibility. Among them the electrolyte would be the bottleneck. In commercial lithium ion batteries liquid electrolytes are widely used. They generally consist of organic solvents and lithium salts. During the solvation lithium ions are separated with the anions and the dissociated ions are moving in a liquid environment so that the ionic conductivity is high and the batteries

could have good performance. However, liquid electrolytes are usually flammable and might lead to fire and explosion in any abuse. Therefore, a rigid case is required to prevent any leakage in the design of the battery because of the fluidity of the liquid electrolytes so that the flexibility of the battery is very limited.

On the contrary, solid electrolytes could eliminate the leakage and safety issue due to their high stability. *Min Koo* and coworkers have developed a bendable inorganic lithium ion battery using a solid ceramic electrolyte [78]. In their design $LiCoO_2$, lithium phosphorus oxynitride electrolyte (LiPON), and lithium metal are used as the cathode, electrolyte and anode, respectively. All the layers including the above materials, the current collector, and the protective encapsulation were deposited in order on the substrate. After the construction the battery could be transferred to a polymer sheet by peeling off the substrate. Finally, another polymer sheet was used to seal the whole device. Because of the high voltage electrode pair ($LiCoO_2$-lithium metal) the obtained all solid-state flexible lithium ion battery was capable of a maximum 4.2 V charging voltage and 106 $\mu Ah/cm^2$ capacity. In bend conditions with various bending radii, however, the capacity would gradually decrease. The authors argued that this reduction on capacity might be a result of the increased internal stress induced by the bending. Another disadvantage of the above battery is the use of lithium metal. Compared to the carbon-based anode the lithium metal is better compatible with solid electrolytes in terms of interfacial resistance. On the other hand, its high activity would result in safety issue. This is more important with the polymer encapsulation because such encapsulation might be easily broken by mechanical impact during the use of the battery. Thus, the exposed

lithium metal would react with the oxygen, moisture in the outside environment and cause the failure of the battery.

In order to develop safer lithium ion batteries with high flexibility, solid polymer electrolytes seem to be good candidates since they exhibit higher chemical and thermal stability. Also they have moderate Young's modulus, much lower than the ceramics but high enough for mechanical support. This is advantageous for reducing the internal stress while the battery is under mechanical strains. On the other hand, they could comply with a certain level of mechanical strain caused by the deformation of the flexible battery. They can maintain their integrated state and will not result in short circuit because of cracking. In addition, they can easily be produced as thin films with any customized shapes for compatibility with different electrodes. However, the low ionic conductivity and high electrode-electrolyte interface resistance, present challenges for their practical applications.

From discussions in previous chapters, we know that the addition of nanofillers could enhance the ionic conductivity of solid polymer electrolytes. We have discussed the mechanisms of the ionic conductivity enhancement induced by the nanofillers. Accomplished research in polymer nanocomposite electrolyte in our groups also confirmed that conclusion. *Mengying Yuan*, a PhD student in our group, has studied the influence of a two dimensional nanofiller—graphene-oxide sheets— on the PEO-$LiClO_4$ solid polymer electrolytes [204]. Graphene oxide (GO) has a similar structure with the graphene. They both have excellent mechanical properties. However, graphene has a very high electrical conductivity so that it is not suitable as filler in the electrolyte for lithium

ion batteries. Graphene oxide, on the other hand, is electrically insulating so the addition of GO will not cause any possible short circuit in the battery. In addition, graphene oxide has ultra-large specific surface area which makes it a promising filler to enhance the performance of solid polymer electrolytes [205-207]. Experimental results have shown that the addition grapheme oxide could enhance both the ionic conductivity and the mechanical strength.

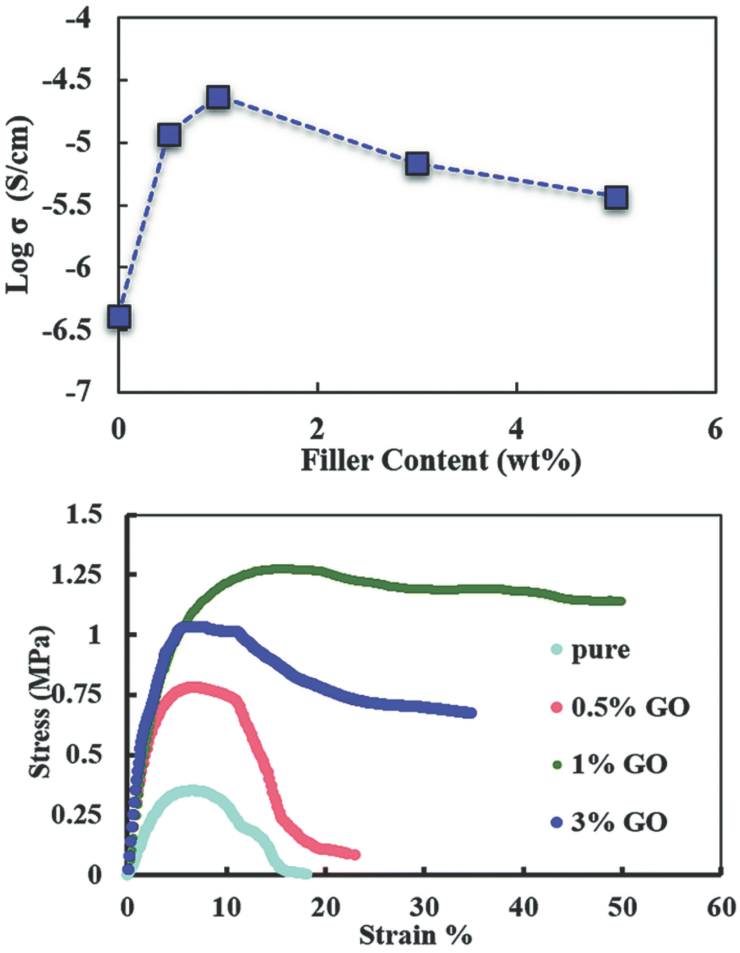

Figure 4.1. Ionic conductivity and mechanical strength enhancement of different grapheme-oxide content in PEO-based solid polymer electrolyte [204].

Figure 4.1 shows the result of the ionic conductivity and tensile tests. For the solid polymer electrolytes with different GO contents, the one containing 1 wt% GO has the maximum ionic conductivity (~10^{-5} S cm^{-1}) which is about two orders of magnitude enhancement compared to that of unfilled solid polymer electrolyte fabricated in our lab (~10^{-7} S cm^{-1}). In addition, the tensile strength of the nanocomposite polymer electrolytes was found to increase compared to that of the unfilled one. The electrolyte with 1 wt% GO has an ultimate tensile strength of 1.27 MPa which is more than 260% improvement in the tensile strength of the unfilled electrolyte (0.35 MPa).

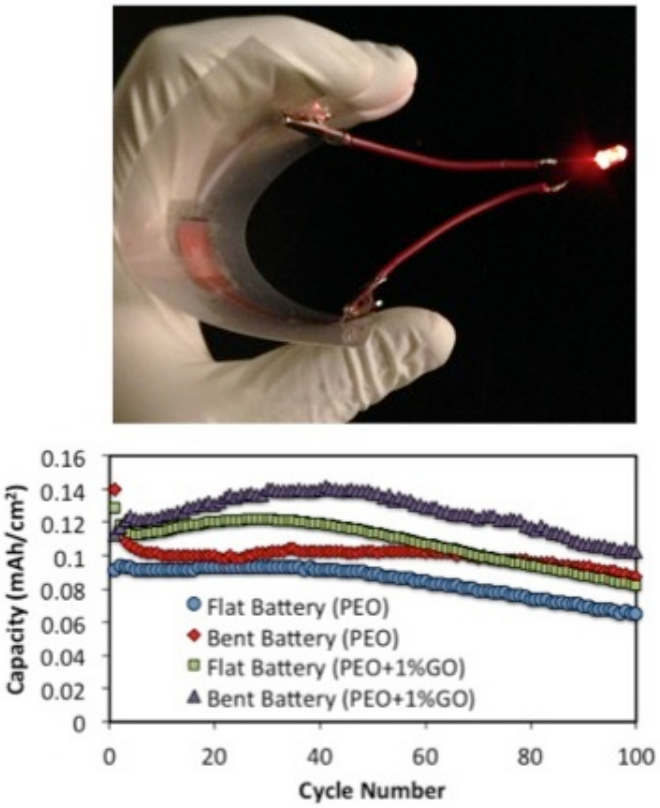

Figure 4.2. A photograph of the laminated flexible lithium ion battery and discharge capacities of two batteries made with different solid polymer electrolytes in flat and bending conditions (Courtesy of Mejdi Kamoun).

Many designs of flexible batteries came out in past decades. Various electrolytes including ceramic solid electrolyte, paper-based electrolyte, and gel polymer electrolytes have been involved in those designs. Since the above PEO-$LiClO_4$-GO nanocomposite polymer electrolyte has shown promising properties, its application in flexible lithium ion batteries is also of interest. This has also been investigated in our group by another PhD student, Mejdi Kammoun [207]. In his study, an economical and scalable thermal laminating process has been used to fabricate thin, flexible lithium ion batteries. In the method, all the layers of the battery are stacking in appropriate order and encapsulated by two thermal adhesive plastic sheets through the laminating machine. Batteries with pristine and graphene oxide filled solid polymer electrolytes were fabricated and their performance have been discussed. Figure 4.2 shows the discharge capacities of flexible batteries made with filled and unfilled solid polymer electrolytes. It can be seen that all the batteries have relatively stable capacity retention up to 100 cycles no matter they are bent or not. We can also observe some differences. First, the battery made with the GO-filled solid polymer electrolyte has higher capacity than the one made with unfilled electrolyte in both flat and bent conditions. This is corresponding to the ionic conductivity results of those two electrolytes. The GO-filled electrolyte has higher ionic conductivity so that he internal resistance of the battery is lower which is important for the battery to approach the maximum capacity. On the contrary, the internal resistance of the battery made with the pristine solid polymer electrolyte would be higher. Larger internal resistance made the battery reach the cutoff voltage faster so the battery would exhibit lower capacity. Second, for the same battery the capacity measured in bent condition is higher than the capacity measured when the battery is flat. This is opposite

with the results from the all-solid-state flexible lithium ion battery made with ceramic solid electrolyte. The reason was revealed by the finite element analysis. For the multilayers structure the contact pressure between the layers will increase as the bending radius decreases. The high contact pressure would reduce the interfacial resistance between the solid polymer electrolyte and the solid electrodes. Therefor, the internal resistance of the battery could be reduced and the battery shows higher capacity.

1.2 PVDF-based solid polymer electrolytes

From the above discussion, we know that the PEO-based solid polymer electrolytes have shown promising performance for application in flexible lithium ion batteries. Also the influence of graphene oxide has been reflected by the capacity difference of the two flexible batteries made with unfilled and filled solid polymer electrolytes. The battery made with GO filled electrolyte has higher capacity compared with the one made with unfilled electrolyte. It is interesting to explore other potential solid polymer electrolytes. In addition to PEO, Poly(vinylidene fluoride) (PVDF) is another commonly used polymer in the field of lithium ion battery. In this chapter, we chose the PVDF as the alternative polymer matrix to make solid polymer electrolytes. The properties of such solid polymer electrolyte and the performance of the lithium ion battery made with that electrolyte will be discussed.

Poly(vinylidene fluoride) has been known since the 1960s and it is a widely used polymer for many applications [208]. In the field of lithium-ion battery, PVDF is usually used as the binder to fabricate electrode slurry. Also, it has been found to be a promising polymer host for gel electrolytes. However, due to its high crystallinity it is usually

copolymerized with hexafluoropropylene (HFP) to enlarge the amorphous regions [69]. The resulting copolymer, PVDF-HFP, has been intensively studied as the most popular polymer host in the preparation of gel polymer electrolytes [67, 68, 209, 210]. In those electrolytes, the ion transport relies on the liquid phase and the PVDF-HFP simply provides the mechanical support. On the other hand, the PVDF-based material also has potential application in solid polymer electrolyte due to some appealing properties. It has strongly electron-withdrawing functional group –(C-F)– which makes it highly anodic stable. Also, its comparatively high dielectric constant (ε=8.4 with ε=5 of PEO) can facilitate the lithium salt dissociation, and thus release more free ions [63]. In addition, like in the case of PEO-based solid polymer electrolytes, incorporating nano-sized fillers with PVDF-based solid polymer electrolytes are found to enhance the ionic conductivity[211, 212]. Based on the above properties we expect that the PVDF-based solid polymer electrolytes would have compatible performance with the PEO-based solid polymer electrolytes and could be applied to lithium ion batteries.

However, the ionic conductivity results of the PVDF-based solid polymer electrolytes in some references are "unusually" high. The ionic conductivity of the PVDF/$LiCoO_2$/TiO_2 membrane at room temperature has been reported to be at the level of 10^{-4} S/cm even it contains no TiO_2 and the maximum ionic conductivity is obtained when it contains 10 wt % TiO_2 [211]. This is about one order of magnitude higher than the ionic conductivity of PEO-based solid electrolytes. The validation of the ionic conductivity results will also be discussed.

2. Experiments

2.1 Preparation of the solid polymer electrolyte

The preparation of the PVDF-based solid polymer electrolytes is following the general solution-casting method. First, PVDF-HFP (Mw=400,000, purchased from Sigma Aldrich) and $LiClO_4$ (Sigma Aldrich) are added into the *N,N*-Dimethylformamide (DMF, Sigma Aldrich). The weight of the $LiClO_4$ is calculated based on the weight of the PVDF-HFP according to the different concentration. The mixture is stirred on a hot plate at temperature of 50 °C for 24 hours to ensure the complete dissolving of the materials. Then, the homogenous solution is poured into a glass petri-dish and placed in a vacuum oven at a temperature of 50 °C to allow the evaporation of the DMF. Finally, the thin film solid polymer electrolytes are obtained. The electrolytes are peeled off from the petri-dish for future testing. In order to investigate the influence of the residual solvent on the ionic conductivity, we measured the ionic conductivity of the same electrolyte sample after different drying durations. Basically, we first set different drying durations (1 to 5 days). Then, we take the sample out of the oven for testing after the first drying duration (1 day) is reached and then we put it back in the oven. When the second drying duration is up, we repeat the above process. Therfore, we can obtain the change of the properties of the prepared electrolytes as drying duration increases to examine if there is a significant influence of the residual solvent.

The preparation of filled solid polymer electrolyte is the same with the above procedures except for the addition of the nanofiller. TiO_2 nanorod (Sigma Aldrich) has

been used as the nanofiller. In order to obtain good dispersion of the nanofiller, it should be added into the DMF first and 1 hour of sonication is necessary to facilitate the dispersion.

2.2 Ionic conductivity measurement

The ionic conductivity of the prepared electrolyte was measured by the electrochemical impedance spectroscopy (EIS) using Autolab, Metrohm. First, the electrolyte was punched to small circular-shape samples. Then, the sample was sandwiched by two stainless circle block electrodes which have the same radii as that of the electrolyte sample. The whole setup was placed in a holder with a clamp on it to ensure intimate contact between the electrolyte sample and the block electrodes. An alternating current signal with frequencies from 500 kHz to 10 Hz was applied to the system during the testing. In addition, the geometry information (thickness and the surface area) of the electrolyte sample was measured to calculate the ionic conductivity.

2.3 Battery assembly and testing

The standard CR2032 coin cell battery was assembled to test the performance of the PVDF-bases solid polymer electrolytes. All the components of the coin cell (case, separator, spring, and the electrodes) were purchased from MTI Corporation. The cathode is $LiCoO_2$ coated onto aluminum foil and the anode is graphite coated onto copper foil. This electrode pair is the most common one used for lithium ion batteries. To assemble the battery the electrodes and the electrolyte film are first punched into small disks. The cathode and anode should have the same size, and the size of the electrolyte should be

slightly larger than that of the electrodes to prevent physical contact. Two drops of liquid electrolyte (1 M $LiPF_6$ in EC+DMC+DEC from MTI Corporation) is deposited on the surface of each electrode to reduce the surface resistance. Because of the porous structure, the electrodes will absorb the added liquid electrolyte. After that, the cathode disk is placed inside the positive case of the battery with the aluminum side down. Other components are stacked on top of the cathode in the order of electrolyte, anode, spacers, spring and the negative case. The graphite side of the anode should be toward the electrolyte and all the above different parts should be concentric. Finally, the battery is sealed using the clamping machine.

To test the cycle performance the battery is placed in a holder and connected to the Arbin battery test equipment. The constant current procedure is used to charge and discharge the battery. The current is controlled to be 0.1mA and the voltage range is from 2.5 V to 4.7 V. Based on the time of charge and discharge the capacities can be obtained.

3. Results and discussion

Figure 4.3 shows the ionic conductivity of PVDF-based solid polymer electrolytes with various contents of lithium salt. For each electrolyte, its ionic conductivity was measured after different drying durations. It can be seen that for all the solid polymer electrolytes the ionic conductivity decreases with the increase of the drying duration. For the electrolyte containing 10% lithium salt, the ionic conductivity reduced nearly one order of magnitude after drying in the oven for three days. This reduction of ionic conductivity may indicate that there was a small amount of solvent left in the polymer

matrix. With increased drying duration, the amount of residual solvent would decrease leading to lower ionic conductivity. We can also observe that for all the electrolytes the ionic conductivity drops fast in the first three days and then it remains at a relatively stable level. This implies that the three days of drying is a minimum suggested drying time for the PVDF-based solid polymer electrolytes.

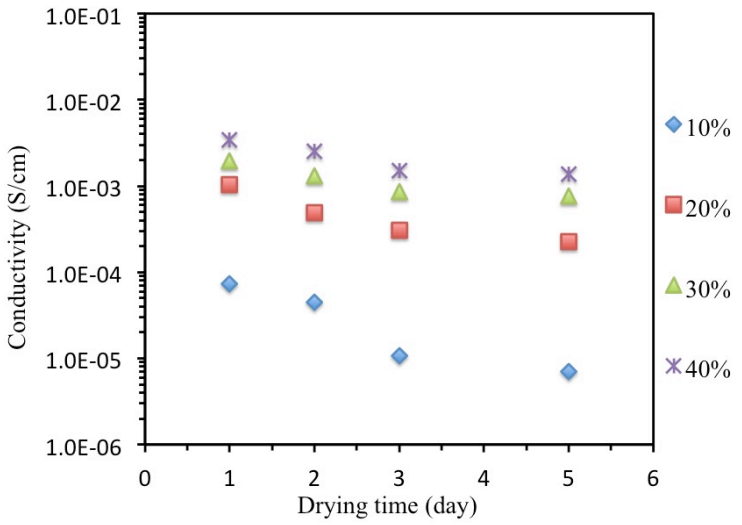

Figure 4.3. Ionic conductivity decreases with the drying time increases.

A possible way to examine the residual solvent in the solid polymer electrolyte is to monitor their weight loss for different drying durations since the PVDF-HFP and the lithium salt are not volatile. The results for the electrolytes with 10% to 40% lithium salt are shown in Figure 4.4. For the solid polymer electrolyte with 40% salt its weight after five days drying is only 80% of its weight after one day drying. This weight loss is smaller for the electrolyte with only 10% lithium salt. Actually, from Figure 4.4 we can observe the trend that the weight loss is more significant for electrolytes containing high weight percentage of lithium salt. This might be attributed to the nature of the lithium salt

that has a tendency to absorb the solvent. Thus, more residual solvent would be found in the electrolyte. This conclusion can also explain the unusually high ionic conductivity observed in Figure 4.3. The ionic conductivity is around 1.0×10^{-3} S/cm for high lithium salt content electrolytes. This is a relatively high value for solid polymer electrolytes. From the weight loss experiment, we would consider increased ion conductivity as a result of residual solvent rather than the high ion concentration.

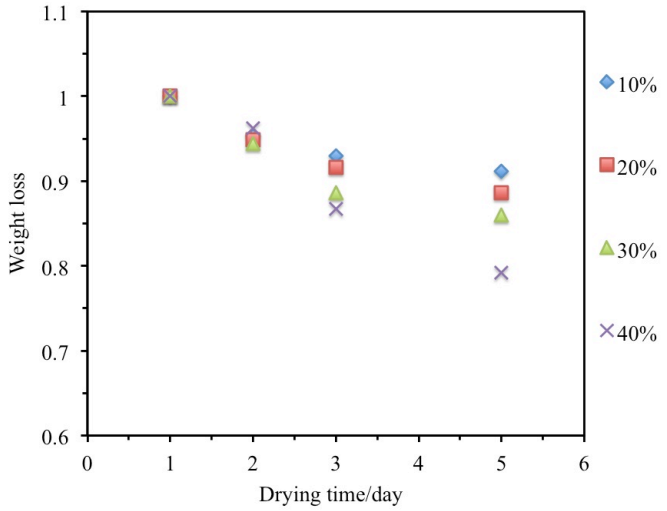

Figure 4.4. Weight loss of solid polymer electrolytes with the drying time increases.

As mentioned before, the additional nanofiller could enhance the ionic conductivity of solid polymer electrolytes by increasing the amorphous phase and increasing the number of free ions. This effect has been confirmed in the PEO-based solid polymer electrolyte with graphene oxide nanosheet as the filler in our lab. Figure 4.5 shows the ionic conductivity comparison of TiO_2 nanorod filled dry PVDF-based solid polymer electrolyte and its unfilled counterpart. It can be seen that the ionic conductivity has been enhanced nearly 1 order of magnitude because of the nanofiller. This is similar to the

result of PEO-based solid polymer electrolytes. This similarity implies that the ion transport in these two polymer hosts has the same mechanism. Thus, the added nanofiller could enhance the ionic conductivity in the same manner as discussed in Chapter II. However, the effect of residual solvent is also observed in the nanocomposite electrolyte. After four days of drying there was a big drop of the ionic conductivity.

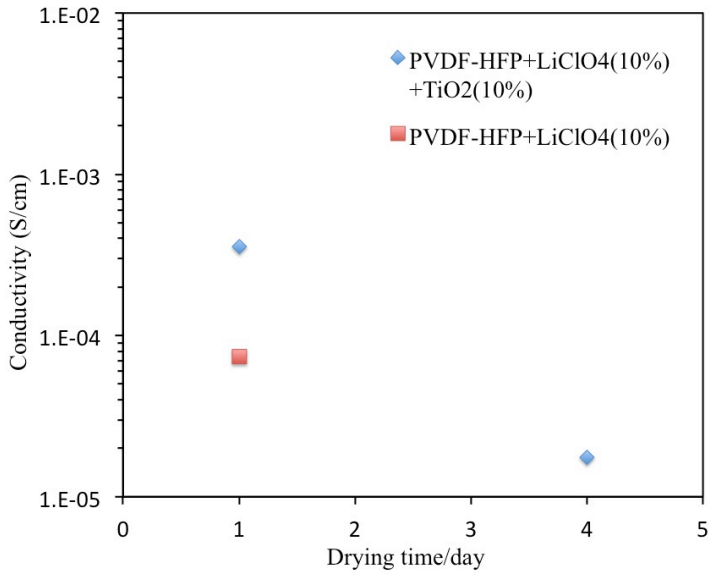

Figure 4.5. Comparison of ionic conductivity of PVDF-based solid polymer electrolyte with and without nanofiller.

The influence of the residual solvent can also be observed in the Nyquist plot of the electrolytes. The Nyquist plot is obtained from the electrochemical impedance spectroscopy. Since the impedance is usually represented as a complex number it has a real part and imaginative part. In the Nyquist plot, the real part of the impedance is the x-axis and the negative of its imagination part is the y-axis. In such plot, each data point represents the impedance of the measured system at certain frequency. Those data points could be fitted by an equivalent circuit [213] consisting of resistors, capacitor and other

elements, and then the information about the system can be obtained. Our ionic conductivity measurement is based on the Nyquist plot. From the equivalent circuit we can obtain the resistance of the electrolyte (R_E) and then the ionic conductivity can be calculated by the following equation

$$\sigma = \frac{t}{R_E A}, \qquad (4.1)$$

where t is the thickness of the electrolyte and A is its surface area.

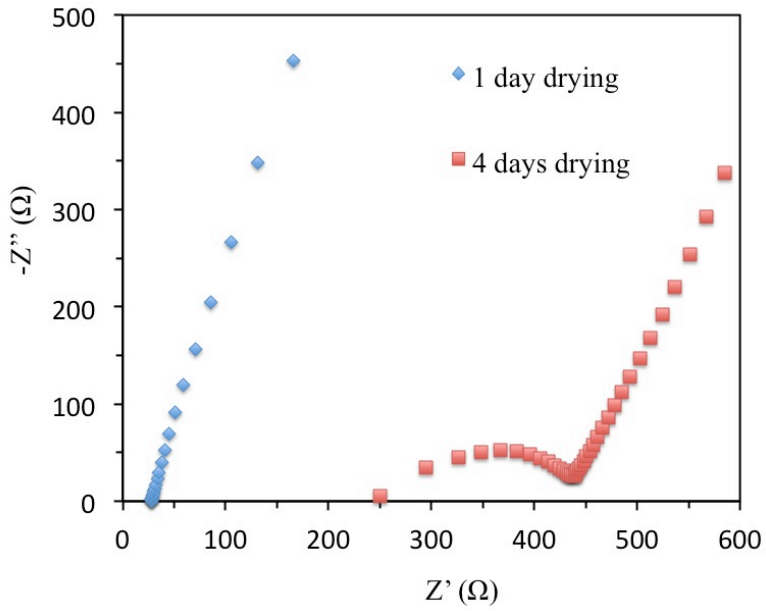

Figure 4.6. Nyquist plots of PVDF-based polymer nanocomposite electrolyte after different drying duration.

Figure 4.6 shows two Nyquist plots for the PVDF-based polymer nanocomposite electrolyte after different drying times. For shorter drying duration (1 day) the Nyquist plot is a straight line through the whole testing frequency range which is typical for gel polymer electrolytes. This might be another evidence that there was some solvent left in

the electrolyte. However, after four days drying the Nyquist plot of the same sample became a depressed semicircle followed by an inclined line. This shape is commonly observed in the PEO-based solid polymer electrolyte. The change of the Nyquist plot represents the transformation of the PVDF-based polymer nanocomposite electrolyte from gel-like ionic conductor to solid-like ionic conductor.

The charge/discharge capacities for 50 cycles of a coin cell battery based on the PVDF-based solid electrolyte are shown in Figure 4.7. The capacity of a battery is the amount of the charge that can be stored/delivered by the battery. In the case of constant current charge/discharge, it could be calculated by the following simple equation

$$Q = It\ , \qquad (4.1)$$

where Q is the capacity and I is the magnitude of the constant current and t is the time duration for the charge and discharge processes.

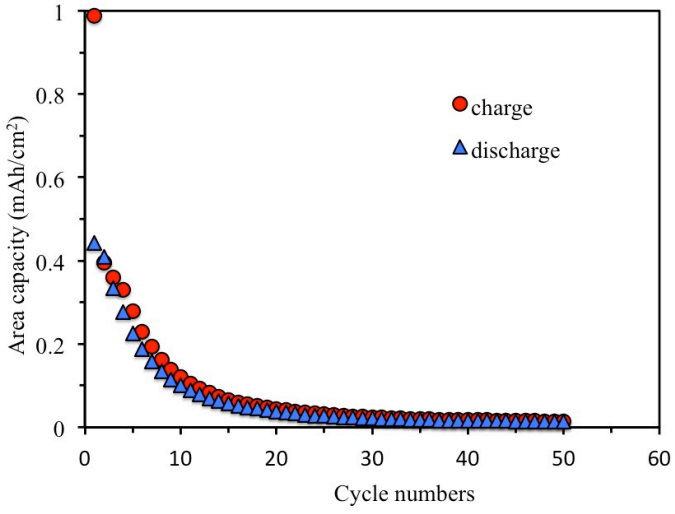

Figure 4.7. Charge/discharge capacities of the coin cell battery made with PVDF (90%)-based solid polymer electrolyte.

It is clear that there are some irreversible reactions present during the first several charge/discharge cycles. Especially in the first cycle, the discharge capacity is less than half of the charge cycle. This significant capacity loss could be attributed to the SEI formation since liquid electrolyte was added in order to reduce the interfacial resistance. This has also been observed in the batteries made with PEO-based solid polymer electrolyte. However, for the battery made with PEO-based solid polymer electrolyte the large capacity loss was only observed in the first cycle and after that the capacity changed slowly (Figure 4.2). The capacity finally became relatively stable although other aging effects (like the degradation of the electrodes) would still cause the decrease for long runs. Thus, the battery is able to deliver a stable power. In the battery made with PVDF-based solid polymer electrolyte after the huge drop in the first cycle, the capacity kept dropping fast until it went down to almost zero. The power delivered by the battery is very unstable and the battery can only work for very few cycles (~10). This difference indicates that some other reaction rather than the SEI formation might have taken place during the charge and discharge cycle. The residual solvent might be the source of those reactions.

4. Conclusions

In this chapter, we have introduced the flexible lithium ion batteries made with PEO-based solid polymer electrolytes. The result shows that those batteries can deliver a stable power when undergoing mechanical deformation. For that solid polymer electrolyte, the addition of the two dimensional nanofiller—graphene oxide—could increase the ionic

conductivity up to 2 orders of magnitude. The flexible battery made with such filled electrolyte also has shown enhancement discharge capacity.

On the contrary, the lithium ion battery made with PVDF-based solid polymer electrolyte has shown different results. In the first several cycles, especially the first cycle, the battery could deliver relatively high capacity. However, it was accompanied with significant decay of capacity. This is because of the side reactions inside the battery. For the PVDF-based solid polymer electrolyte made with DMF solvent we have observed the increased weight loss and decreased ionic conductivity during the five days drying. The change on weight and the ionic conductivity indicated that there might be residual solvent inside the electrolyte and the amount of the left solvent was found to increase with the salt concentration in the electrolytes.

In addition, low ionic conductivity is still a great obstacle for the application of solid polymer electrolytes. The unusual high ionic conductivity ($\sim 1.0\times10^{-3}$ S/cm) of PVDF-based solid polymer electrolyte is attributed to the trapped solvent. In order to obtain higher performance of the battery, gel electrolyte will be discussed further in the next chapters.

Chapter V Gel Polymer Electrolytes for Flexible Lithium Ion Batteries

1. Overview

In the previous chapter, we discussed the solid polymer electrolytes and their applications in flexible lithium ion batteries. The flexible lithium ion batteries made with PEO-based solid polymer electrolytes could deliver a stable capacity in both flat and bent conditions. This capacity could be further enhanced with adding nanofiller (graphene oxide) in the electrolyte due to the induced ionic conductivity enhancement. On the contrary, the battery made with PVDF-based solid polymer electrolyte showed significant capacity degradation and the capacity dropped to almost zero after 10 charge and discharge cycles. In this chapter, we will investigate the application of PVDF-based gel polymer electrolytes.

1.1 Gel polymer electrolytes

Gel polymer electrolytes are characterized by higher room temperature ionic conductivity compared to solid electrolytes and better mechanical properties compared to liquid electrolytes. Therefore, they are expected to have optimized performance. Gel electrolytes are usually obtained by incorporating polymer with a large amount of liquid electrolyte. [63, 214] In those mixtures, the polymer acts as the skeleton to offer mechanical support and stores the liquid electrolyte. It has almost no contribution to the ionic conductivity. The ion transport is mainly governed by the liquid phase electrolyte.

Owing to this bi-phase feature, the ionic conductivity of gel electrolyte is competitive with liquid electrolyte and it is largely decided by the amount of liquid electrolyte stored in the polymer matrix. During the past several decades, various polymers including poly(ethylene oxide) (PEO) [100, 215], polyacrylonitrile (PAN) [198, 216], Poly(methyl methacrylate) (PMMA) [217, 218], and Poly(vinylidene fluoride-co-hexafluoropropene) (PVDF-HFP) [209, 219] have been intensively studied as the polymer matrix for gel electrolytes. Among them PVDF-HFP-based gel polymer electrolytes exhibit excellent mechanical properties as well as high ionic conductivity ($>10^{-3}$ S/cm) thus became the majority in this field.

There are two different methods to produce the PVDF-based gel polymer electrolytes. The first one is the general solution-casting method. In this method, all the components including PVDF-HFP, organic liquids (e.g., EC, PC) or other types of liquids, and lithium salt are added to some common solvent like acetone. During long time stirring all the materials are dissolved in the solvent and completely mixed. Then the solution is ready for drying. The solution could be casted on some flat, smooth substrate like glass petri dish. Because of the high volatility of the solvent, it will evaporate fast and a freestanding film with distributed liquid phase in it could be obtained. This method is very simple and the produced gel polymer electrolytes are stable. The liquid phase is well trapped in the polymer matrix and almost no obvious liquid could be found on the surface. On the contrary, this method would be more affected by the fabrication environment since the lithium salt, which will absorb moisture, is added to the solution at the beginning. Also,

the “dry” surface would result in relatively high electrode-electrolyte interfacial impedance.

In another method the PVDF-HFP itself is first dissolved in the solvent with some non-solvent liquid (e.g., butanol) to allow the phase separation. In the drying process the solvent will evaporate first and then the non-solvent will be removed using future drying or other method like water bath. The obtained PVDF-HFP film has a porous structure which is similar to the commercial separator. Then, that film should go through the so-called activation process where it will be soaked in a liquid electrolyte. Thus, the liquid electrolyte will flow into the pores and the film becomes ionic conductive. The advantage of this method is that all the steps except the activation could be done in a general environment and it is suitable for large-scale manufacturing. However, in this method the amount of liquid electrolyte is difficult to control. Too little liquid electrolyte cannot produce high ionic conductivity and too much liquid electrolyte will loss the benefits of gel polymer electrolytes.

1.2 Influence of nanofillers

The influence of nanofillers on the ionic conductivity of solid polymer electrolytes has been largely demonstrated in literature and also confirmed by experimental results from our lab. The additional nanofillers could increase the ionic conductivity for both PEO- and PVDF- based solid polymer electrolytes. For PVDF-based gel electrolytes the addition of nanofiller also has been found to have some influence on their properties [220]. Experimental results show that because of the different ion transport mechanism compared to the solid polymer electrolyte, the influence of nanofiller on the ionic

conductivity of the gel polymer electrolyte is not obvious. However, the nanofiller can increase the thermal stability of the gel polymer electrolytes. In addition, the composite gel polymer electrolyte is more compatible with lithium metal electrode which is indicated by the slower growth of the interfacial impedance in the EIS.

1.3 Flexible lithium ion batteries using gel polymer electrolytes

There are some designs of flexible lithium ion batteries using different gel polymer electrolytes. *Sheng Xu* et al*.,* developed a stretchable lithium ion battery with self-similar interconnects and a PEO-based gel polymer electrolyte has been used in their battery [80]. The gel polymer electrolyte consisted of 100 g lithium perchlorate ($LiClO_4$), 500 ml ethylene carbonate, 500 ml dimethylcarbonate (DMC) and 10 g polyethylene oxide (4,000,000 g/mol). From the formulation we can seen that the content of PEO is only at additive level. It would be expected that this gel polymer electrolyte would have a relatively higher fluidity. This is required by their specific design in which the electrolyte would be injected into the battery through the edge by a syringe. The battery could be stretched up to 300%. However, the capacity drop (<70%) after 20 cycles has been observed. The authors attributed that degradation to the side reactions caused by the residual water and the detaching of the active materials from the current collector.

Another example is the study reported by *Liangbing Hu and coworkers.* They designed a thin, bendable battery through a simple lamination process. The electrolyte used in their battery is composed of a piece of paper with a thin layer of PVDF coated on both side. Then 1 M solution of $LiPF_6$ in EC/DEC (1:1 in volume) was used to active the

electrolyte [79]. From the detailed description in the study, this battery is a pouch-like battery which has similar structure with that of the conventional batteries except the flexible encapsulation. The cycle performance of the battery has shown relatively low capacity loss. However, the battery was clamped during the test to ensure good contact between different components of the battery. It can be informed from these two examples that the lack of enough compressive pressure, which is one of the major differences between a flexible battery and a coin cell battery, would result in low capacity retention.

In this chapter, different gel polymer electrolytes based on the PVDF-HFP polymer have been fabricated using the solution casting method. The dependence of ionic conductivity on the composition of those gel polymer electrolytes was discussed. Graphene oxide nanosheet, as the filler, has been added to the electrolyte to investigate the influence of nanofiller in this type of electrolytes. The performance of coin cell batteries made with both filled and unfilled gel polymer electrolytes were compared. In addition, results of the attempt to fabricate flexible lithium ion batteries with the PVDF-HFP gel polymer electrolyte are discussed.

2. Experiments

2.1 Preparation and characterization of gel polymer electrolytes

The gel electrolyte was prepared in our lab by the solution-casting method: 1) add 1 gram PVDF-HFP (Mw=400,000, purchased from Sigma Aldrich) in 20 mL acetone and put the mixture on a hot plate for stirring at about 80 °C for 1 hour, the weights of other materials are calculated based on the weight of PVDF-HFP according to the formulation;

2) after the PVDF-HFP is dissolved add graphene oxide nanosheets (only for the filled electrolytes) to the solution and sonication the mixture for 30 minutes; 3) add LiClO4, EC and PC (V_{EC}:V_{PC}=1:1) to the mixture and keep it stirring at about 50 °C for 2 hours; 4) pour the viscos solution into a glass petri-dish to allow the acetone to slowly evaporate. After drying for 4 hours a freestanding, thin-film electrolyte was formed.

Due to the volatility of the EC and PC, the ionic conductivity measurement was performed right after the fabrication of the gel polymer electrolytes. Autolab (Metrohm) was used to obtain the electrochemical impedance spectroscopy (EIS) for ionic conductivity calculation. The frequency range was 100 kHz - 10 Hz.

2.2 Battery assembly and the performance testing

Coin cell batteries are assembled following the same procedure described in Chapter IV. Common lithium-ion battery components including cathode ($LiCoO_2$ on aluminum foil), anode (graphite on copper foil), and liquid electrolyte (1M $LiPF_6$ in EC/DMC/DEC) were purchased from MTI Corporation. The electrodes and the electrolyte film are punched to small circles and stacked in order, inside the battery case. Three drops of liquid electrolyte (1 M $LiPF_6$ in EC+DMC+DEC from MTI Corporation) is painted on the surface of each electrode to reduce the surface resistance. Then, the battery is sealed using the clamping machine. Cycle performance of the coin cell battery was tested by Arbin battery test equipment. The charge/discharge current is 0.5mA (~0.2C) and the voltage range is from 2.7 V to 4.2 V.

The flexible batteries were made using the same materials as in the coin cell battery. The cathode and anode were cut into 2 cm×2.5 cm rectangles. Two small adhesive copper strips were attached to the metal side of each electrode, respectively. A piece of the unfilled gel polymer electrolyte was sandwiched between the two electrodes. Then, the cell was sealed between two plastic sheets with silicone to prevent any moisture into the battery. The two copper strips should be exposed to connect to the test equipment. The cycle performance test of the flexible battery was split into three stages. In order to rule out the environmental factors, the fabricated flexible battery was first tested inside the glove box for 10 charge/discharge cycles. In addition, the battery was clamped to apply pressure and ensure good electrical contact. Then, the clamp was released from the battery and the battery was kept in the glove box for 5 cycles. Finally, the battery was taken out of the glove box and tested for the rest of the cycles. We will refer to this battery as FLB1. Another battery, denoted by FLB2, was made in the same way but it was tested inside the glove box and without the clamp through all the cycles. The current density was 0.3 mA/cm^2 (~0.1 C) and the voltage range was from 2.7 V to 4.2 V for all the charge/discharge cycles of the two batteries.

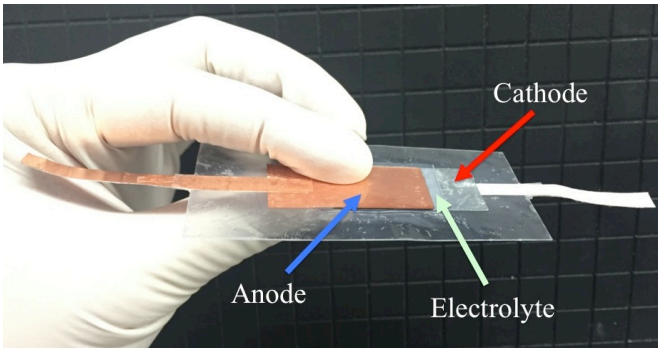

Figure 5.1. A flexible lithium ion battery made with PVDF-based gel polymer electrolyte.

3. Results and discussion

3.1 Dependence of ionic conductivity on the percentage of polymer

The amount of liquid is important to ionic conductivity of the gel polymer electrolyte. From Figure 5.2 we can see the ionic conductivity decrease significantly with the increased weight percentage of PVFDF-HFP. The ionic conductivity dropped 2 orders of magnitude when the wt% of PVDF-HFP increased from 25% to 70%. This result confirms the proposed ion transport mechanism in gel polymer electrolytes. Most of the ion conduction is carried out by the liquid phase (EC+PC) and the PVDF-HFP polymer only has very small contribution. Thus, a large drop in ionic conductivity has been observed.

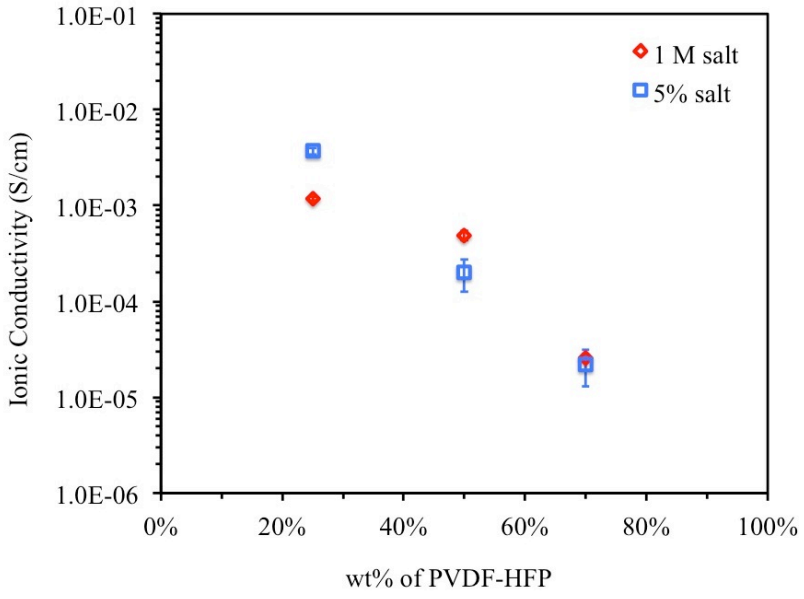

Figure 5.2. Calculated ionic conductivities of different PVDF-HFP/EC+PC/$LiClO_4$ gel electrolytes

In the formulation of gel polymer electrolytes, there are two different ways to measure the lithium salts. First is based on the concentration, usually 1 M lithium salt solution is commonly used. Another one is based on the weight percentage of the salt. It is often taken between 5% and 10% of the total weight of the electrolyte. We have explored both formulation methods and the two types of electrolytes (containing 1 M salt and 5% salt) all followed the same trend that the ionic conductivity decreases with the increase of the PVDF-HFP. However, some difference can be observed. The ionic conductivity drop for the 5% salt-type electrolyte is more dramatic than that of the 1 M slat-type electrolytes. This could be explained by the salt aggregation. In the 1 M salt-type electrolytes when the polymer weight percentage increases the amount of both the salt and the liquid will decrease to keep the constant salt concentration. On the other hand, for the 5% salt-type electrolytes only the liquid amount will decreases while the polymer content is increasing. Thus, the concentration of the lithium salt will be larger and some aggregation of the salt may occur to impair the ionic conductivity.

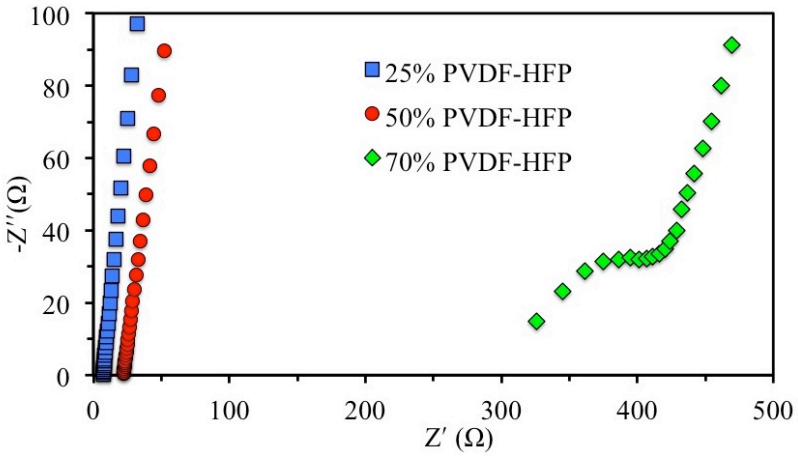

Figure 5.3. Nyquist plots of PVDF gel polymer electrolytes with different content of polymer.

Figure 5.3 shows the corresponding Nyquist plots of the 1 M salt-type gel polymer electrolytes with different polymer content. For the electrolytes containing only 25 wt% and 50 wt% PVDF-HFP their Nyquist plots have same shape, a straight line. On the contrary, the Nyquist plot for the gel polymer electrolyte with 70 wt% PVDF shows a typical solid polymer electrolyte appearance.

3.2 Influence of nanofiller to the gel polymer electrolyte

The influence of graphene oxide nanosheets on ionic conductivity of PVDF-based gel electrolytes is illustrated in Figure 5.4. For the electrolytes with different weight percentages of PVDF-HFP (25% and 50%) the added graphene oxide did not show any obvious influence on the ionic conductivity.

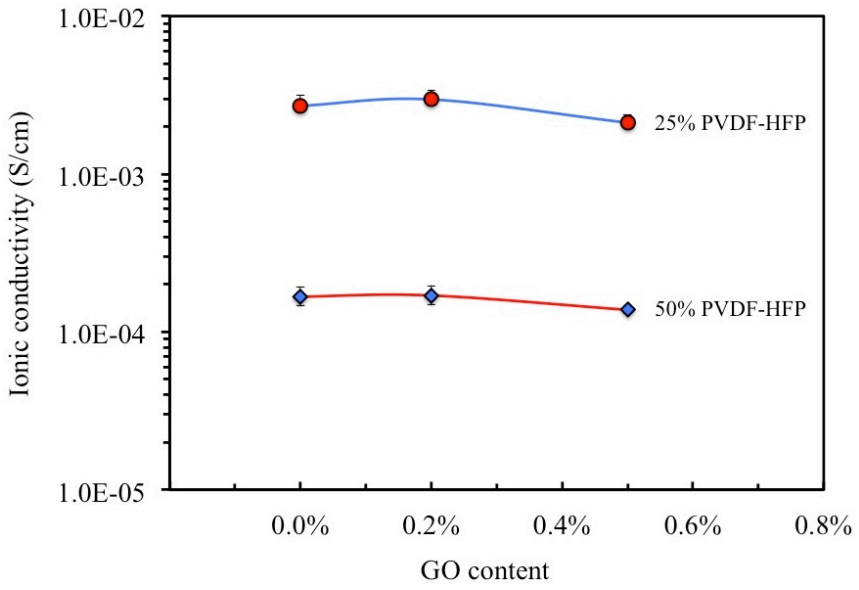

Figure 5.4. Ionic conductivity of PVDF-based gel electrolytes with different content of graphene oxide nanosheets as the filler.

This differs from the results of PEO-based solid polymer electrolytes where the embedded graphene oxide nanosheets enhanced the ionic conductivity significantly. This could be explained by the different conduction mechanisms in those two types of electrolytes. In solid polymer electrolytes the ion conduction mainly relies on the mobility of polymer chains. The nanofillers could increase the amorphous regions of polymer host and thus enhance the mobility of polymer chains and the ionic conductivity. On the other hand, ion transport in gel electrolytes is carried out by the liquid phase which would hardly be affected by the added nanofillers.

3.3 Battery performance

The cycling performances of two coin cell batteries made with GO-filled and GO-free gel electrolytes (both contain 50% PVDF-HFP) are presented in Figure 5.5. Both of the batteries could reach a high discharge capacity, 130 mAh/g for the one made with GO-filled electrolyte and 100 mAh/g for the other, at 0.2 C rate charge and discharge. They also show good capacity retention up to 30 cycles although a small drop could be observed in first few cycles. On the other hand, the Coulombic efficiency of the first cycle is relatively low for each battery. The Coulombic efficiency is defined by the following equation

$$\eta = \frac{Q_{dis}}{Q_{ch}}, \qquad (5.1)$$

where Q_{dis} is the discharge capacity and the Q_{ch} is the charge capacity. This ratio characterizes the reversibility of the electrodes. Unity is desired for it since that means all the capacity stored in the charge process can be completely delivered in the discharge

process. However, no real electrodes can reach that ideal value. This low Coulombic efficiency of the first cycle is usually attributed to the irreversible SEI layer formation during the first charge. An amount of lithium ions as well as the organic solvent (EC, PC) are consumed in those reactions. Thus the reversible capacity will drop and the generated layer on the surface of the electrodes will increase the impedance of the battery. In addition, for the battery made with gel polymer electrolyte the loss of the liquid will also reduce its ionic conductivity. All the above reasons would result in a low Coulombic efficiency in the first cycle. However, after first few cycles the Coulombic efficiency is kept at a pretty high level (> 99%) for each battery.

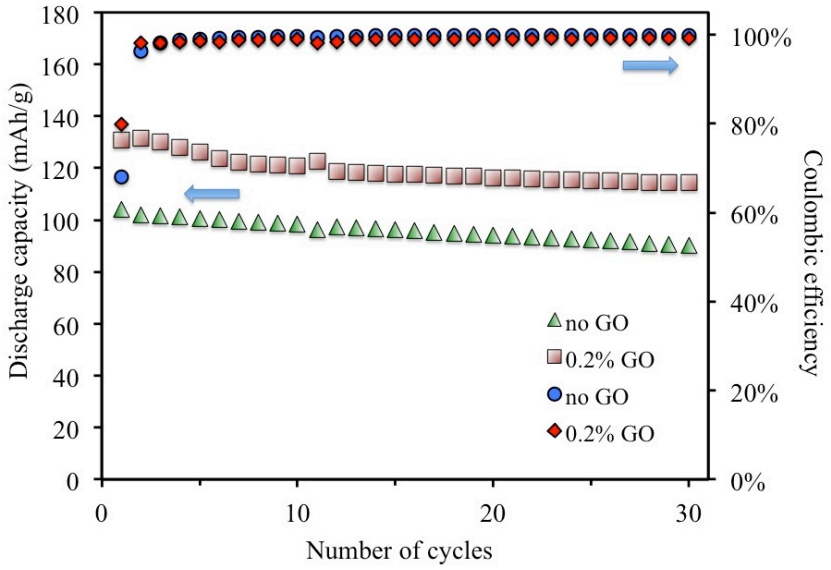

Figure 5.5. Discharge capacities and Coulombic efficiencies of two batteries made with different gel electrolytes at charge/discharge rate of 0.2C.

The above results show that the as-prepared PVDF-HFP gel polymer electrolytes are good candidates for lithium ion batteries. Thus, we expect that the flexible lithium ion battery made with the same materials as in the coin cell batteries would have similar

performance. As described in the experimental section we have made two flexible lithium ion batteries, FLB1 and FLB2, in the same manner and they were subject to different conditions while cycling.

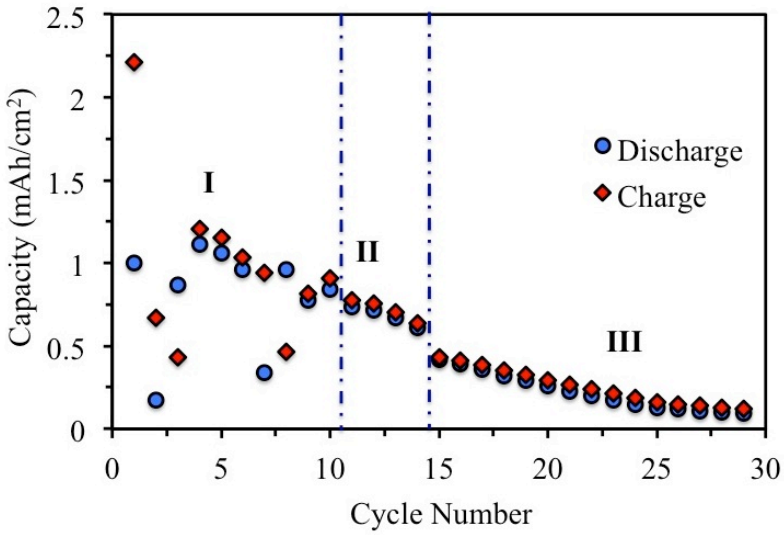

Figure 5.6. Charge/discharge capacities of FLB1 decay during cycling. I, II, III indicate the three different stages during the test as described in the experimental section, respectively.

Figure 5.6 shows the capacities of the flexible lithium ion battery (FLB1) up to 30 charge/discharge cycles. We can first observe that the capacity decreases very fast during the cycling. After 30 cycles the capacity dropped to less than 10% of the capacity of the first cycle. In the results from the first stage of the test (region I) there are some data points deviated from the trend line. Those scatterings might be the result of the non-uniformly distributed pressure applied by the clamp or some incautious vibration of the holder in the glove box. Despite those "noise points" the decay trend of the capacity is obvious and consistent throughout the three different stages. This consistency implies that the applied pressure by the clamp is not enough to prevent the degradation of the battery.

On the other hand, it also indicates that the encapsulation of the battery is sufficient to suppress large influence of the normal room environment on the battery.

The capacities of the FLB2 are given in Figure 5.7. FLB2 was tested in the glove box without applied pressure. Compared to the results in Figure 5.6, the lower capacity of FLB2 confirms the positive effect of the applied pressure to flexible batteries as mentioned before. Although it is not as high as the pressure in the coin cell that could almost prevent the degradation of the battery, it still can enhance the performance of the battery.

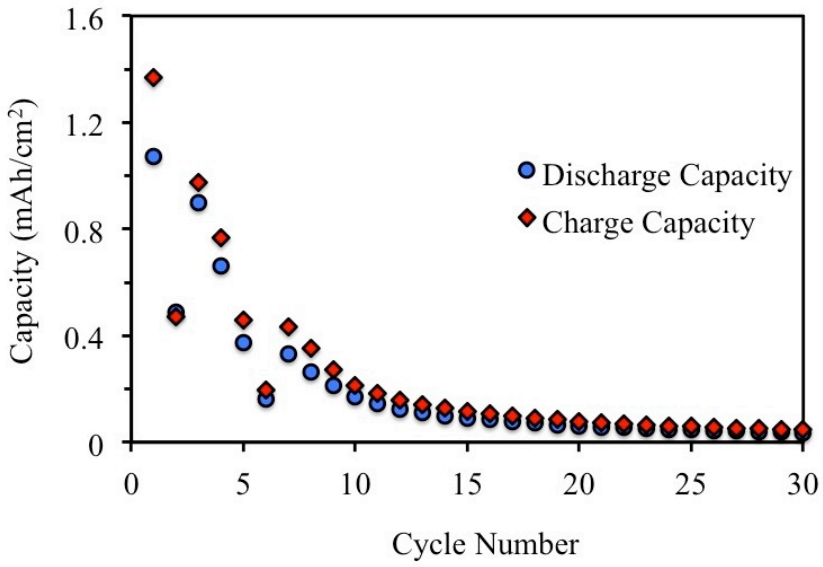

Figure 5.7. Charge/discharge capacities of FLB2 decay during cycling.

The above used gel electrolyte contains large amount of the flammable organic liquids. In order to obtain enhanced safety, we need to reduce the content of the liquids (EC+PC) inside the gel electrolyte. Figure 5.8 (a) gives the ionic conductivity of gel polymer electrolytes with different composition, one is 75 wt% PVDF-HFP/10 wt%

(EC+PC)/15% $LiClO_4$ and another is 75 wt% PVDF-HFP/15 wt% (EC+PC)/10 wt% $LiClO_4$.

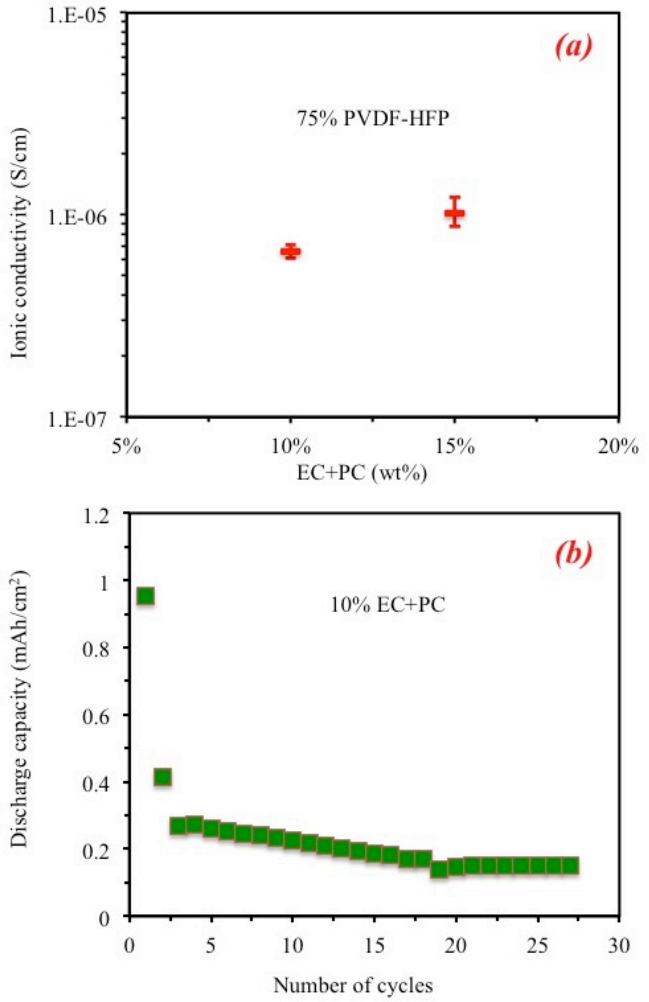

Figure 5.8. (a) Conductivity of gel polymer electrolytes with 75 wt% PVDF-HFP and (b) the cycle performance of a coin cell battery made with 10 wt% EC+PC gel polymer electrolyte.

Compared to Figure 5.2, the ionic conductivity decreased further for both electrolytes and it was higher for the one with more liquid. This confirms that the PVDF-HFP only contributes a little to the ionic conductivity since the high content of salt did not increase

the ionic conductivity even when the liquid phase is very small. Owing to the low conductivity, the capacity of the battery is much lower as shown in Figure 5.5. The large capacity loss in the first three cycles is due to the SEI formation since liquid electrolyte was added to reduce the interface impedance. As a consequence, the internal resistance significantly increased because of the lack of liquid and the generated SEI layer. However, the stable discharge capacity is around 0.15 mAh/cm^2 which is comparable to the capacity of the battery made with PEO-based solid polymer electrolytes.

4. Conclusions

In summary, we have explored the application of the gel polymer electrolytes using PVDF-HFP as the polymer host for both coin and flexible lithium ion batteries. The fabrication of such electrolytes was based on the general solution casting method. Electrochemical impedance spectroscopy was obtained to calculate ionic conductivity of those gel polymer electrolytes with different compositions. The calculated ionic conductivities of gel electrolytes with different weight percentage of PVDF-HFP show that the ionic conductivity is largely decided by the amount of liquids. In addition, the salt concentration also plays an important role. Relatively high concentration of lithium salt will impair the ionic conductivity since the ion transport through the PVDF-HFP in gel electrolytes has very little contribution to the ionic conductivity. Because of this ion conduction mechanism, the addition of graphene oxide nanosheets to the gel electrolyte did not show obvious effect on the ionic conductivity.

Owing to the higher liquid content/ionic conductivity, coin cell lithium ion batteries made with 50 wt% PVDF-HFP have shown promising performance. The discharge capacity could reach 130 mAh/g. The batteries also have good capacity retention after 30 cycles and the Coulombic efficiencies were higher than 99% during the cycling except for the first few cycles. The very low Coulombic efficiency of the first cycle is considered to be the result for SEI formation.

However, the transfer of the same materials to the flexible lithium ion battery has encountered some difficulties. The comparison of cycle performance of two flexible lithium ion batteries made with the same method reveals that the key to a successful flexible lithium ion battery is to maintain sufficient contact pressure in the battery.

Chapter VI Ionic Liquid-based Solid-like Gel Electrolyte for Flexible Lithium Ion Battery

1. Introduction

1.1 Motivation

Flexible energy storage devices offer many advantages including compatibility with the flexible electronics and flexible applications [76]; for example, they can be embedded in textiles/clothing or attached to the biological organs. Among the various energy storage devices, lithium-ion batteries (LIBs) are ideal candidates to transform into flexible devices, due to their superior attributes including higher energy density and efficiency.

In designing flexible LIBs, electrolytes play a crucial role. The common liquid electrolytes – used in many pouch-type flexible batteries – less than ideal due to the risk of leakage and lack of mechanical stability. On the other hand, solid electrolytes are superior in terms of stability and safety but their relatively low ionic conductivity results in insufficient electrochemical performance and power density. In order to develop high-performance LIBs with relatively safer electrolyte – compared to organic liquids – intense efforts have been directed toward the development of gel electrolytes. Gel polymer electrolytes are usually obtained by infusing a large amount of liquid electrolyte into a suitable polymer matrix [63, 130]. The role of the polymer matrix is mainly to store the liquid electrolyte and provide mechanical support. The ionic conductivity of a gel

electrolyte, governed mainly by the conductivity and the amount of the liquid phase, is relatively high and can be competitive with respect to that of traditional organic liquid electrolytes.

Unfortunately, because of the presence of reactive, volatile, and flammable organic solvents (e.g., ethylene carbonate (EC) and propylene carbonate (PC)), common gel electrolytes share some of the same safety concerns as that associated with liquid electrolytes [221]. To further enhance the safety of the gel electrolytes, ionic liquids can be introduced in the polymer matrix to replace the organic liquid phase [222, 223]. Ionic liquids are essentially low-melting temperature salts that remain in liquid phase at room temperature. They possess several favorable properties such as high ionic conductivity, non-volatility, non-flammability, and thermal, chemical stability [224]. Many attempts have been made to replace the traditional organic carbonates with ionic liquids in the solvent-salt and gel electrolytes [210, 225-229]. However, as discussed in a critical review, batteries with these ionic liquid-based liquid or gel electrolytes usually exhibit poor cyclic and power performance compared to those made with conventional organic solvent-based electrolytes even though their ionic conductivities are similar [230].

Although the viscosity of ionic liquids is high there is still a possibility of leakage. Incorporating ionic liquids in polymers could solve this problem. However, this will decrease the ionic conductivity of ionic liquids further. In the PVDF-ionic liquid-lithium salt electrolytes the ionic conductivity also decreases with the increase of concentration of lithium salt [219] as in the case without polymer.

1.2 Ionic liquids

Ionic liquids are molten salts composed of ions only. They are just like the ionic solids, for example, the table salt (NaCl), but with very low melting point so that they could exist as liquids at room temperature or temperatures even below that. Actually, molten NaCl could also be called as an ionic liquid. However, in the patents and academic literature the term "ionic liquids" usually refers to ionic compounds that will melt into fluids at relatively low temperature. In a more accurate definition, "ionic liquids are most commonly defined as materials that are composed of cations and anions which melt at or below 100 °C." This temperature is simply from the first paper describing an ionic liquid. It does not have any scientific significance, but it has persisted until the present day [231].

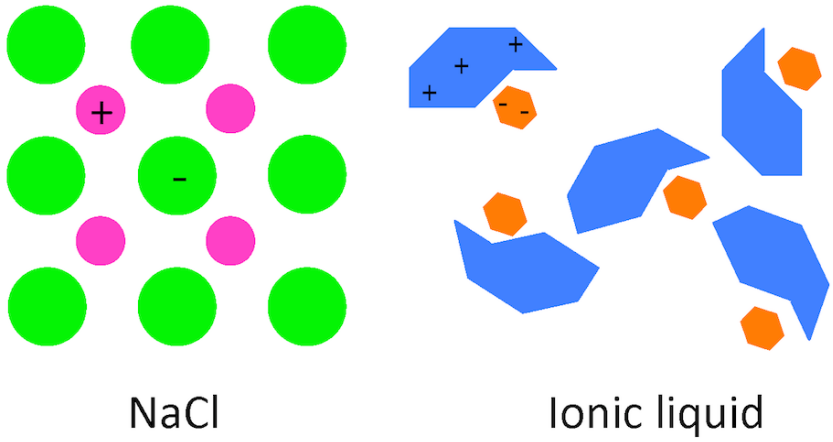

Figure 6.1. Comparison of the structures of NaCl and the ionic liquid

The unusual low melting temperature of the ionic liquids could be explained from their microscopic structure. Compared to the general salts, ionic liquids usually have

distributed charges on both cations and anions as shown in Figure 6.1. Thus, it is difficult to form very strong ionic bonds although the electrostatic force will still hold all the ions together. Therefore, their melting temperatures are much lower.

The primary application of the ionic liquids is to substitute the traditional volatile solvents for various industrial processes [232]. The term "green solvents" [233, 234] indicates the major advantage of ionic liquids. Because of their negligible vapor pressure ionic liquids minimize the risk of atmospheric contamination and reduce associated health concerns.

1.3 Ionic liquid-based electrolytes for lithium ion batteries

Ionic liquids possess several attractive properties including high ionic conductivity, thermal and chemical stability, low volatility, and non-flammability so that they are expected to overcome difficulties spanning a wide range of applications [223]. One of the applications is in the field of energy devices, such as lithium ion batteries, supercapacitors, and fuel cells. Ionic liquids and their mixtures can be excellent electrolytes owing to all the advantages above and can largely improve the stability and safety of those devices. [230]

For an electrolyte, its ionic conductivity is of great importance. The ionic conductivity is usually determined by both the concentration and the mobility of the ions. In ionic liquids those two aspects are dependent on the interactions between cations and anions. One would expect that the weak interactions could suppress the association/aggregation of the ions and also reduce the drag forces to ions' movements as

well. Therefore, high ionic conductivity could be achieved. Some studies have investigated the transport properties of ionic liquids [235-238]. Generally speaking, in order to have a high ionic conductivity, both the cation and anion of the ionic liquid should be small and bear a well-delocalized charge [235]. For the popular imidazolium-based ionic liquids the transport properties are correlated with the chemical structure. The type of the anion and the length of the alkyl chain are two key features. It has been found that increasing the size of the anion will slightly increase the diffusion coefficient of the cation. In the contrast, the conductivity and the diffusion coefficient of cation decrease with increasing alkyl chain length [236]. *Alan and coworkers* observed that the specific conductivity of ionic liquids follows Stokes law to a good approximation. Also, they found that adding solvents to the ionic liquids, would reduce the viscosity rapidly and increase the conductivity [237]. Overall, the ionic conductivity is related to the viscosity, molecular weight, density, and the radii of the ions [238].

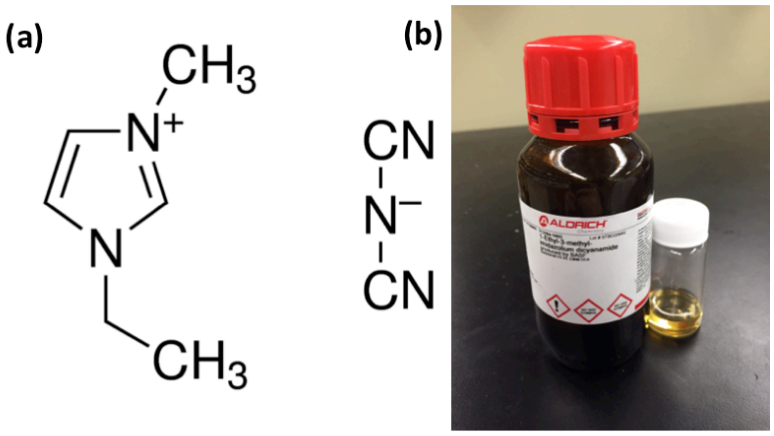

Figure 6.2. (a) Molecular structure and (b) a photograph of EMIMDCA ionic liquid purchased from Sigma Aldrich.

Among all the available ionic liquids, 1-Ethyl-3-methylimidazolium dicyanamide (EMIMDCA) is found to have relatively high ionic conductivity (27 S/cm). This could be attributed to the small size of the dicyanamide anion [239, 240]. Figure 6.2 shows the molecular structure of EMIMDCA.

However, in the application of lithium ion batteries the ionic liquids themselves could not be used as the electrolytes although they have high ionic conductivity. They must be combined with lithium salts to make the lithium ion intercalation-deintercalation at the electrodes possible as in the general liquid electrolytes. In general, liquid electrolytes based on a lithium salt dissolved in organic solvents (like EC and PC) lithium ions and anions are separated by polar solvent molecules. Then, the solvated ion and its solvation shell would move as a whole under the applied electric field. This model is also suggested in the case of using ionic liquids as the solvents [241]. Unfortunately, adding lithium salts usually will increase the viscosity and thus decrease the ionic conductivity [222]. For example, for the mixture of $EMIMBF_4$ and $LiBF_4$, when the concentration of $LiBF_4$ increases, the viscosity will also increase which results in a decrease of the ionic conductivity [242]. Another important aspect is the transport number of lithium ions. There are up to four different types of ions in the salt/ionic liquid mixture contributing to the ionic conductivity but only lithium ions are relevant for the charge and discharge process. Therefore, the ionic conductivity alone does not exactly indicate the performance of this kind of electrolyte in lithium ion batteries.

In Chapter V, we explored the application of PVDF/EC-PC/$LiClO_4$ gel polymer electrolyte in lithium ion batteries. The coin cells made with such electrolyte have shown

excellent performance. On the contrary, the flexible batteries with the same materials suffered from significant capacity decay such that they were not able to deliver a stable power. In this chapter, we aim to improve the performance of the flexible lithium ion battery by using ionic liquid-based electrolyte because of its high thermal and chemical stability.

2. Experimental

2.1 Preparation of the gel electrolyte

The electrolyte consists of 30% PVDF-HFP, 60% EMIMDCA, and 10% $LiClO_4$. It was prepared by the same solution-casting method: 1) 0.6 gram PVDF-HFP (Mw=400,000, purchased from Sigma Aldrich) was added in 20 mL N,N-Dimethylformamide (purity 99.8%, Sigma Aldrich) and the mixture was stirred at about 80 °C for 1 hour; the weights of other materials were calculated based on the weight of PVDF-HFP; 2) after the PVDF-HFP was dissolved, the EMIMDCA (Sigma Aldrich) and $LiClO_4$ (Sigma Aldrich) were added to the solution and stirred at 50 °C overnight (about 12 hours); 3) the viscous solution was poured into a glass petri-dish and placed in the vacuum oven at a temperature of 50 °C for 24 hours to allow the solvent to evaporate. Since the ionic liquid is not volatile, there is no risk of composition change of the gel electrolyte during the long-period drying. This is different for the case of volatile organic liquids in gel polymer electrolytes and the risk of compositional changes can be present. After drying, the PVDF-HFP/ EMIMDCA electrolytes were removed from the oven and placed inside the glove box for further use.

2.2 Characterizations of the electrolytes

The ionic conductivity of the electrolyte is the primary property of our concern. It can be calculated by the electrochemical impedance spectroscopy of the PVDF-IL electrolyte which could be obtained by Metrohm Autolab. The sample was sandwiched between two stainless steel electrode discs and the complex impedance spectroscopy was obtained with the frequency response analysis (FRA) module in the frequency range of 10 Hz to 500 kHz.

The thermal stability of the PVDF-IL electrolyte was examined by the thermogravimetric analysis (TGA). The experiment was performed by Q50 TGA, TA Instruments. The PVDF-IL electrolyte sample was heated from 20 to 200 °C at a rate of 10 °C/min. Then, the weight change of the sample was recorded. Thus, we can get the weight loss of the sample caused by the evaporation of the components in it.

2.3 Battery assembly

To prepare the anode first we dissolve all the materials ($Li_4Ti_5O_{12}$: Carbon black: PVDF=8:1:1, purchased from MTI Corporation) in N-Methyl-2-pyrrolidone. $Li_4Ti_5O_{12}$ is the active material which is for lithium ion de-intercalation. Carbon black is used to increase the electrical conductivity of the electrode. PVDF is the binder. The prepared slurry was coated onto the aluminum foil by a doctor blade and dried in the vacuum oven at 80 °C for 24 hours. The cathode ($LiCoO_2$ on aluminum foil with mass loading of about 12 mg/cm^2) was purchased from MTI Corporation.

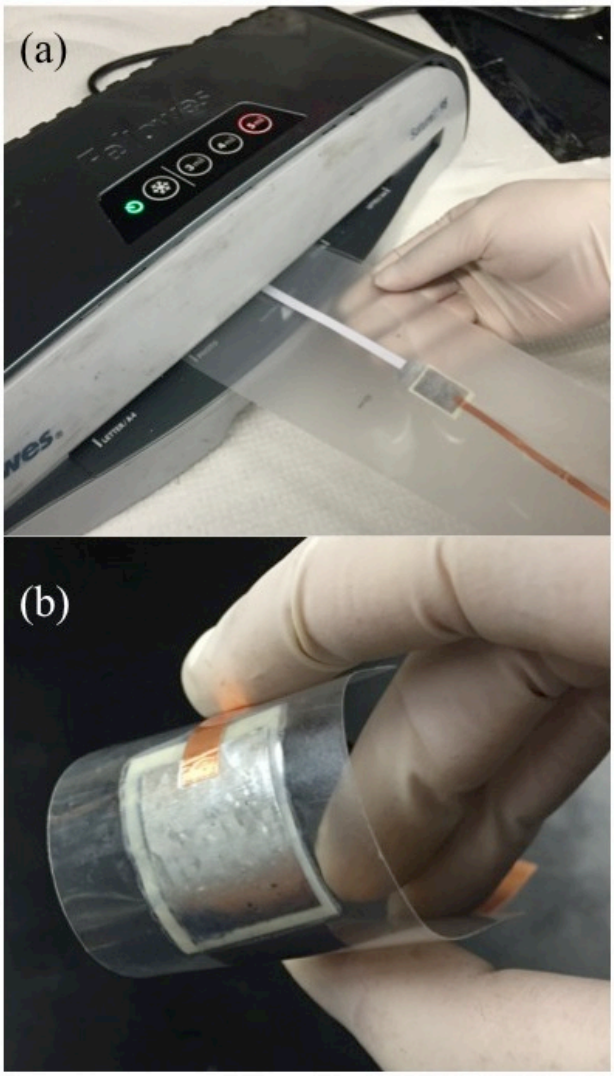

Figure 6.3. (a) All components of the lithium ion battery are stacked in appropriate order and fed to the laminating machine. (b) A photograph of the fabricated flexible lithium ion battery.

Both the cathode and anode were cut into about 1.5 cm×2.0 cm rectangles and a copper strip was placed on the aluminum side of each electrode for the electrical connection to the external devices. A piece of the PVDF-IL electrolyte was sandwiched between the cathode and anode and one drop (about 2 mg) of 1M $LiClO_4$ in EMIMDCA was spread on the surface of each electrode to further reduce the interfacial resistance.

Then, the whole cell was placed on a thermal-adhesive plastic laminating sheet and the laminating machine (Saturn SL-95 Laminating Machine, Amazon) was used to laminate the battery. Figure 6.3a shows how to use the laminator to make the battery. After the lamination process, the extra parts of the sheet were cut and removed, and the copper strips were exposed for battery testing. The fabricated battery is very thin and bendable (as shown in Figure 6.3b). In addition, it is very easy to make batteries with different shapes and sizes based on this method.

2.4 Battery testing

The cyclic voltammograms of the battery were obtained with Metrohm Autolab. The battery was connected to the equipment and a voltage profile was applied to the battery. The voltage was slowly increased from 1.5 V to 2.8 V at a scan rate of 0.05 mV/s. When the voltage reached the maximum it would go back down to the 1.5 V at the same scan rate. We tested three such cycles to obtain information about the electrode reactions.

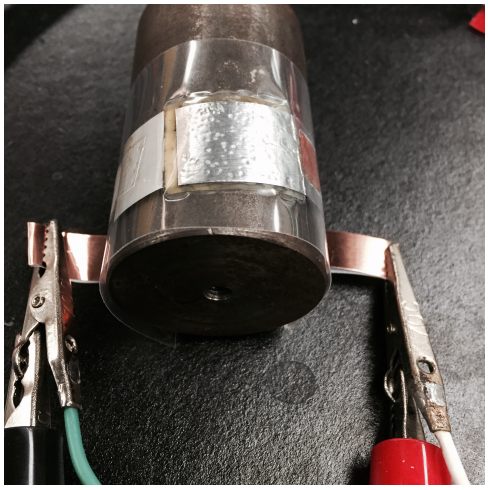

Figure 6.4. The battery is wrapped around a steel cylinder of two cm radius for testing.

The cycle performance of the battery was tested by Arbin battery test equipment at a constant current density of 35 mA/mg (0.25 C of $LiCoO_2$) in the voltage range of 1.6 V to 2.7 V. The battery was first tested in the normal/flat condition. To evaluate the electrochemical performance of the laminated battery in bending condition, the battery was wrapped around a 2 cm radius steel cylinder (as shown in Figure 6.4).

3. Results and discussion

3.1 Properties of the PVDF-IL electrolyte

Figure 6.5a shows a sample of the obtained freestanding gel polymer electrolyte film composed of polyvinylidene fluoride-co-hexafluoropropene (PVDF-HFP), **1-**Ethyl-3-methylimidazolium dicyanamide (EMIMDCA) ionic liquid and $LiClO_4$ lithium salt. It appears as a solid material although it contains 60 wt% ionic liquid. The properties of the solid-like gel polymer electrolyte (PVDF-IL hereinafter) including microstructure, ionic conductivity, and thermal stability were examined.

Due to the micro-porous structure of PVDF-HFP, the liquid phase — ionic liquid combined with dissolved lithium salt — are well trapped inside the electrolyte film. The microporous structure of the film is clearly evident from the scanning electron microscope (SEM) image shown in Figure 6.5b. It can be see that the PVDF-HFP forms a network to provide the mechanical support and the liquid phase is distributed inside the pores for ion conduction.

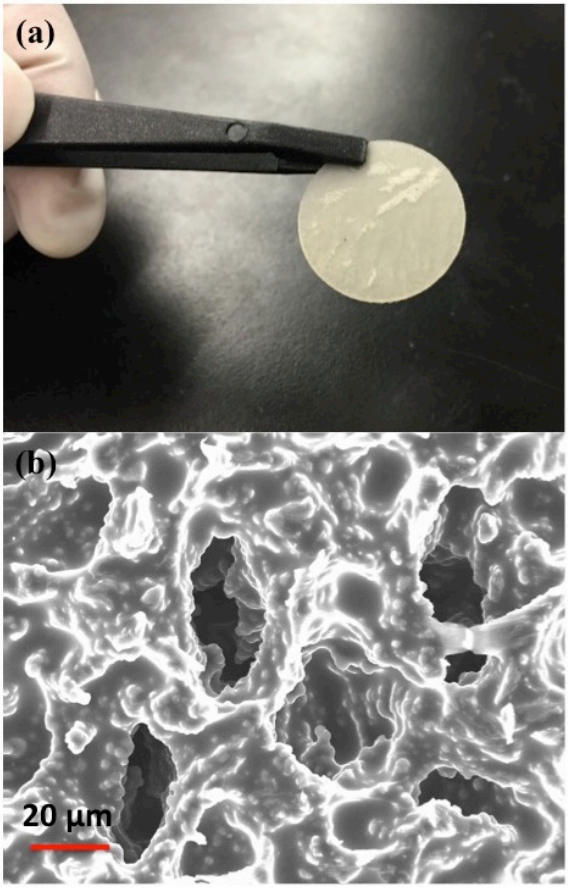

Figure 6.5. (a) A photograph of the electrolyte sample, (b) the SEM image of the PVDF-IL electrolyte showing microporous structure.

The electrolyte film was punched into thin disk-shaped samples for complex impedance spectroscopy based ion conductivity measurements. The frequency ranged from 500 kHz to 10 Hz. Figure 6.6 shows the Nyquist plot of the electrolyte. Unlike the case of common PEO-based solid polymer electrolytes, the Nyquist plot for the fabricated PVDF-IL electrolyte does not exhibit a semi-circle in the high frequency region. The intrinsic resistance is estimated by fitting an equivalent circuit to the Nyquist plot. The calculated ionic conductivity of the fabricated PVDF-IL electrolyte is about 6 $\times 10^{-4}$ S cm^{-1}.

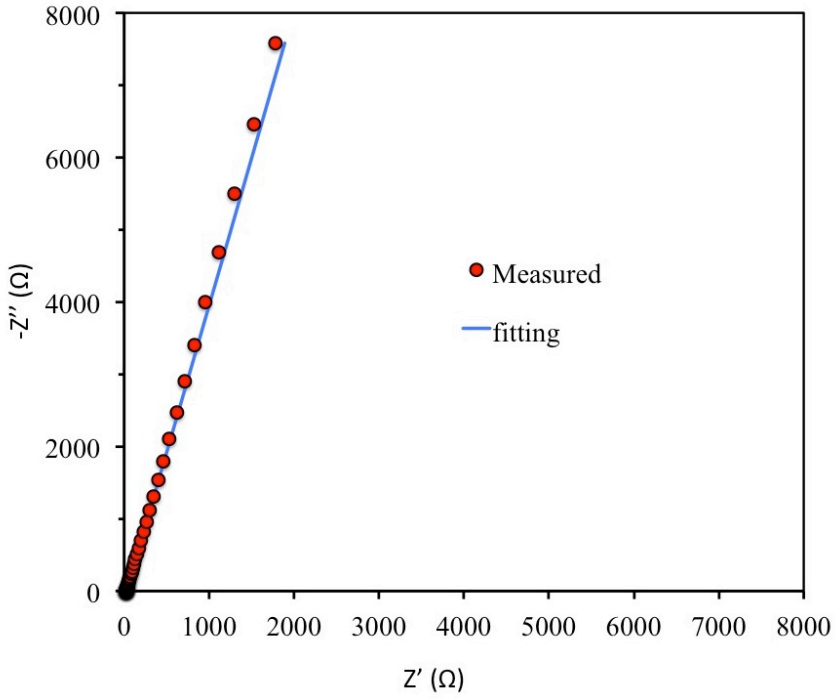

Figure 6.6. Nyquist plot (•) and the fitting curve (solid line) of the PVDF-IL electrolyte.

For gel electrolytes made with general organic carbonates, thermal stability is a significant concern. Due to its intrinsic volatility, the liquid phase will be gradually released during fabrication and storage. This leads to the degradation of the gel electrolyte since the ionic conductivity is predominantly determined by the amount of liquid in the gel. In sharp contrast, ionic liquids are nonvolatile so that the PVDF-IL gel electrolyte can maintain stable composition. Figure 6.7 compares the thermogravimetric analysis (TGA) results of our PVDF-IL electrolyte and gel electrolyte composed of PVDF-EC+PC. The weight loss of the former is negligible even when the temperature rises to 200 °C.

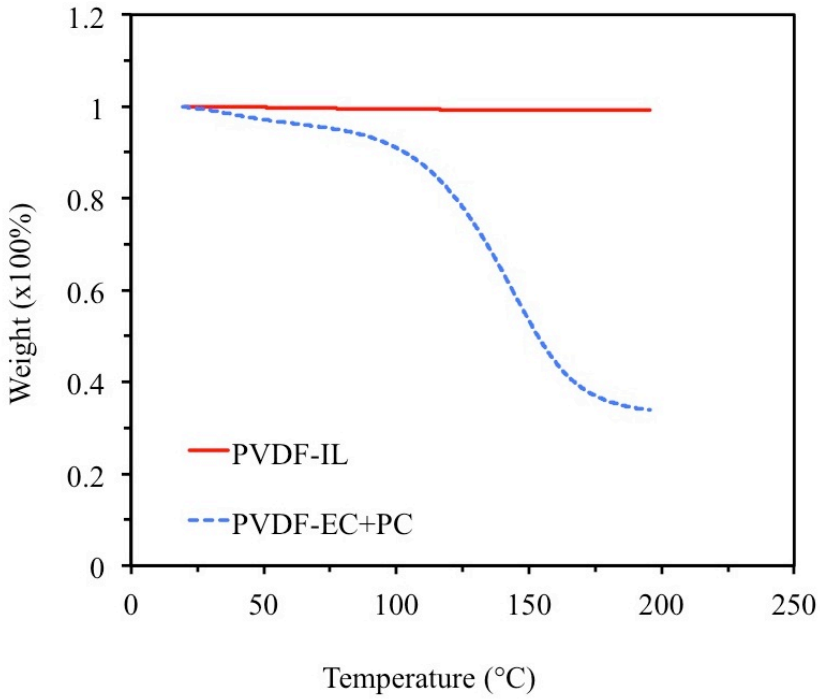

Figure 6.7. Comparison of TGA results of PVDF-IL and PVDF-HFP/EC/PC electrolytes.

3.2 Structure examination of the flexible battery

Using a simple and economical approach, a flexible lithium ion battery was fabricated based on the solid-like PVDF-IL gel electrolyte. The fabrication processes of the electrolyte and the flexible battery are described in the experimental section. A common office-type laminating machine (Figure 6.3a) was used to laminate the flexible battery layers covered by thermal-adhesive plastic sheets with a total process time just under a few minutes. The obtained laminated lithium ion battery (Figure 6.3b) has a multi-layer structure as illustrated in Figure 6.8. The thermal-adhesive laminating plastic sheet acts as the encapsulation to protect the battery from the outside environment and the lamination process produces the pressure to keep all the layers in good contact.

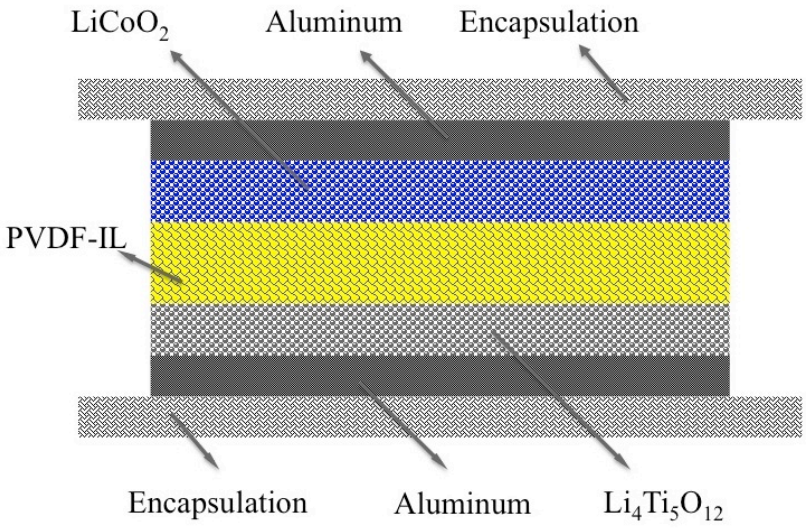

Figure 6.8. Schematics of the flexible Li ion battery, (c) photo of the multi-layer LIB, and (d) SEM image of the battery cross-section.

As mentioned before, maintaining adequate contact between the layers is essential for developing a high performance flexible lithium ion battery. This aspect is especially critical for the traditional carbon-based anodes and organic carbonate-based electrolytes due to the swelling caused by the gas generated from the electrolyte/electrode reactions. Even after replacing carbon-based anode with $Li_4Ti_5O_{12}$ this problem persists [243] and a degassing process is generally required. Because of the high stability of ionic liquids, the gassing problem appears to be suppressed in the flexible batteries fabricated in this study. From the scanning electron microscopy (SEM) image of the cross-section of the flexible battery (Figure 6.9), it can be observed that the boundary between the active material ($LiCoO_2$ or $Li_4Ti_5O_{12}$) and the PVDF-IL layers has disappeared, indicating that the two layers have merged after the hot laminating process. On the other hand, there appears to be a small gap between the active material and the aluminum current collector. This is

most likely due to the process of cutting and removal of the sample from the flexible battery causing the release of the applied pressure from encapsulation.

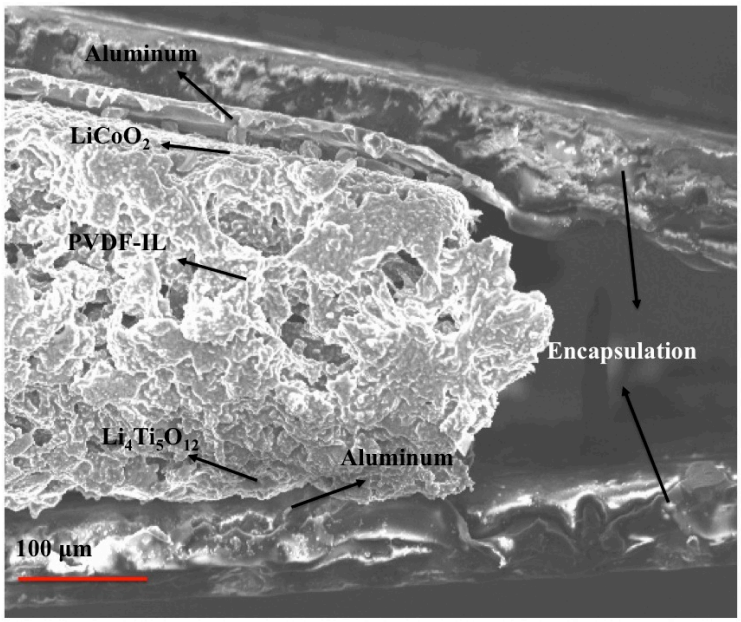

Figure 6.9. The SEM image of the battery cross-section.

3.3 Battery performance

The electrochemical performance of the flexible battery was evaluated. The electrochemical stability of the battery was examined by cyclic voltammetry as shown in Figure 6.10. In the voltage range 1.5 V to 2.8 V, two obvious peaks are observed in the voltammograms corresponding to the intercalation/deintercalation of lithium ions. The heights of these two peaks are almost identical which indicates good reversibility of the lithium ion insertion and extraction. No other peaks are found in the voltage range thus confirming that no side reaction has occurred. In addition, we found a slight difference between the first cycle and the following two cycles. This might be due to the very small

amount of impurity inside the battery. Also, the structural change of the electrodes could be another reason.

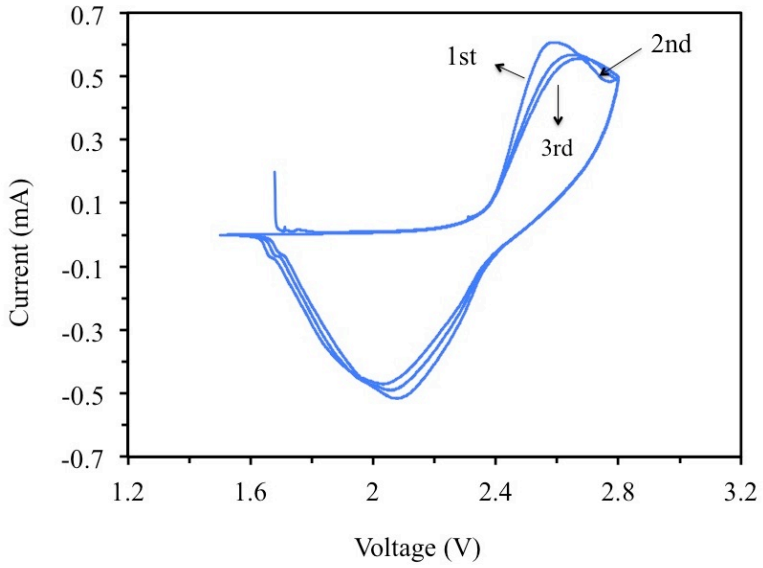

Figure 6.10. Cyclic voltammograms (CVs) of the flexible battery with $LiCoO_2$/Al cathode, $Li_4Ti_5O_{12}$/Al anode, and PVDF-IL electrolyte.

Figure 6.11 shows the galvanostatic charge-discharge profiles of the battery for selected cycles. We can see that at the beginning of the charging, the voltage increases dramatically because of the accumulated charge at the two electrodes. When the voltage reached about 2.5 V, the intercalation of lithium ions occurred and the increasing of the voltage became slow. Instead of the flat plateaus at this reaction region that are usually observed for the batteries based on organic liquid electrolytes, the voltage for the fabricated flexible LIBs, however, exhibits an increasing/decreasing trend. This trend was also observed in the case of the battery based on polyethylene oxide (PEO) gel electrolyte and it may be attributed to the high polarization of the polymer electrolyte [80]. The

increased polarization would create an addition electrical field in the electrolyte and impair the transport of the lithium ions.

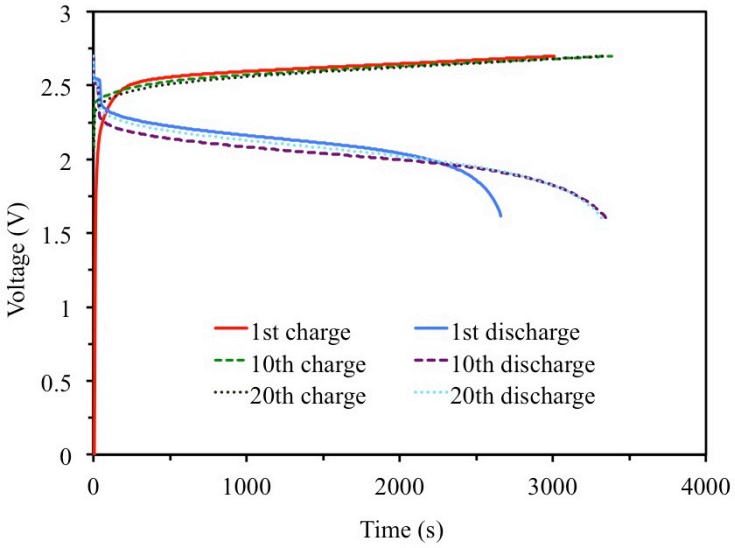

Figure 6.11. Charge-discharge profiles of the battery for 1st (flat), 10th (flat), and 20th (bending) cycles.

The battery is charged and discharged in both flat and bent positions and the results are shown in Figure 6.12. It can be seen that except for the first cycle, the Coulombic efficiencies of all the cycles are about 98%. This result is consistent with the cyclic voltammograms as shown in Figure 6.10 where the first cycle is different with the following cycles. In average, the battery can deliver about 300 μAh/cm^2 capacity for 20 cycles. However, we can still observe the slow degradation of the capacity. It is not as significant as in the case of flexible battery made with EC and PC in the Chapter V, but still not desirable for practical use. In addition, we found that when the flat battery is bent, a capacity jump occurs. This may be attributed to the increased pressure between the layers under bending and the consequent reduction of the interfacial resistance.

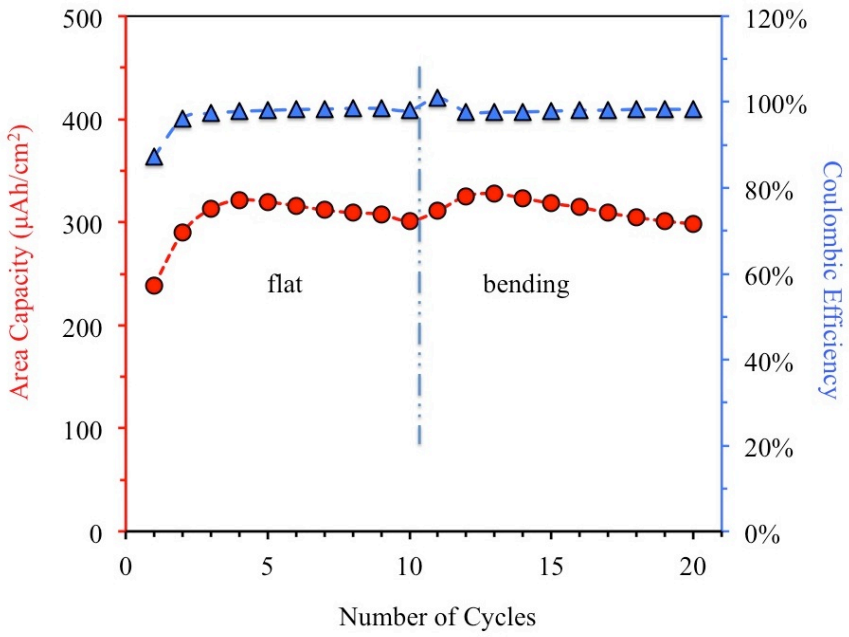

Figure 6.12. Discharge capacities and Coulombic efficiencies of the battery for 20 cycles in flat and bent (2 cm radius) positions.

From the discharge profile, we can find that the average working voltage of the battery is about 2.1 V. It is lower than that of the lithium metal- or graphite-based lithium ion batteries. However, the battery safety is ensured through the use of non-volatile, inflammable PVDF-IL electrolyte. Also, the battery can work functionally (in some cases, even better) while its shape is changing. In Figure 6.13, a red LED (~2.0 V) is lighting up by a bent flexible lithium ion battery. Therefore, the flexible battery fabricated in this study, based on PVDF-ionic liquid electrolyte, can be a promising energy storage device for integration with flexible electronics and applications.

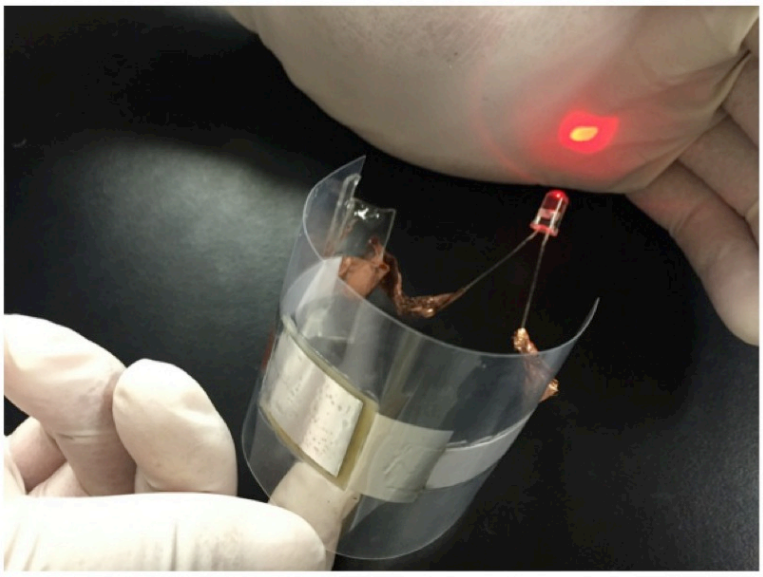

Figure 6.13. Bent flexible battery lighting up a red LED (~2.0 V).

4. Conclusions

In summary, a safer flexible lithium ion battery is fabricated based on a solid-like gel electrolyte consisting of EMIMDCA ionic liquid and PVDF-HFP polymer matrix. The ionic conductivity nearly reached 6 $\times 10^{-4}$ S cm^{-1} with a polymer to ionic liquid ratio of 1:2. This solid-like electrolyte is non-volatile with a stable composition up to 200 °C. This electrolyte is an ideal candidate for a low-cost, simple lamination method to fabricate high performance flexible lithium ion batteries. The battery shows relatively stable energy delivery capability and can function in both flat and bent configurations.

Chapter VII Conclusions and Future Work

1. Conclusions

1.1 Polymer electrolytes for lithium ion batteries

In this study, we have investigated the properties of several different polymer-based electrolytes and explored their applications for lithium ion batteries by means of theoretical modeling, computer simulation, and experiments. In general, the polymer-based electrolytes have high thermal and chemical stability and thus could enhance the safety of the battery. Also, their thin-film manufacturing ability and high mechanical strength make them excellent candidates for the development of thin, flexible lithium in batteries.

Mixture of polyethylene oxide (PEO) and lithium salt is the widely used solid polymer electrolytes for lithium ion batteries. It has been used in our lab to fabricate flexible lithium ion batteries as we introduced in Chapter IV. Those batteries could deliver a stable power while they are bending and they could work functionally even after hundreds of bending cycles. In order to expand this research field, another polymer, polyvinylidene fluoride-*co*-hexafluoropropylene (PVDF-HFP), has been used as the alternative polymer host. The obtained solid polymer electrolytes have shown promising ionic conductivity but we found that might be due to the residual solvent inside the electrolytes. The decay of both the weight and the ionic conductivity with increasing drying time supported our conclusion. The coin cell made with such solid polymer

electrolyte suffered from the large capacity loss in the first several charge/discharge cycles due to the side reactions.

For solid polymer electrolytes, low ionic conductivity is still a big obstacle for their applications in lithium ion batteries. Gel polymer electrolytes, which are characterized by higher room temperature ionic conductivity and better mechanical properties, thus have gained attention. In Chapter V, we explored the application of the gel polymer electrolytes using PVDF-HFP as the polymer host in lithium ion batteries. We found that the ionic conductivity of this electrolyte is largely decided by the amount of liquids and the salt concentration also plays a role. With low polymer content (25 wt%), its ionic conductivity could reach 10^{-3} S/cm. Coin cell lithium ion batteries made with the gel electrolyte have shown promising performance including high discharge capacity, high Coulombic efficiency and good capacity retention for up to 30 cycles.

1.2 Performance enhancement by functional additives

In order to enhance the performance of polymer electrolytes, different additives have been added. In Chapter IV, we have shown that the added graphene oxide nanosheets could increase ionic conductivity and the performance of the flexible lithium ion batteries. The possible mechanisms of this behavior have been investigated in Chapter II. We proposed a model of the ion conductivity enhancement of polymer nanocomposite electrolytes as a function of nanofiller content. Based on the free volume theory, we derived an expression of the ionic conductivity for unfilled solid polymer electrolytes. Then, we split the effects of nanofillers according to the interaction between polymer, nanofillers and lithium salt. Both enhancement and adverse effects of nanofillers on ion

conductivity were considered including salt dissociation, free volume expansion and distribution, diffusion blocking, filler aggregation, ion trapping, and chain confinement. Finally, an equation of ionic conductivity enhancement using several adjustable k-parameters was obtained. We fitted the equation to some ionic conductivity experimental data of polymer nanocomposite electrolytes with different nanofillers and the results have shown that our model agrees very well with the experimental results. It could explain ionic conductivity enhancement and degradation as well. It could also be used to fit the temperature dependency of the ionic conductivity. In our model, several k-parameters are involved and each of them has some physical meaning behind it. Their contributions to the final ionic enhancement were studied by the following method: each k-parameter was doubled while other parameters remained the same and the resulting ionic conductivities were compared. We identified that the free volume factor has more significant influence on ionic conductivity enhancement. Overall, this model can offer insight into the fundamental mechanisms of ion conductivity in the polymer-salt-filler system and facilitate a more effective design of polymer nanocomposite electrolytes.

Molecular dynamics simulation can help to understand the behavior of materials in the microscopic level. In Chapter III, we performed molecular dynamics simulations of a polymer nanocomposite electrolyte. The model consisted of a TiO_2 nanofiller embedded in PEO/$LiClO_4$ electrolyte. Each PEO chain had 200 repeated units and a EO:Li ratio of 10:1. The $LiClO_4$ was added as dissociated ions and they were distributed in the model randomly at the beginning. We constructed several models with different TiO_2 nanofiller to study the influence of the nanofiller's properties (size, shape, and surface feature) on

the electrolyte. Also, a model without the nanofiller was generated as the reference. The structural and dynamic properties of all the models were compared. From the comparison, we have found that the nanofillers can affect the salt dissociation, lithium-ion mobility, and the dynamics of PEO chains. Among all the nanofillers, those with repulsive surface showed good performance in both the suppression of ion-cluster formation and the enhancement of lithium ion mobility. This indicates that the surface property of nanofillers plays a crucial role in ionic conductivity of polymer nanocomposite electrolytes. Also, the smaller size (lower volume fraction) nanofiller is found to better increase the mobility of lithium ions. Regarding the shape of the nanofiller, we could not observe significant effects for two nanofillers with different shapes in the condition of equal volume.

In addition to nanofillers, various liquids can also be used as additives to enhance the ion conductivity of polymer electrolyte. It results in a mixture of polymer and liquid electrolyte. The choice of the liquid and its amount will decide the properties of this generated gel polymer electrolyte. Organic carbonates are widely used in this type of electrolyte. However, those liquids have low thermal and chemical stability and thus, may carry some safety issues with respect to batteries. This concern will become more significant in flexible batteries. In order to maintain the stability of the solid polymer electrolyte and meanwhile obtain enhanced performance, ionic liquids have been used in the development of polymer electrolytes. In Chapter VI, a highly conductive (ionic conductivity of 27 S/cm) ionic liquid, EMIMDCA, was incorporated with PVDF-HFP and lithium salt to make a gel polymer electrolyte. The obtained electrolyte is a

freestanding thin film and exhibited solid appearance. The ionic conductivity of such polymer electrolyte could reach 6×10^{-4} S cm^{-1} with a polymer to ionic liquid ratio of 1:2. This solid-like electrolyte is non-volatile showing stable composition up to 200 °C. Because of the high stability, it has been used for a low-cost, simple lamination method to fabricate high performance flexible lithium ion batteries. The battery shows relatively stable energy delivery capability and can function in both flat and bent configurations.

2. Future work

2.1 Modification of ionic conductivity enhancement model

In Chapter II, we derived an equation (Equation 2.17) for the dependence of ionic conductivity enhancement on the loading of nanofiller. The equation is based on the free volume model for diffusion. It is able to fit to some sets of experimental data and from the fitting parameters we could obtain some insight regarding the effects of different nanofillers. However, compared to the well-known Arrhenius/VTF equation for temperature dependency of ionic conductivity, our proposed model is more complex. Thus, we are interested in further simplification of the model. From the derivation we can see that the complexity mainly comes from the free volume expansion induced by the nanofiller. Therefore, more detailed study for free volume in the polymer materials would be the key step for this work. Also, more fitting of our model to different experimental results would be helpful.

2.2 Challenges of MD simulation

2.2.1 Equilibration times

In Chapter III, we have performed the MD simulation for PEO/Li salt/nanofiller system. One difficulty we have encountered is the simulation time. For each model, less than 4 ns simulation took about 2 weeks in a computer cluster with 16 cores. This time-consuming calculation makes long equilibration times unrealistic. However, for polymer materials, because of the very slow relaxation of the long chain molecules longer equilibration time might be desired. Thus, it would be important to know that how much equilibration is needed for polymer systems to ensure reliable results. A fundamental investigation of this issue is of our interest. It could provide insight into the role of equilibration times in MD simulations of polymer materials.

2.2.2 Nanofiller dispersion

Another difficulty is the modeling of nanofiller. In this study we cut the TiO_2 from a periodic crystal so that the structure of the nanofiller is the same as the bulk material. This seems a practical method to obtain a nanoparticle of certain material. However, in reality the structure of the nanofiller might have some difference with the bulk material.

More important is that in the study of polymer nanocomposite electrolytes, their properties are usually measured at different concentration of nanofiller. In MD simulation, this means that a large model with several nanofillers is required. In order to limit such a simulation to a practical time, such a model should have simplified structure

(e.g., a nanofiller is represented by a single bead). However, that simplification might need a thorough consideration on the force field.

2.3 Improvement of flexible lithium ion batteries

From some results reported in literature and in this study, the performance of flexible lithium ion batteries still needs more progress. Because of the lack of rigid case, the common degradation problem might become more critical in flexible lithium ion batteries including the SEI formation. For coin cell battery, the SEI formation usually means the loss of reversible capacity. In flexible battery, that may result in the failure of the whole device since the accompanied gas generation may damage the encapsulation. This problem can be circumvented using "dry" solid polymer electrolyte and ceramic electrolytes. However, their ionic conductivity is lower than that of the liquid/gel counterparts.

To further improve the performance of flexible batteries, two different approaches can be employed: First would be using new designs and fabrication methods of the electrodes to make them more compatible with solid electrolytes that generally exhibit no SEI formation. The goal is to reduce the high interface impedance. Also, this method requires high ionic conductivity solid electrolytes. In the second method, we can keep the current electrodes and put the focus on developing more stable and highly Li-conducting liquid/gel electrolytes. Ionic liquids are promising materials for this purpose. However, the conduction of lithium ions in these room temperature molten salts needs more investigation.

References

[1] Armand, M., and Tarascon, J. M., 2008, "Building better batteries," pp. 652-657.

[2] Tarascon, J. M., and Armand, M., 2001, "Issues and challenges facing rechargeable lithium batteries," Nature, 414(6861), pp. 359-367.

[3] Whittingham, M. S., 2008, "Materials challenges facing electrical energy storage," Mrs Bulletin, 33(4), pp. 411-419.

[4] Scrosati, B., and Garche, J., 2010, "Lithium batteries: Status, prospects and future," Journal of Power Sources, 195(9), pp. 2419-2430.

[5] Hadjipaschalis, I., Poullikkas, A., and Efthimiou, V., 2009, "Overview of current and future energy storage technologies for electric power applications," Renewable & Sustainable Energy Reviews, 13(6-7), pp. 1513-1522.

[6] Ibrahim, H., Ilinca, A., and Perron, J., 2008, "Energy storage systems - Characteristics and comparisons," Renewable & Sustainable Energy Reviews, 12(5), pp. 1221-1250.

[7] Chen, H., Cong, T. N., Yang, W., Tan, C., Li, Y., and Ding, Y., 2009, "Progress in electrical energy storage system: A critical review," Progress in Natural Science, 19(3), pp. 291-312.

[8] Winter, M., and Brodd, R. J., 2004, "What are batteries, fuel cells, and supercapacitors?," Chemical Reviews, 104(10), pp. 4245-4269.

[9] Takamura, T., 2002, "Trends in advanced batteries and key materials in the new century," Solid State Ionics, 152, pp. 19-34.

[10] Dell, R. M., 2000, "Batteries - fifty years of materials development," Solid State Ionics, 134(1-2), pp. 139-158.

[11] Scrosati, B., 1995, "BATTERY TECHNOLOGY - CHALLENGE OF PORTABLE POWER," Nature, 373(6515), pp. 557-558.

[12] Jayalakshmi, M., and Balasubramanian, K., 2008, "Simple Capacitors to Supercapacitors - An Overview," International Journal of Electrochemical Science, 3(11), pp. 1196-1217.

[13] Simon, P., and Gogotsi, Y., 2008, "Materials for electrochemical capacitors," Nature Materials, 7(11), pp. 845-854.

[14] Zhang, L. L., Zhou, R., and Zhao, X. S., 2010, "Graphene-based materials as supercapacitor electrodes," Journal of Materials Chemistry, 20(29), pp. 5983-5992.

[15] Zhang, Y., Feng, H., Wu, X., Wang, L., Zhang, A., Xia, T., Dong, H., Li, X., and Zhang, L., 2009, "Progress of electrochemical capacitor electrode materials: A review," International Journal of Hydrogen Energy, 34(11), pp. 4889-4899.

[16] Kotz, R., and Carlen, M., 2000, "Principles and applications of electrochemical capacitors," Electrochimica Acta, 45(15-16), pp. 2483-2498.

[17] Ekanayake, S. R., Cortie, M. B., and Ford, M. J., 2004, "Design of nanocapacitors and associated materials challenges," Current Applied Physics, 4(2-4), pp. 250-254.

[18] Cohen, R., 2009, "NANOCAPACITORS Undead layers breathe new life," Nature Materials, 8(5), pp. 366-368.

[19] Haspert, L. C., Lee, S. B., and Rubloff, G. W., 2012, "Nanoengineering Strategies for Metal-Insulator-Metal Electrostatic Nanocapacitors," Acs Nano, 6(4), pp. 3528-3536.

[20] Stengel, M., Vanderbilt, D., and Spaldin, N. A., 2009, "Enhancement of ferroelectricity at metal-oxide interfaces," Nature Materials, 8(5), pp. 392-397.

[21] Majdoub, M. S., Maranganti, R., and Sharma, P., 2009, "Understanding the origins of the intrinsic dead layer effect in nanocapacitors," Physical Review B, 79(11).

[22] Li, Q., Patel, C., and Ardebili, H., 2012, "Mitigating the dead-layer effect in nanocapacitors using graded dielectric films," International Journal of Smart and Nano Materials, 3(1), pp. 23-32.

[23] Vincent, C. A., 2000, "Lithium batteries: a 50-year perspective, 1959-2009," Solid State Ionics, 134(1-2), pp. 159-167.

[24] Nishi, Y., 2001, "Lithium ion secondary batteries; past 10 years and the future," Journal of Power Sources, 100(1-2), pp. 101-106.

[25] Li, Y. F., and Wu, H. Q., 1989, "THEORETICAL TREATMENT OF KINETICS OF INTERCALATION ELECTRODE-REACTION," Electrochimica Acta, 34(2), pp. 157-159.

[26] Whittingham, M. S., 2004, "Lithium batteries and cathode materials," Chemical Reviews, 104(10), pp. 4271-4301.

[27] Ellis, B. L., Lee, K. T., and Nazar, L. F., 2010, "Positive Electrode Materials for Li-Ion and Li-Batteries," Chemistry of Materials, 22(3), pp. 691-714.

[28] Wang, B., Bates, J. B., Hart, F. X., Sales, B. C., Zuhr, R. A., and Robertson, J. D., 1996, "Characterization of thin-film rechargeable lithium batteries with lithium cobalt oxide cathodes," Journal of the Electrochemical Society, 143(10), pp. 3203-3213.

[29] Yamada, A., Chung, S. C., and Hinokuma, K., 2001, "Optimized LiFePO4 for lithium battery cathodes," Journal of the Electrochemical Society, 148(3), pp. A224-A229.

[30] Padhi, A. K., Nanjundaswamy, K. S., and Goodenough, J. B., 1997, "Phospho-olivines as positive-electrode materials for rechargeable lithium batteries," Journal of the Electrochemical Society, 144(4), pp. 1188-1194.

[31] Megahed, S., and Scrosati, B., 1994, "LITHIUM-ION RECHARGEABLE BATTERIES," Journal of Power Sources, 51(1-2), pp. 79-104.

[32] Scrosati, B., 2000, "Recent advances in lithium ion battery materials," Electrochimica Acta, 45(15-16), pp. 2461-2466.

[33] Agubra, V. A., and Fergus, J. W., 2014, "The formation and stability of the solid electrolyte interface on the graphite anode," Journal of Power Sources, 268, pp. 153-162.

[34] Wakihara, M., 2001, "Recent developments in lithium ion batteries," Materials Science & Engineering R-Reports, 33(4), pp. 109-134.

[35] Poizot, P., Laruelle, S., Grugeon, S., Dupont, L., and Tarascon, J. M., 2000, "Nano-sized transition-metaloxides as negative-electrode materials for lithium-ion batteries," Nature, 407(6803), pp. 496-499.

[36] Zaghib, K., Armand, M., and Gauthier, M., 1998, "Electrochemistry of anodes in solid-state Li-ion polymer batteries," Journal of the Electrochemical Society, 145(9), pp. 3135-3140.

[37] Wang, Y.-Q., Guo, L., Guo, Y.-G., Li, H., He, X.-Q., Tsukimoto, S., Ikuhara, Y., and Wan, L.-J., 2012, "Rutile-TiO2 Nanocoating for a High-Rate Li4Ti5O12 Anode of a Lithium-Ion Battery," Journal of the American Chemical Society, 134(18), pp. 7874-7879.

[38] Xu, K., 2004, "Nonaqueous liquid electrolytes for lithium-based rechargeable batteries," Chemical Reviews, 104(10), pp. 4303-4417.

[39] Goodenough, J. B., and Kim, Y., 2010, "Challenges for Rechargeable Li Batteries," Chemistry of Materials, 22(3), pp. 587-603.

[40] Arora, P., and Zhang, Z. M., 2004, "Battery separators," Chemical Reviews, 104(10), pp. 4419-4462.

[41] Lee, J. K., Smith, K. B., Hayner, C. M., and Kung, H. H., 2010, "Silicon nanoparticles-graphene paper composites for Li ion battery anodes," Chemical Communications, 46(12), pp. 2025-2027.

[42] Natarajan, C., Setoguchi, K., and Nogami, G., 1998, "Preparation of a nanocrystalline titanium dioxide negative electrode for the rechargeable lithium ion battery," Electrochimica Acta, 43(21-22), pp. 3371-3374.

[43] Beck, F., and Ruetschi, P., 2000, "Rechargeable batteries with aqueous electrolytes," Electrochimica Acta, 45(15-16), pp. 2467-2482.

[44] Hayashi, K., Nemoto, Y., Tobishima, S., and Yamaki, J., 1999, "Mixed solvent electrolyte for high voltage lithium metal secondary cells," Electrochimica Acta, 44(14), pp. 2337-2344.

[45] Osaka, T., Naoi, K., Sakai, H., and Ogano, S., 1987, "EFFECT OF PF6- ANION ON THE PROPERTIES OF LITHIUM-POLYPYRROLE BATTERY DURING POLYPYRROLE FILM FORMATION," Journal of the Electrochemical Society, 134(2), pp. 285-289.

[46] Campion, C. L., Li, W. T., and Lucht, B. L., 2005, "Thermal decomposition of LiPF6-based electrolytes for lithium-ion batteries," Journal of the Electrochemical Society, 152(12), pp. A2327-A2334.

[47] Le Bideau, J., Ducros, J.-B., Soudan, P., and Guyomard, D., 2011, "Solid-State Electrode Materials with Ionic-Liquid Properties for Energy Storage: the Lithium Solid-State Ionic-Liquid Concept," Advanced Functional Materials, 21(21), pp. 4073-4078.

[48] Sawai, K., Iwakoshi, Y., and Ohzuku, T., 1994, "CARBON MATERIALS FOR LITHIUM-ION (SHUTTLECOCK) CELLS," Solid State Ionics, 69(3-4), pp. 273-283.

[49] Tarascon, J. M., and Guyomard, D., 1994, "NEW ELECTROLYTE COMPOSITIONS STABLE OVER THE O-V TO 5-V VOLTAGE RANGE AND COMPATIBLE WITH THE LI1+XMN2O4 CARBON LI-ION CELLS," Solid State Ionics, 69(3-4), pp. 293-305.

[50] Jasinski, R., and Carroll, S., 1970, "THERMAL STABILITY OF A PROPYLENE CARBONATE ELECTROLYTE," Journal of the Electrochemical Society, 117(2), pp. 218-&.

[51] Armand, M. B., 1986, "Polymer Electrolytes," Annu. Rev. Mater. Sci., pp. 245-261.

[52] Du, J., and Chen, C.-H., 2012, "Structure and lithium ion diffusion in lithium silicate glasses and at their interfaces with lithium lanthanum titanate crystals," Journal of Non-Crystalline Solids, 358(24), pp. 3531-3538.

[53] Bruce, P. G., 1995, "STRUCTURE AND ELECTROCHEMISTRY OF POLYMER ELECTROLYTES," Electrochimica Acta, 40(13-14), pp. 2077-2085.

[54] Fergus, J. W., 2010, "Ceramic and polymeric solid electrolytes for lithium-ion batteries," Journal of Power Sources, 195(15), pp. 4554-4569.

[55] Yang, X. Q., Lee, H. S., Hanson, L., McBreen, J., and Okamoto, Y., 1995, "DEVELOPMENT OF A NEW PLASTICIZER FOR POLY(ETHYLENE OXIDE)-

BASED POLYMER ELECTROLYTE AND THE INVESTIGATION OF THEIR ION-PAIR DISSOCIATION EFFECT," Journal of Power Sources, 54(2), pp. 198-204.

[56] Kelly, I. E., Owen, J. R., and Steele, B. C. H., 1985, "POLY(ETHYLENE OXIDE) ELECTROLYTES FOR OPERATION AT NEAR ROOM-TEMPERATURE," Journal of Power Sources, 14(1-3), pp. 13-21.

[57] Kumar, Y., Hashmi, S. A., and Pandey, G. P., 2011, "Lithium ion transport and ion-polymer interaction in PEO based polymer electrolyte plasticized with ionic liquid," Solid State Ionics, 201(1), pp. 73-80.

[58] Croce, F., Appetecchi, G. B., Persi, L., and Scrosati, B., 1998, "Nanocomposite polymer electrolytes for lithium batteries," Nature, 394(6692), pp. 456-458.

[59] Fullerton-Shirey, S. K., and Maranas, J. K., 2010, "Structure and Mobility of PEO/LiClO4 Solid Polymer Electrolytes Filled with Al2O3 Nanoparticles," Journal of Physical Chemistry C, 114(20), pp. 9196-9206.

[60] D'Epifanio, A., Fiory, F. S., Licoccia, S., Traversa, E., Scrosati, B., and Croce, F., 2004, "Metallic-lithium, LiFePO4-based polymer battery using PEO-ZrO2 nanocomposite polymer electrolyte," Journal of Applied Electrochemistry, 34(4), pp. 403-408.

[61] Chung, S. H., Wang, Y., Persi, L., Croce, F., Greenbaum, S. G., Scrosati, B., and Plichta, E., 2001, "Enhancement of ion transport in polymer electrolytes by addition of nanoscale inorganic oxides," Journal of Power Sources, 97-8, pp. 644-648.

[62] Ahn, J. H., Wang, G. X., Liu, H. K., and Dou, S. X., 2003, "Nanoparticle-dispersed PEO polymer electrolytes for Li batteries," Journal of Power Sources, 119, pp. 422-426.

[63] Song, J. Y., Wang, Y. Y., and Wan, C. C., 1999, "Review of gel-type polymer electrolytes for lithium-ion batteries," Journal of Power Sources, 77(2), pp. 183-197.

[64] Watanabe, M., Kanba, M., Nagaoka, K., and Shinohara, I., 1982, "IONIC-CONDUCTIVITY OF HYBRID FILMS BASED ON POLYACRYLONITRILE AND THEIR BATTERY APPLICATION," Journal of Applied Polymer Science, 27(11), pp. 4191-4198.

[65] Bohnke, O., Frand, G., Rezrazi, M., Rousselot, C., and Truche, C., 1993, "FAST-ION TRANSPORT IN NEW LITHIUM ELECTROLYTES GELLED WITH PMMA .1. INFLUENCE OF POLYMER CONCENTRATION," Solid State Ionics, 66(1-2), pp. 97-104.

[66] Bohnke, O., Frand, G., Rezrazi, M., Rousselot, C., and Truche, C., 1993, "FAST-ION TRANSPORT IN NEW LITHIUM ELECTROLYTES GELLED WITH PMMA .2. INFLUENCE OF LITHIUM SALT CONCENTRATION," Solid State Ionics, 66(1-2), pp. 105-112.

[67] Song, J. Y., Wang, Y. Y., and Wan, C. C., 2000, "Conductivity study of porous plasticized polymer electrolytes based on poly(vinylidene fluoride) - A comparison with polypropylene separators," Journal of the Electrochemical Society, 147(9), pp. 3219-3225.

[68] Kim, H. S., Periasamy, P., and Moon, S. I., 2005, "Electrochemical properties of the Li-ion polymer batteries with P(VdF-co-HFP)-based gel polymer electrolyte," Journal of Power Sources, 141(2), pp. 293-297.

[69] Tarascon, J. M., Gozdz, A. S., Schmutz, C., Shokoohi, F., and Warren, P. C., 1996, "Performance of Bellcore's plastic rechargeable Li-ion batteries," Solid State Ionics, 86-8, pp. 49-54.

[70] Hu, M., Pang, X., and Zhou, Z., 2013, "Recent progress in high-voltage lithium ion batteries," Journal of Power Sources, 237, pp. 229-242.

[71] Hautier, G., Jain, A., and Ong, S. P., 2012, "From the computer to the laboratory: materials discovery and design using first-principles calculations," Journal of Materials Science, 47(21), pp. 7317-7340.

[72] Plimpton, S., 1995, "FAST PARALLEL ALGORITHMS FOR SHORT-RANGE MOLECULAR-DYNAMICS," Journal of Computational Physics, 117(1), pp. 1-19.

[73] Alder, B. J., and Wainwright, T. E., 1957, "PHASE TRANSITION FOR A HARD SPHERE SYSTEM," Journal of Chemical Physics, 27(5), pp. 1208-1209.

[74] Kresse, G., and Hafner, J., 1993, "ABINITIO MOLECULAR-DYNAMICS FOR LIQUID-METALS," Physical Review B, 47(1), pp. 558-561.

[75] Isralewitz, B., Gao, M., and Schulten, K., 2001, "Steered molecular dynamics and mechanical functions of proteins," Current Opinion in Structural Biology, 11(2), pp. 224-230.

[76] Nishide, H., and Oyaizu, K., 2008, "Materials science - Toward flexible batteries," Science, 319(5864), pp. 737-738.

[77] Zhou, G., Li, F., and Cheng, H.-M., 2014, "Progress in flexible lithium batteries and future prospects," Energy & Environmental Science, 7(4), pp. 1307-1338.

[78] Koo, M., Park, K. I., Lee, S. H., Suh, M., Jeon, D. Y., Choi, J. W., Kang, K., and Lee, K. J., 2012, "Bendable Inorganic Thin-Film Battery for Fully Flexible Electronic Systems," Nano Letters, 12(9), pp. 4810-4816.

[79] Hu, L. B., Wu, H., La Mantia, F., Yang, Y. A., and Cui, Y., 2010, "Thin, Flexible Secondary Li-Ion Paper Batteries," Acs Nano, 4(10), pp. 5843-5848.

[80] Xu, S., Zhang, Y. H., Cho, J., Lee, J., Huang, X., Jia, L., Fan, J. A., Su, Y. W., Su, J., Zhang, H. G., Cheng, H. Y., Lu, B. W., Yu, C. J., Chuang, C., Kim, T. I., Song, T., Shigeta, K., Kang, S., Dagdeviren, C., Petrov, I., Braun, P. V., Huang, Y. G., Paik, U., and Rogers, J. A., 2013, "Stretchable batteries with self-similar serpentine interconnects and integrated wireless recharging systems," Nature Communications, 4.

[81] Wu, M.-S., Lee, J.-T., Chiang, P.-C. J., and Lin, J.-C., 2007, "Carbon-nanofiber composite electrodes for thin and flexible lithium-ion batteries," Journal of Materials Science, 42(1), pp. 259-265.

[82] Goyal, A., Reddy, A. L. M., and Ajayan, P. M., 2011, "Flexible Carbon Nanotube-Cu2O Hybrid Electrodes for Li-Ion Batteries," Small, 7(12), pp. 1709-1713.

[83] Chew, S. Y., Ng, S. H., Wang, J., Novak, P., Krumeich, F., Chou, S. L., Chen, J., and Liu, H. K., 2009, "Flexible free-standing carbon nanotube films for model lithium-ion batteries," Carbon, 47(13), pp. 2976-2983.

[84] Wang, J.-Z., Zhong, C., Chou, S.-L., and Liu, H.-K., 2010, "Flexible free-standing graphene-silicon composite film for lithium-ion batteries," Electrochemistry Communications, 12(11), pp. 1467-1470.

[85] Li, N., Chen, Z., Ren, W., Li, F., and Cheng, H.-M., 2012, "Flexible graphene-based lithium ion batteries with ultrafast charge and discharge rates," Proceedings of the

National Academy of Sciences of the United States of America, 109(43), pp. 17360-17365.

[86] Noerochim, L., Wang, J.-Z., Chou, S.-L., Wexler, D., and Liu, H.-K., 2012, "Free-standing single-walled carbon nanotube/SnO2 anode paper for flexible lithium-ion batteries," Carbon, 50(3), pp. 1289-1297.

[87] Lee, S.-Y., Choi, K.-H., Choi, W.-S., Kwon, Y. H., Jung, H.-R., Shin, H.-C., and Kim, J. Y., 2013, "Progress in flexible energy storage and conversion systems, with a focus on cable-type lithium-ion batteries," Energy & Environmental Science, 6(8), pp. 2414-2423.

[88] Balakrishnan, P. G., Ramesh, R., and Kumar, T. P., 2006, "Safety mechanisms in lithium-ion batteries," Journal of Power Sources, 155(2), pp. 401-414.

[89] Arbizzani, C., Gabrielli, G., and Mastragostino, M., 2011, "Thermal stability and flammability of electrolytes for lithium-ion batteries," Journal of Power Sources, 196(10), pp. 4801-4805.

[90] Schoonman, J., and Kelder, E. M., 1997, "Thin film solid electrolytes and electrodes for rechargeable lithium-ion batteries," Journal of Power Sources, 68(1), pp. 65-68.

[91] Skaarup, S., West, K., Zachau-Christiansen, B., Popall, M., Kappel, J., Kron, J., Eichinger, G., and Semrau, G., 1998, "Towards solid state lithium batteries based on ORMOCER electrolytes," Electrochimica Acta, 43(10-11), pp. 1589-1592.

[92] Dias, F. B., Plomp, L., and Veldhuis, J. B. J., 2000, "Trends in polymer electrolytes for secondary lithium batteries," Journal of Power Sources, 88(2), pp. 169-191.

[93] Minami, T., Hayashi, A., and Tatsumisago, M., 2006, "Recent progress of glass and glass-ceramics as solid electrolytes for lithium secondary batteries," Solid State Ionics, 177(26-32), pp. 2715-2720.

[94] Maitra, A., and Heuer, A., 2007, "Cation transport in polymer electrolytes: A microscopic approach," Physical Review Letters, 98(22).

[95] Stolwijk, N. A., and Obeidi, S., 2004, "Radiotracer diffusion and ionic conduction in a PEO-NaI polymer electrolyte," Physical Review Letters, 93(12).

[96] Wang, Y., Agapov, A. L., Fan, F., Hong, K., Yu, X., Mays, J., and Sokolov, A. P., 2012, "Decoupling of Ionic Transport from Segmental Relaxation in Polymer Electrolytes," Physical Review Letters, 108(8).

[97] Papke, B. L., Ratner, M. A., and Shriver, D. F., 1982, "CONFORMATION AND ION-TRANSPORT MODELS FOR THE STRUCTURE AND IONIC-CONDUCTIVITY IN COMPLEXES OF POLYETHERS WITH ALKALI-METAL SALTS," Journal of the Electrochemical Society, 129(8), pp. 1694-1701.

[98] Sheldon, M. H., Glasse, M. D., Latham, R. J., and Linford, R. G., 1989, "THE EFFECT OF PLASTICIZER ON ZINC POLYMER ELECTROLYTES," Solid State Ionics, 34(1-2), pp. 135-138.

[99] Michael, M. S., Jacob, M. M. E., Prabaharan, S. R. S., and Radhakrishna, S., 1997, "Enhanced lithium ion transport in PEO-based solid polymer electrolytes employing a novel class of plasticizers," Solid State Ionics, 98(3-4), pp. 167-174.

[100] Qian, X. M., Gu, N. Y., Cheng, Z. L., Yang, X. R., Wang, E. K., and Dong, S. J., 2002, "Plasticizer effect on the ionic conductivity of PEO-based polymer electrolyte," Materials Chemistry and Physics, 74(1), pp. 98-103.

[101] Nan, C. W., Fan, L. Z., Lin, Y. H., and Cai, Q., 2003, "Enhanced ionic conductivity of polymer electrolytes containing nanocomposite SiO2 particles," Physical Review Letters, 91(26).

[102] Bruce, P. G., Scrosati, B., and Tarascon, J.-M., 2008, "Nanomaterials for rechargeable lithium batteries," Angewandte Chemie-International Edition, 47(16), pp. 2930-2946.

[103] Weston, J. E., and Steele, B. C. H., 1982, "EFFECTS OF INERT FILLERS ON THE MECHANICAL AND ELECTROCHEMICAL PROPERTIES OF LITHIUM SALT POLY (ETHYLENE-OXIDE) POLYMER ELECTROLYTES," Solid State Ionics, 7(1), pp. 75-79.

[104] Przyluski, J., and Wieczorek, W., 1989, "INCREASING THE CONDUCTIVITY OF POLYMER SOLID ELECTROLYTES - A REVIEW," Solid State Ionics, 36(3-4), pp. 165-169.

[105] Capuano, F., Croce, F., and Scrosati, B., 1991, "COMPOSITE POLYMER ELECTROLYTES," Journal of the Electrochemical Society, 138(7), pp. 1918-1922.

[106] Croce, F., Curini, R., Martinelli, A., Persi, L., Ronci, F., Scrosati, B., and Caminiti, R., 1999, "Physical and chemical properties of nanocomposite polymer electrolytes," Journal of Physical Chemistry B, 103(48), pp. 10632-10638.

[107] Wang, C. X., Xia, Y. Y., Koumoto, K., and Sakai, T., 2002, "All solid-state Li/LixMnO2 polymer battery using ceramic modified polymer electrolytes," Journal of the Electrochemical Society, 149(8), pp. A967-A972.

[108] Golodnitsky, D., Ardel, G., and Peled, E., 2002, "Ion-transport phenomena in concentrated PEO-based composite polymer electrolytes," Solid State Ionics, 147(1-2), pp. 141-155.

[109] Adebahr, J., Ciccosillo, N., Shekibi, Y., MacFarlane, D. R., Hill, A. J., and Forsyth, M., 2006, "The "filler-effect" in organic ionic plastic crystals: Enhanced conductivity by the addition of nano-sized TiO2," Solid State Ionics, 177(9-10), pp. 827-831.

[110] Tan, S. M., and Johan, M. R., 2011, "Effects of MnO2 nano-particles on the conductivity of PMMA-PEO-LiClO4-EC polymer electrolytes," Ionics, 17(6), pp. 485-490.

[111] Do, N. S. T., Schaetzl, D. M., Dey, B., Seabaugh, A. C., and Fullerton-Shirey, S. K., 2012, "Influence of Fe2O3 Nanofiller Shape on the Conductivity and Thermal Properties of Solid Polymer Electrolytes: Nanorods versus Nanospheres," Journal of Physical Chemistry C, 116(40), pp. 21216-21223.

[112] Croce, F., Persi, L., Scrosati, B., Serraino-Fiory, F., Plichta, E., and Hendrickson, M. A., 2001, "Role of the ceramic fillers in enhancing the transport properties of composite polymer electrolytes," Electrochimica Acta, 46(16), pp. 2457-2461.

[113] Persi, L., Croce, F., Scrosati, B., Plichta, E., and Hendrickson, M. A., 2002, "Poly(ethylene oxide)-based, nanocomposite electrolytes as improved separators for rechargeable lithium polymer batteries - The Li/LiMn3O6 case," Journal of the Electrochemical Society, 149(2), pp. A212-A216.

[114] Vaia, R. A., Vasudevan, S., Krawiec, W., Scanlon, L. G., and Giannelis, E. P., 1995, "New Polymer Electrolyte Nanocomposites-Melt Intercalation of Polymer(ethylen oxide) in Mica-type Silicates," Advanced Materials, 7(2), pp. 154-156.

[115] Gadjourova, Z., Andreev, Y. G., Tunstall, D. P., and Bruce, P. G., 2001, "Ionic conductivity in crystalline polymer electrolytes," Nature, 412(6846), pp. 520-523.

[116] Przyluski, J., Siekierski, M., and Wieczorek, W., 1995, "EFFECTIVE-MEDIUM THEORY IN STUDIES OF CONDUCTIVITY OF COMPOSITE POLYMERIC ELECTROLYTES," Electrochimica Acta, 40(13-14), pp. 2101-2108.

[117] Wieczorek, W., Zalewska, A., Siekierski, M., and Przyluski, J., 1996, "Modelling the ac conductivity behaviour of composite polymeric electrolytes by the effective medium theory," Solid State Ionics, 86-8, pp. 357-362.

[118] Stramare, S., Thangadurai, V., and Weppner, W., 2003, "Lithium lanthanum titanates: A review," Chemistry of Materials, 15(21), pp. 3974-3990.

[119] Sviridov, S. I., 2007, "Influence of the composition of a molten salt on the field-assisted diffusion of potassium ions in the 20Na(2)O center dot 80SiO(2) glass," Glass Physics and Chemistry, 33(6), pp. 550-555.

[120] Zielinski, J. M., and Duda, J. L., 1992, "PREDICTING POLYMER SOLVENT DIFFUSION-COEFFICIENTS USING FREE-VOLUME THEORY," Aiche Journal, 38(3), pp. 405-415.

[121] Hong, S. U., 1997, "Predictive methods to estimate solvent free-volume parameters and diffusion coefficients in polymer/solvent systems," Industrial & Engineering Chemistry Research, 36(2), pp. 501-505.

[122] Ramesh, N., Davis, P. K., Zielinski, J. M., Danner, R. P., and Duda, J. L., 2011, "Application of Free-Volume Theory to Self Diffusion of Solvents in Polymers Below the Glass Transition Temperature: A Review," Journal of Polymer Science Part B-Polymer Physics, 49(23), pp. 1629-1644.

[123] Nagel, C., Gunther-Schade, K., Fritsch, D., Strunskus, T., and Faupel, F., 2002, "Free volume and transport properties in highly selective polymer membranes," Macromolecules, 35(6), pp. 2071-2077.

[124] Jiang, W. H., and Han, R., 2000, "Prediction of solvent-diffusion coefficient in polymer by a modified free-volume theory," Journal of Applied Polymer Science, 77(2), pp. 428-436.

[125] Thornton, A. W., Nairn, K. M., Hill, A. J., and Hill, J. M., 2009, "New relation between diffusion and free volume: I. Predicting gas diffusion," Journal of Membrane Science, 338(1-2), pp. 29-37.

[126] Cohen, M. H., and Turnbull, D., 1959, "MOLECULAR TRANSPORT IN LIQUIDS AND GLASSES," Journal of Chemical Physics, 31(5), pp. 1164-1169.

[127] Ratner, M. A., and Shriver, D. F., 1988, "ION-TRANSPORT IN SOLVENT-FREE POLYMERS," Chemical Reviews, 88(1), pp. 109-124.

[128] Xiong, H. M., Zhao, X., and Chen, J. S., 2001, "New polymer-inorganic nanocomposites: PEO-ZnO and PEO-ZnO-LiClO4 films," Journal of Physical Chemistry B, 105(42), pp. 10169-10174.

[129] Shukla, N., and Thakur, A. K., 2011, "Enhancement in electrical and stability properties of amorphous polymer based nanocomposite electrolyte," Journal of Non-Crystalline Solids, 357(22-23), pp. 3689-3701.

[130] Stephan, A. M., and Nahm, K. S., 2006, "Review on composite polymer electrolytes for lithium batteries," Polymer, 47(16), pp. 5952-5964.

[131] Ji, K. S., Moon, H. S., Kim, J. W., and Park, J. W., 2003, "Role of functional nano-sized inorganic fillers in poly(ethylene) oxide-based polymer electrolytes," Journal of Power Sources, 117(1-2), pp. 124-130.

[132] Mohapatra, S. R., Thakur, A. K., and Choudhary, A. K., 2009, "Vibrational spectroscopy analysis of ion conduction mechanism in dispersed phase polymer nanocomposites," Journal of Polymer Science, Part B: Polymer Physics, 47(1), pp. 60-71.

[133] Forsyth, M., MacFarlane, D. R., Best, A., Adebahr, J., Jacobsson, P., and Hill, A. J., 2002, "The effect of nano-particle TiO2 fillers on structure and transport in polymer electrolytes," Solid State Ionics, 147(3-4), pp. 203-211.

[134] Liu, Y., Lee, J. Y., and Hong, L., 2004, "In situ preparation of poly(ethylene oxide)-SiO2 composite polymer electrolytes," Journal of Power Sources, 129(2), pp. 303-311.

[135] Ramesh, S., and Wen, L. C., 2010, "Investigation on the effects of addition of SiO2 nanoparticles on ionic conductivity, FTIR, and thermal properties of nanocomposite PMMA-LiCF3SO3-SiO2," Ionics, 16(3), pp. 255-262.

[136] Merkel, T. C., Freeman, B. D., Spontak, R. J., He, Z., Pinnau, I., Meakin, P., and Hill, A. J., 2003, "Sorption, transport, and structural evidence for enhanced free volume in poly(4-methyl-2-pentyne)/fumed silica nanocomposite membranes," Chemistry of Materials, 15(1), pp. 109-123.

[137] Lue, S. J., Lee, D.-T., Chen, J.-Y., Chiu, C.-H., Hu, C.-C., Jean, Y. C., and Lai, J.-Y., 2008, "Diffusivity enhancement of water vapor in poly(vinyl alcohol)-fumed silica nano-composite membranes: Correlation with polymer crystallinity and free-volume properties," Journal of Membrane Science, 325(2), pp. 831-839.

[138] Takeuchi, H., Roe, R. J., and Mark, J. E., 1990, "MOLECULAR-DYNAMICS SIMULATION OF DIFFUSION OF SMALL MOLECULES IN POLYMERS .2. EFFECT OF FREE-VOLUME DISTRIBUTION," Journal of Chemical Physics, 93(12), pp. 9042-9048.

[139] Racko, D., Capponi, S., Alvarez, F., Colmenero, J., and Bartos, J., 2009, "The free-volume structure of a polymer melt, poly(vinyl methylether) from molecular dynamics simulations and cavity analysis," Journal of Chemical Physics, 131(6).

[140] Chang, K.-S., Chung, Y.-C., Yang, T.-H., Lue, S. J., Tung, K.-L., and Lin, Y.-F., 2012, "Free volume and alcohol transport properties of PDMS membranes: Insights of nano-structure and interfacial affinity from molecular modeling," Journal of Membrane Science, 417, pp. 119-130.

[141] Li, Q., Wood, E., and Ardebili, H., 2013, "Elucidating the mechanisms of ion conductivity enhancement in polymer nanocomposite electrolytes for lithium ion batteries," Applied Physics Letters, 102(24).

[142] Shen, L., and Chen, Z., 2007, "Critical review of the impact of tortuosity on diffusion," Chemical Engineering Science, 62(14), pp. 3748-3755.

[143] Munshi, M. Z. A., and Owens, B. B., 1988, "IONIC TRANSPORT IN POLY(ETHYLENE OXIDE) (PEO)-LIX POLYMERIC SOLID ELECTROLYTE," Polymer Journal, 20(7), pp. 577-586.

[144] Cui, T., Ding, J., and Chen, J. Z. Y., 2008, "Dynamics of a self-avoiding polymer chain in slit, tube, and cube confinements," Physical Review E, 78(6).

[145] Kimmich, R., Fatkullin, N., Mattea, C., and Fischer, E., 2005, "Polymer chain dynamics under nanoscopic confinements," Magnetic Resonance Imaging, 23(2), pp. 191-196.

[146] Gao, J., Qu, R., Tang, B., Wang, C., Ma, Q., and Sun, C., 2011, "Control of the aggregation behavior of silver nanoparticles in polyurethane matrix," Journal of Nanoparticle Research, 13(10), pp. 5289-5299.

[147] Oberdisse, J., 2006, "Aggregation of colloidal nanoparticles in polymer matrices," Soft Matter, 2(1), pp. 29-36.

[148] Ellison, J., Wykoff, G., Paul, A., Mohseni, R., and Vasiliev, A., 2014, "Efficient dispersion of coated silver nanoparticles in the polymer matrix," Colloids and Surfaces a-Physicochemical and Engineering Aspects, 447, pp. 67-70.

[149] Tang, C., Hackenberg, K., Fu, Q., Ajayan, P. M., and Ardebili, H., 2012, "High Ion Conducting Polymer Nanocomposite Electrolytes Using Hybrid Nanofillers," Nano Letters, 12(3), pp. 1152-1156.

[150] Pitawala, H. M. J. C., Dissanayake, M. A. K. L., and Seneviratne, V. A., 2007, "Combined effect of Al2O3 nano-fillers and EC plasticizer on ionic conductivity enhancement in the solid polymer electrolyte (PEO)(9)LiTf," Solid State Ionics, 178(13-14), pp. 885-888.

[151] Walls, H. J., Zhou, J., Yerian, J. A., Fedkiw, P. S., Khan, S. A., Stowe, M. K., and Baker, G. L., 2000, "Fumed silica-based composite polymer electrolytes: synthesis, rheology, and electrochemistry," Journal of Power Sources, 89(2), pp. 156-162.

[152] Yang, X., Zhang, F., Zhang, L., Zhang, T., Huang, Y., and Chen, Y., 2013, "A High-Performance Graphene Oxide-Doped Ion Gel as Gel Polymer Electrolyte for All-

Solid-State Supercapacitor Applications," Advanced Functional Materials, 23(26), pp. 3353-3360.

[153] Keplinger, C., Sun, J.-Y., Foo, C. C., Rothemund, P., Whitesides, G. M., and Suo, Z., 2013, "Stretchable, Transparent, Ionic Conductors," Science, 341(6149), pp. 984-987.

[154] Zhang, J., Huang, X., Wei, H., Fu, J., Liu, W., and Tang, X., 2011, "Preparation and electrochemical behaviors of composite solid polymer electrolytes based on polyethylene oxide with active inorganic-organic hybrid polyphosphazene nanotubes as fillers," New Journal of Chemistry, 35(3), pp. 614-621.

[155] Potts, J. R., Dreyer, D. R., Bielawski, C. W., and Ruoff, R. S., 2011, "Graphene-based polymer nanocomposites," Polymer, 52(1), pp. 5-25.

[156] Aravindan, V., and Vickraman, P., 2007, "Effects of TiO2 and ZrO2 nanofillers in LiBOB based PVdF/PVC composite polymer electrolytes (CPE)," Journal of Physics D-Applied Physics, 40(21), pp. 6754-6759.

[157] Uddin, N. M., Capaldi, F. M., and Farouk, B., 2011, "Molecular dynamics simulations of the interactions and dispersion of carbon nanotubes in polyethylene oxide/water systems," Polymer, 52(2), pp. 288-296.

[158] Cho, J., and Sun, C. T., 2007, "A molecular dynamics simulation study of inclusion size effect on polymeric nanocomposites," Computational Materials Science, 41(1), pp. 54-62.

[159] Smith, J. S., Bedrov, D., and Smith, G. D., 2003, "A molecular dynamics simulation study of nanoparticle interactions in a model polymer-nanoparticle composite," Composites Science and Technology, 63(11), pp. 1599-1605.

[160] Brown, D., Mele, P., Marceau, S., and Alberola, N. D., 2003, "A molecular dynamics study of a model nanoparticle embedded in a polymer matrix," Macromolecules, 36(4), pp. 1395-1406.

[161] Starr, F. W., Schroder, T. B., and Glotzer, S. C., 2002, "Molecular dynamics simulation of a polymer melt with a nanoscopic particle," Macromolecules, 35(11), pp. 4481-4492.

[162] Hong, B., and Panagiotopoulos, A. Z., 2012, "Molecular Dynamics Simulations of Silica Nanoparticles Grafted with Poly(ethylene oxide) Oligomer Chains," Journal of Physical Chemistry B, 116(8), pp. 2385-2395.

[163] Liu, J., Gao, Y., Cao, D., Zhang, L., and Guo, Z., 2011, "Nanoparticle Dispersion and Aggregation in Polymer Nanocomposites: Insights from Molecular Dynamics Simulation," Langmuir, 27(12), pp. 7926-7933.

[164] Borodin, O., Smith, G. D., Bandyopadhyaya, R., and Byutner, E., 2003, "Molecular dynamics study of the influence of solid interfaces on poly(ethylene oxide) structure and dynamics," Macromolecules, 36(20), pp. 7873-7883.

[165] Kuppa, V., and Manias, E., 2003, "Dynamics of poly(ethylene oxide) in nanoscale confinements: A computer simulations perspective," Journal of Chemical Physics, 118(7), pp. 3421-3429.

[166] Hackett, E., Manias, E., and Giannelis, E. P., 2000, "Computer simulation studies of PEO/layer silicate nanocomposites," Chemistry of Materials, 12(8), pp. 2161-2167.

[167] Siqueira, L. J. A., and Ribeiro, M. C. C., 2005, "Molecular dynamics simulation of the polymer electrolyte poly(ethylene oxide)/LiClO4. I. Structural properties," Journal of Chemical Physics, 122(19).

[168] Siqueira, L. J. A., and Ribeiro, M. C. C., 2006, "Molecular dynamics simulation of the polymer electrolyte poly(ethylene oxide)/LiClO4. II. Dynamical properties," Journal of Chemical Physics, 125(21).

[169] Halley, J. W., Duan, Y., Curtiss, L. A., and Baboul, A. G., 1999, "Lithium perchlorate ion pairing in a model of amorphous polyethylene oxide," Journal of Chemical Physics, 111(7), pp. 3302-3308.

[170] Duan, Y. H., Halley, J. W., Curtiss, L., and Redfern, P., 2005, "Mechanisms of lithium transport in amorphous polyethylene oxide," Journal of Chemical Physics, 122(5).

[171] Diddens, D., and Heuer, A., 2013, "Lithium Ion Transport Mechanism in Ternary Polymer Electrolyte-Ionic Liquid Mixtures: A Molecular Dynamics Simulation Study," Acs Macro Letters, 2(4), pp. 322-326.

[172] Laasonen, K., and Klein, M. L., 1995, "MOLECULAR-DYNAMICS SIMULATIONS OF THE STRUCTURE AND ION DIFFUSION IN POLY(ETHYLENE OXIDE)," Journal of the Chemical Society-Faraday Transactions, 91(16), pp. 2633-2638.

[173] Wu, H., and Wick, C. D., 2010, "Computational Investigation on the Role of Plasticizers on Ion Conductivity in Poly(ethylene oxide) LiTFSI Electrolytes," Macromolecules, 43(7), pp. 3502-3510.

[174] Neyertz, S., and Brown, D., 1996, "Local structure and mobility of ions in polymer electrolytes: A molecular dynamics simulation study of the amorphous PEO(x)NaI system," Journal of Chemical Physics, 104(10), pp. 3797-3809.

[175] Balbuena, P. B., Lamas, E. J., and Wang, Y. X., 2005, "Molecular modeling studies of polymer electrolytes for power sources," Electrochimica Acta, 50(19), pp. 3788-3795.

[176] Neyertz, S., Brown, D., and Thomas, J. O., 1995, "MOLECULAR-DYNAMICS SIMULATION OF THE CRYSTALLINE PHASE OF POLY(ETHYLENE OXIDE)-SODIUM IODIDE, PEO(3)NAI," Electrochimica Acta, 40(13-14), pp. 2063-2069.

[177] Aabloo, A., and Thomas, J., 2001, "Molecular dynamics simulation of lithium ion mobility in a PEO surface," Solid State Ionics, 143(1), pp. 83-87.

[178] Kasemagi, H., Klintenberg, M., Aabloo, A., and Thomas, J. O., 2001, "Molecular dynamics simulation of the effect of adding an Al2O3 nanoparticle to PEO-LiCl/LiBr/LiI systems," Journal of Materials Chemistry, 11(12), pp. 3191-3196.

[179] Liivat, A., Brandell, D., and Thomas, J. O., 2007, "A molecular dynamics study of ion-conduction mechanisms in crystalline low-M-w LiPF6 center dot PEO6," Journal of Materials Chemistry, 17(37), pp. 3938-3946.

[180] Brandell, D., Liivat, A., Kasemagi, H., Aabloo, A., and Thomas, J. O., 2005, "Molecular dynamics simulation of the LiPF6 center dot PEO6 structure," Journal of Materials Chemistry, 15(14), pp. 1422-1428.

[181] Forsyth, M., Payne, V. A., Ratner, M. A., Deleeuw, S. W., and Shriver, D. F., 1992, "MOLECULAR-DYNAMICS SIMULATIONS OF HIGHLY CONCENTRATED SALT-SOLUTIONS - STRUCTURAL AND TRANSPORT EFFECTS IN POLYMER ELECTROLYTES," Solid State Ionics, 53, pp. 1011-1026.

[182] Borodin, O., and Smith, G. D., 2000, "Molecular dynamics simulation study of LiI-doped diglyme and poly(ethylene oxide) solutions," Journal of Physical Chemistry B, 104(33), pp. 8017-8022.

[183] Lin, B., Boinske, P. T., and Halley, J. W., 1996, "A molecular dynamics model of the amorphous regions of polyethylene oxide," Journal of Chemical Physics, 105(4), pp. 1668-1681.

[184] Ferreira, B. A., Muller-Plathe, F., Bernardes, A. T., and De Almeida, W. B., 2002, "A comparison of Li+ transport in dimethoxyethane, poly(ethylene oxide) and poly(tetramethylene oxide) by molecular dynamics simulations," Solid State Ionics, 147(3-4), pp. 361-366.

[185] Karo, J., and Brandell, D., 2009, "A Molecular Dynamics study of the influence of side-chain length and spacing on lithium mobility in non-crystalline LiPF6 center dot PEOx; x=10 and 30," Solid State Ionics, 180(23-25), pp. 1272-1284.

[186] Borodin, O., Smith, G. D., Bandyopadhyaya, R., Redfern, P., and Curtiss, L. A., 2004, "Molecular dynamics study of nanocomposite polymer electrolyte based on poly(ethylene oxide)/LiBF4," Modelling and Simulation in Materials Science and Engineering, 12(3), pp. S73-S89.

[187] Kasemagi, H., Aabloo, A., Klintenberg, M. K., and Thomas, J. O., 2004, "Molecular dynamics simulation of the effect of nanoparticle fillers on ion motion in a polymer host," Solid State Ionics, 168(3-4), pp. 249-254.

[188] Boulet, P., Covency, P. V., and Stackhouse, S., 2004, "Simulation of hydrated Li+-, Na+- and K+-montmorillonite/polymer nanocomposites using large-scale molecular dynamics," Chemical Physics Letters, 389(4-6), pp. 261-267.

[189] Kasemagi, H., Klintenberg, M., Aabloo, A., and Thomas, J. O., 2003, "Molecular dynamics simulation of temperature and concentration dependence of the 'filler' effect for

the LiCl/PEO/Al2O3-nanoparticle system," Electrochimica Acta, 48(14-16), pp. 2273-2278.

[190] Borodin, O., and Smith, G. D., 2009, "Quantum Chemistry and Molecular Dynamics Simulation Study of Dimethyl Carbonate: Ethylene Carbonate Electrolytes Doped with LiPF6," Journal of Physical Chemistry B, 113(6), pp. 1763-1776.

[191] Ennari, J., Neelov, I., and Sundholm, F., 2000, "Molecular dynamics simulation of the structure of PEO based solid polymer electrolytes," Polymer, 41(11), pp. 4057-4063.

[192] Ennari, J., Pietila, L. O., Virkkunen, V., and Sundholm, F., 2002, "Molecular dynamics simulation of the structure of an ion-conducting PEO-based solid polymer electrolyte," Polymer, 43(20), pp. 5427-5438.

[193] Darinskii, A. A., Zarembo, A., Balabaev, N. K., Neelov, I. M., and Sundholm, F., 2006, "Molecular dynamic simulation of side-chain liquid crystalline elastomer," Macromolecular Symposia, 237, pp. 119-127.

[194] Costa, L. T., and Ribeiro, M. C. C., 2006, "Molecular dynamics simulation of polymer electrolytes based on poly(ethylene oxide) and ionic liquids. I. Structural properties," Journal of Chemical Physics, 124(18).

[195] Costa, D., Munao, G., Saija, F., and Caccamo, C., 2007, "Reference interaction site model and molecular dynamics study of structure and thermodynamics of methanol," Journal of Chemical Physics, 127(22).

[196] Lin, K.-J., and Maranas, J. K., 2012, "Cation Coordination and Motion in a Poly(ethylene oxide)-Based Single Ion Conductor," Macromolecules, 45(15), pp. 6230-6240.

[197] Humphrey, W., Dalke, A., and Schulten, K., 1996, "VMD: Visual molecular dynamics," Journal of Molecular Graphics & Modelling, 14(1), pp. 33-38.

[198] Slane, S., and Salomon, M., 1995, "COMPOSITE GEL ELECTROLYTE FOR RECHARGEABLE LITHIUM BATTERIES," Journal of Power Sources, 55(1), pp. 7-10.

[199] Li, Q., Sun, H. Y., Takeda, Y., Imanishi, N., Yang, J., and Yamamoto, O., 2001, "Interface properties between a lithium metal electrode and a poly(ethylene oxide) based composite polymer electrolyte," Journal of Power Sources, 94(2), pp. 201-205.

[200] Borghini, M. C., Mastragostino, M., Passerini, S., and Scrosati, B., 1995, "ELECTROCHEMICAL PROPERTIES OF POLYETHYLENE OXIDE-LI (CF3SO2)(2)N -GAMMA-LIALO2 COMPOSITE POLYMER ELECTROLYTES," Journal of the Electrochemical Society, 142(7), pp. 2118-2121.

[201] Mastragostino, M., Soavi, F., and Zanelli, A., 1999, "Improved composite materials for rechargeable lithium metal polymer batteries," Journal of Power Sources, 81, pp. 729-733.

[202] Chen, C. X., Depa, P., Sakai, V. G., Maranas, J. K., Lynn, J. W., Peral, I., and Copley, J. R. D., 2006, "A comparison of united atom, explicit atom, and coarse-grained simulation models for poly(ethylene oxide)," Journal of Chemical Physics, 124(23).

[203] Koirala, R., Gunugunuri, K. R., Pratsinis, S. E., and Smirniotis, P. G., 2011, "Effect of Zirconia Doping on the Structure and Stability of CaO-Based Sorbents for CO2 Capture during Extended Operating Cycles," Journal of Physical Chemistry C, 115(50), pp. 24804-24812.

[204] Yuan, M., Erdman, J., Tang, C., and Ardebili, H., 2014, "High performance solid polymer electrolyte with graphene oxide nanosheets," Rsc Advances, 4(103), pp. 59637-59642.

[205] Gao, S., Zhong, J., Xue, G., and Wang, B., 2014, "Ion conductivity improved polyethylene oxide/lithium perchlorate electrolyte membranes modified by graphene oxide," Journal of Membrane Science, 470, pp. 316-322.

[206] Shim, J., Kim, D.-G., Kim, H. J., Lee, J. H., Baik, J.-H., and Lee, J.-C., 2014, "Novel composite polymer electrolytes containing poly(ethylene glycol)-grafted graphene oxide for all-solid-state lithium-ion battery applications," Journal of Materials Chemistry A, 2(34), pp. 13873-13883.

[207] Akhtar, M. S., Kwon, S., Stadler, F. J., and Yang, O. B., 2013, "High efficiency solid state dye sensitized solar cells with graphene-polyethylene oxide composite electrolytes," Nanoscale, 5(12), pp. 5403-5411.

[208] Abbrent, S., Plestil, J., Hlavata, D., Lindgren, J., Tegenfeldt, J., and Wendsjo, A., 2001, "Crystallinity and morphology of PVdF-HFP-based gel electrolytes," Polymer, 42(4), pp. 1407-1416.

[209] Jiang, Z., Carroll, B., and Abraham, K. M., 1997, "Studies of some poly(vinylidene fluoride) electrolytes," Electrochimica Acta, 42(17), pp. 2667-2677.

[210] Yang, P., Liu, L., Li, L., Hou, J., Xu, Y., Ren, X., An, M., and Li, N., 2014, "Gel polymer electrolyte based on polyvinylidenefluoride-co-hexafluoropropylene and ionic liquid for lithium ion battery," Electrochimica Acta, 115, pp. 454-460.

[211] Wang, Y.-J., and Kim, D., 2007, "Crystallinity, morphology, mechanical properties and conductivity study of in situ formed PVdF/LiClO4/TiO2 nanocomposite polymer electrolytes," Electrochimica Acta, 52(9), pp. 3181-3189.

[212] Stephan, A. M., Nahm, K. S., Kumar, T. P., Kulandainathan, M. A., Ravi, G., and Wilson, J., 2006, "Nanofiller incorporated poly(vinylidene fluoride-hexafluoropropylene) (PVdF-HFP) composite electrolytes for lithium batteries," Journal of Power Sources, 159(2), pp. 1316-1321.

[213] Chang, B.-Y., and Park, S.-M., 2010, "Electrochemical Impedance Spectroscopy," Annual Review of Analytical Chemistry, Vol 3, 3, pp. 207-229.

[214] Stephan, A. M., 2006, "Review on gel polymer electrolytes for lithium batteries," European Polymer Journal, 42(1), pp. 21-42.

[215] Ito, Y., Kanehori, K., Miyauchi, K., and Kudo, T., 1987, "IONIC-CONDUCTIVITY OF ELECTROLYTES FORMED FROM PEO-LICF3SO3 COMPLEX WITH LOW-MOLECULAR-WEIGHT POLY(ETHYLENE GLYCOL)," Journal of Materials Science, 22(5), pp. 1845-1849.

[216] Abraham, K. M., and Alamgir, M., 1990, "LI+-CONDUCTIVE SOLID POLYMER ELECTROLYTES WITH LIQUID-LIKE CONDUCTIVITY," Journal of the Electrochemical Society, 137(5), pp. 1657-1657.

[217] Bohnke, O., Rousselot, C., Gillet, P. A., and Truche, C., 1992, "GEL ELECTROLYTE FOR SOLID-STATE ELECTROCHROMIC CELL," Journal of the Electrochemical Society, 139(7), pp. 1862-1865.

[218] Appetecchi, G. B., Croce, F., and Scrosati, B., 1995, "Kinetics and Stability of the Lithium Electrode in Poly(methylmethacrylate)-based gel Electrolytes," Electrochimica Acta, 40(8), pp. 991-997.

[219] Ye, H., Huang, J., Xu, J. J., Khalfan, A., and Greenbaum, S. G., 2007, "Li ion conducting polymer gel electrolytes based on ionic liquid/PVDF-HFP blends," Journal of the Electrochemical Society, 154(11), pp. A1048-A1057.

[220] Gentili, V., Panero, S., Reale, P., and Scrosati, B., 2007, "Composite gel-type polymer electrolytes for advanced, rechargeable lithium batteries," Journal of Power Sources, 170(1), pp. 185-190.

[221] Meyer, W. H., 1998, "Polymer electrolytes for lithium-ion batteries," Advanced Materials, 10(6), pp. 439-+.

[222] Lewandowski, A., and Swiderska-Mocek, A., 2009, "Ionic liquids as electrolytes for Li-ion batteries-An overview of electrochemical studies," Journal of Power Sources, 194(2), pp. 601-609.

[223] Armand, M., Endres, F., MacFarlane, D. R., Ohno, H., and Scrosati, B., 2009, "Ionic-liquid materials for the electrochemical challenges of the future," Nature Materials, 8(8), pp. 621-629.

[224] Kunze, M., Jeong, S., Paillard, E., Schoenhoff, M., Winter, M., and Passerini, S., 2011, "New Insights to Self-Aggregation in Ionic Liquid Electrolytes for High-Energy Electrochemical Devices," Advanced Energy Materials, 1(2), pp. 274-281.

[225] Shin, J.-H., Henderson, W. A., Tizzani, C., Passerini, S., Jeong, S.-S., and Kim, K.-W., 2006, "Characterization of solvent-free polymer electrolytes consisting of ternary

PEO-LiTFSI-PYR14 TFSI," Journal of the Electrochemical Society, 153(9), pp. A1649-A1654.

[226] Bansal, D., Cassel, F., Croce, F., Hendrickson, M., Plichta, E., and Salomon, M., 2005, "Conductivities and transport properties of gelled electrolytes with and without an ionic liquid for Li and Li-ion batteries," Journal of Physical Chemistry B, 109(10), pp. 4492-4496.

[227] Zheng, H. H., Jiang, K., Abe, T., and Ogumi, Z., 2006, "Electrochemical intercalation of lithium into a natural graphite anode in quaternary ammonium-based ionic liquid electrolytes," Carbon, 44(2), pp. 203-210.

[228] Nakagawa, H., Izuchi, S., Kuwana, K., Nukuda, T., and Aihara, Y., 2003, "Liquid and polymer gel electrolytes for lithium batteries composed of room-temperature molten salt doped by lithium salt," Journal of the Electrochemical Society, 150(6), pp. A695-A700.

[229] Garcia, B., Lavallee, S., Perron, G., Michot, C., and Armand, M., 2004, "Room temperature molten salts as lithium battery electrolyte," Electrochimica Acta, 49(26), pp. 4583-4588.

[230] Galinski, M., Lewandowski, A., and Stepniak, I., 2006, "Ionic liquids as electrolytes," Electrochimica Acta, 51(26), pp. 5567-5580.

[231] Plechkova, N. V., and Seddon, K. R., 2008, "Applications of ionic liquids in the chemical industry," Chemical Society Reviews, 37(1), pp. 123-150.

[232] Welton, T., 1999, "Room-temperature ionic liquids. Solvents for synthesis and catalysis," Chemical Reviews, 99(8), pp. 2071-2083.

[233] Rogers, R. D., and Seddon, K. R., 2003, "Ionic liquids - Solvents of the future?," Science, 302(5646), pp. 792-793.

[234] Earle, M. J., and Seddon, K. R., 2000, "Ionic liquids. Green solvents for the future," Pure and Applied Chemistry, 72(7), pp. 1391-1398.

[235] Bonhote, P., Dias, A. P., Papageorgiou, N., Kalyanasundaram, K., and Gratzel, M., 1996, "Hydrophobic, highly conductive ambient-temperature molten salts," Inorganic Chemistry, 35(5), pp. 1168-1178.

[236] Every, H. A., Bishop, A. G., MacFarlane, D. R., Oradd, G., and Forsyth, M., 2004, "Transport properties in a family of dialkylimidazolium ionic liquids," Physical Chemistry Chemical Physics, 6(8), pp. 1758-1765.

[237] McEwen, A. B., Ngo, H. L., LeCompte, K., and Goldman, J. L., 1999, "Electrochemical properties of imidazolium salt electrolytes for electrochemical capacitor applications," Journal of the Electrochemical Society, 146(5), pp. 1687-1695.

[238] Papageorgiou, N., Athanassov, Y., Armand, M., Bonhote, P., Pettersson, H., Azam, A., and Gratzel, M., 1996, "The performance and stability of ambient temperature molten salts for solar cell applications," Journal of the Electrochemical Society, 143(10), pp. 3099-3108.

[239] MacFarlane, D. R., Golding, J., Forsyth, S., Forsyth, M., and Deacon, G. B., 2001, "Low viscosity ionic liquids based on organic salts of the dicyanamide anion," Chemical Communications(16), pp. 1430-1431.

[240] MacFarlane, D. R., Forsyth, S. A., Golding, J., and Deacon, G. B., 2002, "Ionic liquids based on imidazolium, ammonium and pyrrolidinium salts of the dicyanamide anion," Green Chemistry, 4(5), pp. 444-448.

[241] Saito, Y., Umecky, T., Niwa, J., Sakai, T., and Maeda, S., 2007, "Existing condition and migration property of ions in lithium electrolytes with ionic liquid solvent," Journal of Physical Chemistry B, 111(40), pp. 11794-11802.

[242] Hayamizu, K., Aihara, Y., Nakagawa, H., Nukuda, T., and Price, W. S., 2004, "Ionic conduction and ion diffusion in binary room-temperature ionic liquids composed of emim BF4 and LiBF4," Journal of Physical Chemistry B, 108(50), pp. 19527-19532.

[243] He, Y.-B., Li, B., Liu, M., Zhang, C., Lv, W., Yang, C., Li, J., Du, H., Zhang, B., Yang, Q.-H., Kim, J.-K., and Kang, F., 2012, "Gassing in Li4Ti5O12-based batteries and its remedy," Scientific Reports, pp. 2.

[244] Engheta, N., Salandrino, A., and Alu, A., 2005, "Circuit elements at optical frequencies: Nanoinductors, nanocapacitors, and nanoresistors," Physical Review Letters, 95(9), pp. 095504.

[245] Scott, J. F., 1998, “High-dielectric constant thin films for dynamic random access memories (DRAM),” Annual Reviews of materials Science, 28, pp.79-100.

[246] Son, J. Y., Shin, Y.-H., Kim, H., and Jang, H. M., 2010, "NiO Resistive Random Access Memory Nanocapacitor Array on Graphene," Acs Nano, 4(5), pp. 2655-2658.

[247] Nagaraj, B., Sawhney, T., Perusse, S., Aggarwal, S., Ramesh, R., Kaushik, V. S., Zafar, S., Jones, R. E., Lee, J. H., Balu, V., and Lee, J., 1999, "(BaSr)TiO3 thin films with conducting perovskite electrodes for dynamic random access memory applications," Applied Physics Letters, 74(21), pp. 3194-3196.

[248] Ekanayake, S. R., Cortie, M. B., and Ford, M. J., 2004, "Design of nanocapacitors and associated materials challenges," Current Applied Physics, 4(2-4), pp. 250-254.

[249] Cortie, M. B., Zareie, M. H., Ekanayake, S. R., and Ford, M. J., 2005, "Conduction, storage, and leakage in particle-on-SAM nanocapacitors," Ieee Transactions on Nanotechnology, 4(4), pp. 406-414.

[250] Saha, S. K., DaSilva, M., Hang, Q., Sands, T., and Janes, D. B., 2006, "A nanocapacitor with giant dielectric permittivity," Nanotechnology, 17(9), pp. 2284-2288.

[251] Sohn, J. I., Kim, Y. S., Nam, C., Cho, B. K., Seong, T. Y., and Lee, S., 2005, "Fabrication of high-density arrays of individually isolated nanocapacitors using anodic aluminum oxide templates and carbon nanotubes," Applied Physics Letters, 87(12).

[252] Ekanayake, S. R., Ford, M., and Cortie, M., 2004, Metal-insulator-metal (MIM) nanocapacitors and effects of material properties on their operation, Materials Forum, 27, 15-20 (2004).

[253] Hunter, D. N., Pickering, S. L., and Jia, D., 2007, "Thin-film nanocapacitor and its characterization," European Journal of Physics, 28(2), pp. 161-170.

[254] Rabe, K. M., 2006, "Nanoelectronics - New life for the 'dead layer'," Nature Nanotechnology, 1(3), pp. 171-U174.

[255] Cohen, R., 2009, "NANOCAPACITORS Undead layers breathe new life," Nature Materials, 8(5), pp. 366-368.

[256] Ekanayake, S. R., Rodanski, B. S., Cortie, M. B., Ford, A. J., and Ieee, I., 2003, "Quantum electrical characteristics of nanocapacitors," 2003 Third Ieee Conference on Nanotechnology, Vols One and Two, Proceedings, pp. 756-759.

[257] Park, H. C., and Ahn, K.-H., 2008, "Admittance and noise in an electrically driven nanostructure: Interplay between quantum coherence and statistics," Physical Review Letters, 101(11).

[258] Mead, C. A., 1961, "ANOMALOUS CAPACITANCE OF THIN DIELECTRIC STRUCTURES," Physical Review Letters, 6(10), pp. 545-&.

[259] Kim, D. J., Jo, J. Y., Kim, Y. S., Chang, Y. J., Lee, J. S., Yoon, J. G., Song, T. K., and Noh, T. W., 2005, "Polarization relaxation induced by a depolarization field in ultrathin ferroelectric BaTiO3 capacitors," Physical Review Letters, 95(23).

[260] Sinnamon, L. J., Bowman, R. M., and Gregg, J. M., 2001, "Investigation of dead-layer thickness in SrRuO3/Ba0.5Sr0.5TiO3/Au thin-film capacitors," Applied Physics Letters, 78(12), pp. 1724-1726.

[261] Stengel, M., and Spaldin, N. A., 2006, "Origin of the dielectric dead layer in nanoscale capacitors," Nature, 443(7112), pp. 679-682.

[262] Zhou, C., and Newns, D. M., 1997, "Intrinsic dead layer effect and the performance of ferroelectric thin film capacitors," Journal of Applied Physics, 82(6), pp. 3081-3088.

[263] Black, C. T., and Welser, J. J., 1999, "Electric-field penetration into metals: Consequences for high-dielectric-constant capacitors," Ieee Transactions on Electron Devices, 46(4), pp. 776-780.

[264] Natori, K., Otani, D., and Sano, N., 1998, "Thickness dependence of the effective dielectric constant in a thin film capacitor," Applied Physics Letters, 73(5), pp. 632-634.

[265] Saad, M. M., Baxter, P., Bowman, R. M., Gregg, J. M., Morrison, F. D., and Scott, J. F., 2004, "Intrinsic dielectric response in ferroelectric nano-capacitors," Journal of Physics-Condensed Matter, 16(41), pp. L451-L456.

[266] Hong, J., Catalan, G., Scott, J. F., and Artacho, E., 2010, "The flexoelectricity of barium and strontium titanates from first principles," Journal of Physics-Condensed Matter, 22(11).

[267] Resta, R., 2010, "Towards a Bulk Theory of Flexoelectricity," Physical Review Letters, 105(12).

[268] Suresh, S., 2001, "Graded materials for resistance to contact deformation and damage," Science, 292(5526), pp. 2447-2451.

[269] Mindlin, R. D., 1968, "Polarization gradient in elastic dielectrics," International Journal of Solids and Structures, 4(6), pp. 637-642.

[270] D. Mindlin, R., 1969, "Continuum and lattice theories of influence of electromechanical coupling on capacitance of thin dielectric films," International Journal of Solids and Structures, 5(11), pp. 1197-1208.

[271] Majdoub, M. S., Maranganti, R., and Sharma, P., 2009, "Understanding the origins of the intrinsic dead layer effect in nanocapacitors," Physical Review B, 79(11), pp. 115412.

[272] Sharma, N. D., Landis, C. M., and Sharma, P., 2010, "Piezoelectric thin-film superlattices without using piezoelectric materials," Journal of Applied Physics, 108(2), pp. 024304.

Appendix A

Mitigating the Dead-layer Effect in Nanocapacitors Using Graded Dielectric Films

1. Introduction

Nanocapacitors have received considerable attention in recent years due to the promise of high energy and power densities and utilization in nanoelectronic applications [244-246]. Using high dielectric constant materials (i.e., $BaTiO_3$ and $SrTiO_3$ with perovskite structures [247]) and nanoscale dielectric films, the capacitance of nanocapacitors can theoretically approach very high levels. However, there are certain challenges and bottlenecks that must be overcome [248, 249]. Several studies have addressed design, materials and fabrication issues associated with nanocapacitors [250-253], unexpected low capacitance or "dead-layer" effect [254, 255], and quantum electrical phenomena in nanocapacitors [256, 257]. In this study, we focused on mitigating the "dead-layer" effect by grading the dielectric film properties.

The promise of high energy density in nanocapacitors emerges from the basic capacitance and energy storage theories. As the classical capacitance is inversely proportional to the distance between the parallel plates and the energy stored in a capacitor is directly proportional to the capacitance, transitioning from microscale to nanoscale capacitor can lead to several orders of magnitude increase in capacitance and subsequently, significant enhancement in energy storage. However, experimental

measurements have shown rather unexpected results and the capacitance of nanocapacitors are found to be much lower than that predicted from classical theories [258-260]. Recent *ab intio* simulation [261] by Stengel and Spaldin has verified that for a 2.7 nm $SrTiO_3$ (STO) capacitor, the actual capacitance is 258 $fF\mu m^{-2}$ rather than the classical theory prediction which is 1600 $fF\mu m^{-2}$ (Figure A1a). It appears as if a layer of very low permittivity ("dead layer") is present at the metal/dielectric interface, *"C_i"*, and when in series with the dielectric film, *"C_d"*, causes a dramatic drop in the overall capacitance, *"C_{eff}"*. The relation of those capacitances is

$$\frac{1}{c_{eff}} = \frac{1}{C_i} + \frac{1}{C_d} + \frac{1}{C_i}. \qquad \text{(A1)}$$

Thus, the term "dead layer" has been coined in relation to this observed phenomenon [262-264]. The overall capacitance of is The cause of dead-layer effect was initially attributed to the material defects, but improved manufacturing process [265] disproved this notion, verified by the *ab intio* simulation [261], and the problem of low capacitance continued to persist even in defect-free nanocapacitors. Recent studies have identified two main causes for the "dead-layer" effect: flexoelectricity and incomplete screening. Flexoelectricity refers to the behavior of centrosymmetric, non-piezoelectric materials (Figure A1b) that when subjected to non-uniform strain, can exhibit polarization [266, 267]. Incomplete screening refers to the phenomenon where the electric field penetrates into the metal as shown in Figure A1c [254].

In order to mitigate the "dead-layer" effect in nanocapacitors, we can focus on either the electrodes or the dielectric films. The results of the *ab initio* simulation [261] by

Stengel and Spaldin indicated that using metals such as P_t or A_u with shorter electronic screening length could reduce the dead-layer effect. On the other hand, since graded materials have been used to improve mechanical and electrical performances [268], in this study, we explore graded dielectric films to enhance the capacitance of nanocapacitors.

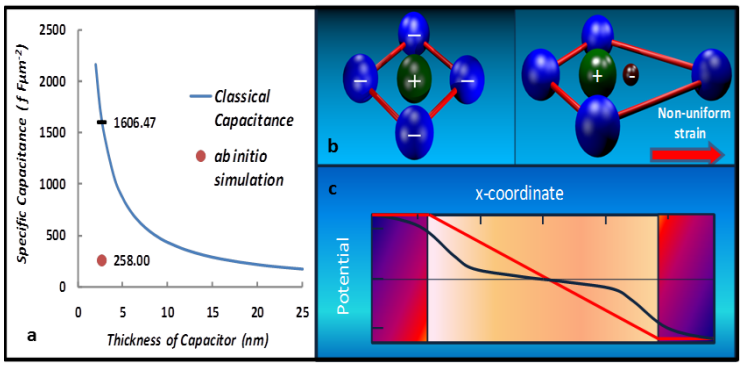

Figure A1. (a) Classical capacitance (per unit area) prediction ($C = \varepsilon/d$, $\varepsilon_r = 490$), at nanoscale dielectric film lengths and *ab intio* simulation result (b) Schematics of centrosymmetric nonpiezoelectric material exhibiting polarization when subjected to non-uniform strain (c) Incomplete screening caused by electric field penetration into electrode metal.

2. Theoretical Analysis

Capacitance is defined as the ratio of free charge to the voltage drop. Using Gauss's law, we can relate the electric field, *"E"*, polarization vector, *"P"*, and permittivity, *"ε_o"*, to free charge density, "ρ_f", in the capacitor by Equation A2

$$\nabla \cdot \left(\varepsilon_0 \vec{E} + \vec{P}\right) = \rho_f \ . \qquad \text{(A2)}$$

The term inside the parenthesis in Equation A2 is known as the electric displacement, *"$\vec{D}$"*.

For a parallel-plate capacitor, the magnitude of electric displacement is equal to the free charge density at the plate surface and the direction is from positive to negative electrode. Therefore, the specific capacitance can be expressed as

$$C_s = \frac{D}{V}. \qquad \text{(A3)}$$

2.1. Homogeneous dielectric film

For the homogeneous dielectric film capacitor system illustrated in Figure A2, we can use Mindlin's model [269, 270] for 1-D case to describe the relations between three independent fields, namely displacement *"u"*, polarization *"P"*, and electric potential "ϕ". The governing equations can be expressed as

$$\begin{cases} c\partial^2 u + d\partial^2 P = 0 \\ d\partial^2 u + b\partial^2 P - aP - \partial\phi = 0 \\ -\varepsilon_0 \partial^2 \phi + \partial P = 0 \end{cases}, \qquad \text{(A4)}$$

where "*c*" is the elastic constant, "*d*" is a coupling factor that addresses both polarization-gradient to strain and polarization to strain-gradient coupling, "*b*" is the polarization-gradient coupling factor, and *"a"* is the reciprocal dielectric susceptibility ($\varepsilon_o a = \eta^{-1}$) [269].

The boundary conditions are

$$\begin{cases} (c\partial u + d\partial P)_{x=\pm h} = 0 \\ P(-h) = P(h) = -\varepsilon_0 k\eta V_d/h \\ (\phi)_{x=\pm h} = \pm V_d \end{cases}. \qquad \text{(A5)}$$

Where *"h"* is the half thickness of the dielectric film, *"k"* is the penetration constant, *"η"* is dielectric susceptibility, and V_d is the voltage at the metal electrodes. The parameter *"k"* controls the depth at which the electric filed penetration occurs [270, 271].

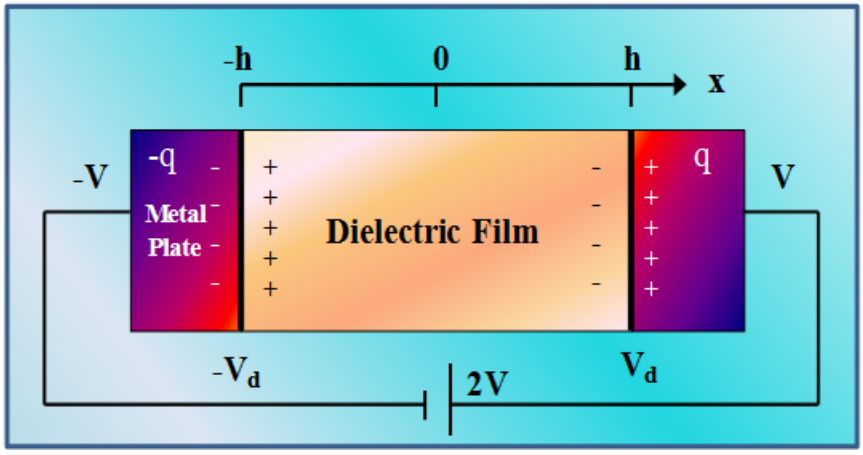

Figure A2. Schematic of a parallel-plate capacitor.

The solution to the specific capacitance is obtained as

$$C_{s0} = \frac{\varepsilon_0 \partial\phi - P}{2V_d} = \frac{\varepsilon_0 \varepsilon_r}{2h} \frac{1+\left(\frac{k\eta l}{h}\right)\tanh\left(\frac{h}{l}\right)}{1+\left(\frac{\eta l}{h}\right)\tanh\left(\frac{h}{l}\right)} = \frac{\varepsilon_0 \varepsilon_r}{2h} \frac{\frac{1}{\varepsilon_r - 1}+\left(\frac{kl}{h}\right)\tanh\left(\frac{h}{l}\right)}{\frac{1}{\varepsilon_r - 1}+\left(\frac{l}{h}\right)\tanh\left(\frac{h}{l}\right)}, \quad \text{(A6)}$$

where "ε_r" is the relative permittivity and

$$l = \sqrt{(b - d^2/c)/(a + 1/\varepsilon_0)}\,. \quad \text{(A7)}$$

The parameter *"l"* is defined as the longitudinal flexoelectric length scale and it is a real number due to the positive definiteness of energy density [269]. This solution can be found in Mindlin's papers [269, 270] and recent work by P. Sharma's group [271].

2.2.Graded dielectric film

In order to increase the effective capacitance, the properties of the dielectric film are graded (Figure A3a) with a linear grading function as depicted in Equation A8 and Figure A3b. The main graded properties are relative permittivity *"ε_r"* (Equation A9) and elastic constant *"c"* (Equation A10). Those equations are listed below

$$g(x) = w\left(\frac{x+h}{h}\right), \qquad \text{(A8)}$$

$$\varepsilon_r = \varepsilon_{r0}\{1 + \lambda g(x)\};\ \ 0 \le \lambda \le 1, \text{ and} \qquad \text{(A9)}$$

$$c = c_0\{1 + \lambda g(x)\}, \qquad \text{(A10)}$$

where w is the grading direction and the subscript "0"represents the original (ungraded) parameters. The overall capacitance of a graded film can be determined by using perturbation theory as

$$C_s = C_{s0} + \lambda C_{s1}, \qquad \text{(A11)}$$

where *"C_{s0}"* is the capacitance of the original homogeneous film (Equation A6) and *"C_{s1}"* is the added capacitance due to grading. It should be noted that the parameter "λ" in Equation A10 and A11 has different meanings, respectively. In Equation A10, it is related to how you grade the films. However, in Equation A11, it is just a number more less than 1 which comes from the perturbation theory. In our current work, we assume they are identical (=0.1) to make the calculation simple.

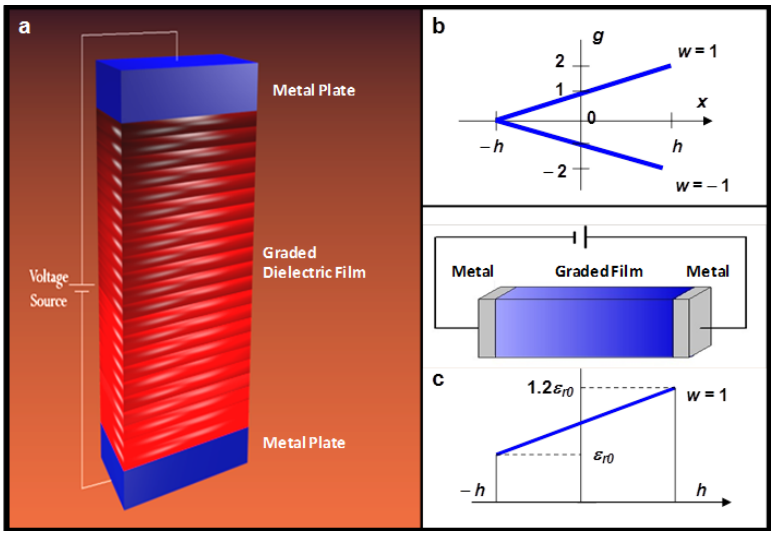

Figure A3. (a) The capacitor with graded dielectric film (b) Linear grading function *g(x)* (c) Dielectric film with graded relative permittivity *"ε_r"*.

First, we grade the relative permittivity *"ε_r"* and elastic constant *"c"*, separately. When we grade *"ε_r"* the relation between the coefficients *"a"* and *"ε_r"* should be considered. According to Equation A9 and the following relation

$$a\varepsilon_0 = (\varepsilon_r - 1)^{-1}\,, \qquad \text{(A12)}$$

we obtain

$$a^{-1} = a_0^{-1}\{1 + \lambda g(x)\} + \varepsilon_0 \lambda g(x)\,. \qquad \text{(A13)}$$

By substituting Equation A13 into the G.E and B.C. equations (Equation A4, A5), we found that the added capacitance due to grading *"ε_r"* only is

$$C_{s1} = -w\frac{1}{4a_0hV_d\eta_0\left(h-l\eta_0+e^{2h/l}(h+l\eta_0)\right)}e^{\frac{h}{l}}\left(-4a_0A_2h^2\cosh\left(\frac{h}{l}\right)+2l(2a_0A_2h+\right.$$

$$\left.V_d(k_1+k_2+2a_0k_2\varepsilon_0)\eta_0)\sinh\left(\frac{h}{l}\right)+a_0B_2h\left(2h-lsinh\left(\frac{2h}{l}\right)\right)\right). \quad \text{(A14)}$$

The added capacitance due to grading *"c"* only is

$$C_{s1} = -w\frac{B_1d\varepsilon_0\eta_0\left(-2h+lsinh\left(\frac{2h}{l}\right)\right)}{8l^2V_d\left(h\cosh\left(\frac{h}{l}\right)+l\eta_0\sinh\left(\frac{h}{l}\right)\right)}. \quad \text{(A15)}$$

Then, we grade both *"c"* (w=w_1= −1) and *"ε_r"* (w=w_2=1), simultaneously, to obtain

$$C_{s1} = \frac{1}{8a_0hl^2V_d\eta_0\left(h-l\eta_0+e^{2h/l}(h+l\eta_0)\right)}e^{-\frac{h}{l}}\left(-2e^{\frac{h}{l}}\left(-1+e^{\frac{2h}{l}}\right)(k_1+k_2)l^3V_d\eta_0(1+\right.$$

$$\eta_0)w_2+a_0\left(4A_2e^{\frac{h}{l}}hl^2\left(h+e^{\frac{2h}{l}}(h-l)+l\right)(1+\eta_0)w_2+2e^{\frac{2h}{l}}\left(-4k_2l^3V_d\varepsilon_0(1+\right.\right.$$

$$\left.\left.\left.\eta_0)\sinh\left(\frac{h}{l}\right)w_2+h(-B_1f\varepsilon_0\eta_0^2w_1+B_2l^2(1+\eta_0)w_2)\left(-2h+lsinh\left(\frac{2h}{l}\right)\right)\right)\right)\right), \quad \text{(A16)}$$

where the parameters B_1, B_2, B_3, A_2, and A_3 are defined as [271]

$$B_3 = (1-k_0)\eta_0V_d/[\eta_0\,sinh\left(\frac{h}{l}\right)+\left(\frac{h}{l}\right)cosh\left(\frac{h}{l}\right)] \ ,$$

$$A_3 = (B_3/\eta_0l)cosh\,(h/l)+k_0V_d/h] \ ,$$

$$A_2 = -\varepsilon_0\eta_0A_3;\ B_2 = \varepsilon_0B_3/l = -c_0B_1d \ , \text{and}$$

$$k_1 = k_0 = 0.3;\ k_2 = 1.2k_0 = 0.36. \qquad \text{(A17)}$$

The details of solving the PDEs can be found in the appendix.

3. Results and discussion

The material constant values used in the calculations of specific capacitance for the 2.7 nm $SrTiO_3$ nanocapacitor are listed in Table A1[272].

Table A1. Selected parameters and their values for $SrTiO_3$ dielectric film.

Parameter	Value	Units
ε_r	3.00×10^{2}	unitless
b	4.14×10^{-6}	Nm^4/C^2
c	3.5×10^{11}	N/m^2
d	-1.2×10^{3}	Nm/C

The results of the specific capacitance of uniform and graded dielectric films are tabulated in Table A2. The relationships between the original capacitance *"C_{s0}"* and the added capacitance *"C_{s1}"* (for three different grading cases) with the longitudinal flexoelectric length scale *"l"* and other parameters are shown in Figure A4 and A5.

Table A2. Specific capacitance of uniform and graded dielectric film.

Capacitance Parameter	Graded Parameter	Grading Direction, W	Specific Capacitance ($fF\mu m^{-2}$)	Added Capacitance $0.1*C_{s1}$ ($fF\mu m^{-2}$)	Enhancement $0.1*C_{s1}/C_{s0}$
C_{s0}	Not Graded	0	301.65	0	0%
C_{s1}	ε_r	1	320.895	32.09	10.64%
C_{s1}	c	-1	495.701	49.57	16.43%
C_{s1}	ε_r & c	1&-1	816.596	81.66	27.07%

From Figure A4, we notice that the capacitance exhibits linear behavior with respect to the relative permittivity, which can also be verified by inspecting Equation A6, A7 and A12. Since we generally use materials with high relative permittivity (in the order of 10^2 or 10^3), the constant *"a"* will be several orders of magnitude smaller than *"*$\frac{1}{\varepsilon_0}$*"* (Equation A12) and similarly, the term *"*$\frac{1}{\varepsilon_r - 1}$*"* will be several orders smaller than the rest of the summation (Equation A6). Consequently, changing of *"*ε_r*"* does not affect the value of *"l"* and furthermore, the second fraction of Equation A6. Considering the linear grading function *g(x)* in the case of *w*=1, its range is [0, 2]. Therefore, the graded relative permittivity *"*ε_r*"* is in the range of $[\varepsilon_{r0}, 1.2\varepsilon_{r0}]$. According to the linear relation shown in Figure 4A, the overall capacitance of the dielectric film with graded *"*ε_r*"* based on ε_r=300 should fall into the range of [301.65 $fF\mu m^{-2}$, 360.683 $fF\mu m^{-2}$] which includes our result of 320.895 $fF\mu m^{-2}$.

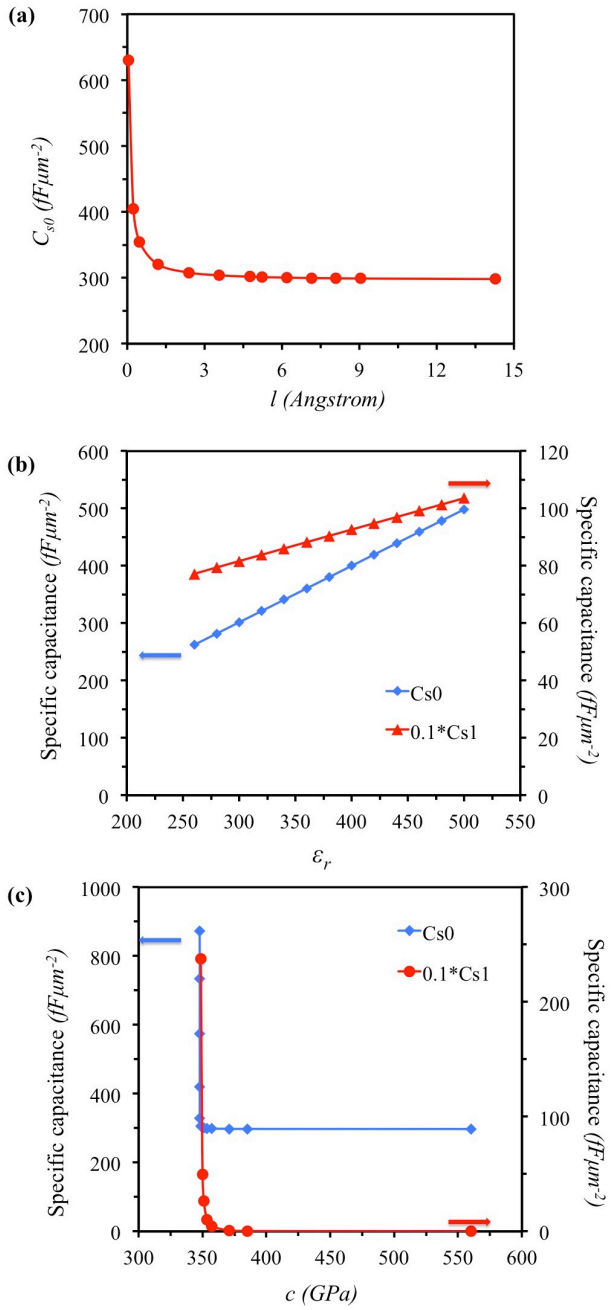

Figure A4. The relations between *"C_{s0}"* and *"0.1*C_{s1}"* (due to grading either *"c"* or *"ε_r"*) with *"l"* (a), *"ε_r"* (b), and *"c"* (c), respectively.

For the case of grading *"c"*, we have found a large window of capacitance enhancement. That can be attributed to the high sensitivity of "*l"* with respect to the

values of *"b"*, *"c"* and *"d"* and thus, its impact on the overall capacitance. Generally, increasing *"l"* will lead to reduction in capacitance. We observed a critical value of "*l*" around 1 Å below which the curve is very sharp. Above this value (*l*=1 Å), the curve is nearly flat (slightly decreasing with *"l"*). Therefore, there are corresponding critical values of *"b"*, *"c"* and *"d"* (Equation A7). We have found that below those values, the added capacitance becomes unstable, i.e., a slight change in the parameter will result in a very large added capacitance (Figure A4 and A5). Thus, it is recommended to use parametric values above the critical points to remain in the "stable" regions of the C_{s1} curves.

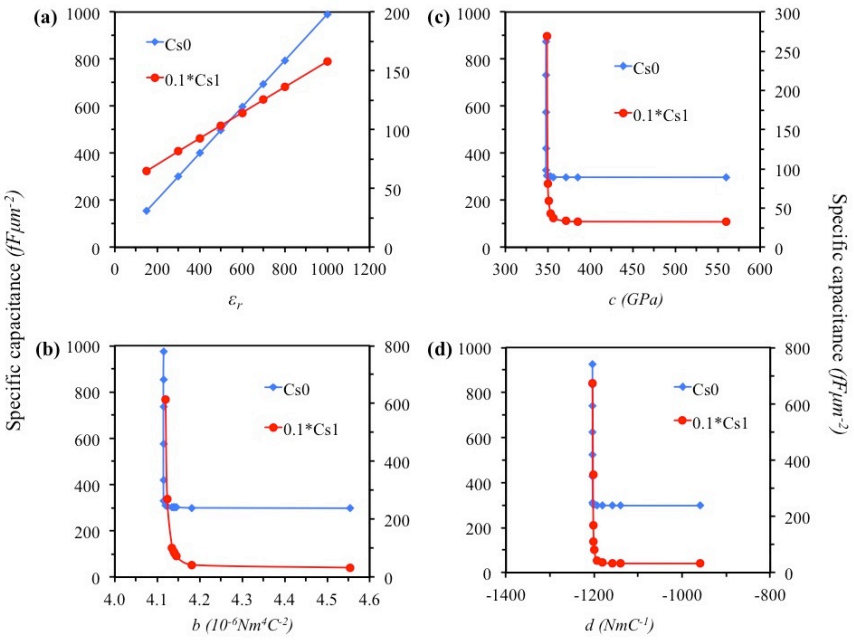

Figure A5. The relations between *"C_{s0}"* and *"0.1*C_{s1}"* (due to grading both *"c"* and *"ε_r"*) with *"ε_r"* (a), *"b"* (b), *"c"* (c), and *"d"* (d).

Based on the parametric values we used for the 2.7 nm $SrTiO_3$ nanocapacitor (Table A1), larger capacitance enhancement was achieved by combined grading of *"ε_r"* with *w*

=1 and *"c"* with $w = -1$. The results of the original capacitance *"C_{s0}"*, the added capacitance *"0.1*C_{s1}"*, and the total capacitance *"C_s"* of different size nanocapacitors are shown in Figure A6. For $2h$=2.7nm, the capacitance enhancement is found to be as large as 27%. Thus, based on our results, grading appears to be an effective method for enhancing capacitance in nanocapacitors.

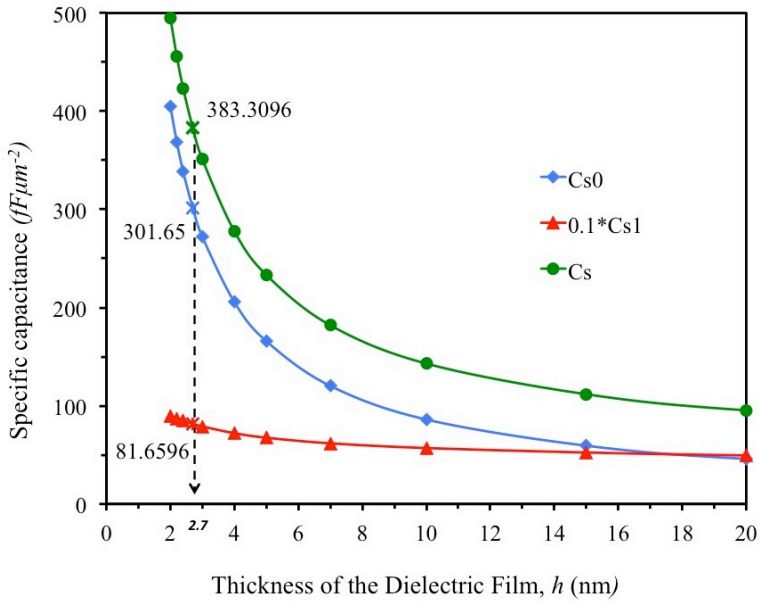

Figure 6. The change of the original (*"C_{s0}"*), added (*"0.1*C_{s1}"*) and overall (*"C_s"*) specific capacitance (due to grading both *"c"* and *"ε_r"*) as the thickness of the dielectric film increases.

4. Conclusion

By using perturbation theory, we have calculated the enhancements of capacitance due to grading of selected properties of the dielectric films in the parallel-plate nanocapacitors. Combined grading of the relative permittivity *"ε_r"* and the elastic constant *"c"*, resulted in the enhancement of 27% for the 2.7nm $SrTiO_3$ nanocapacitors. We also studied the impact of various parameters on the capacitance. Higher *"ε_r"* and

lower longitudinal flexoelectric length scale *"l"* will lead to higher capacitance enhancement especially when *"l"* reduces to 1 Å. However, the value of *"l"* was found to be very sensitive around 1 Å with altering "b", *"c"* and *"d"*.

Appendix B

Table B1. The force field parameters used in the Chapter III (Equation 3.1 and 3.2)

Bonds	K_{ij} (kcal mol^{-1} Å^{-2})	r_0 (Å)		
C-C	309.194	1.513		
C-O	369.733	1.390		
C-H	327.717	1.090		
Cl-O	350.000	1.440		
Angles	K_{ijk} (kcal mol^{-1} rad^{-2})	Θ_0 (deg)		
C-C-H	42.924	98.400		
H-C-H	38.551	93.400		
O-C-C	59.535	96.500		
O-C-H	56.034	100.800		
C-O-C	74.544	107.100		
O-Cl-O	100.000	109.500		
Dihedrals	K_1 (kcal mol^{-1})	K_2 (kcal mol^{-1})	K_3 (kcal mol^{-1})	K_4 (kcal mol^{-1})
O-C-C-H	0.278	0.000	0.000	-0.278
H-C-C-H	0.278	0.000	0.000	-0.278
C-O-C-H	0.808	0.000	0.000	-0.808
O-C-C-O	2.602	0.050	-2.552	0.000
C-O-C-C	2.021	-1.001	-0.701	-0.320
Non-bonded	A_{ij} (kcal mol^{-1}) or A'_{ij}(kcal mol^{-1} Å^{12})	B_{ij} (Å^{-1})	C_{ij} (kcal mol^{-1} Å^6)	
H-H	2651.299	0.267	27.389	
H-C	4322.793	0.293	138.332	
H-O_{PEO}	14185.128	0.256	104.539	
H-Li	5002.437	0.192	0.000	
H-Cl	5284.667	0.297	207.110	

Table B1 (continued)

H-O_{LiClO4}	5284.928	0.276	86.977
H-Ti	88630.000[a]	N/A	32.000
H-O_{TiO2}	14175.980	0.256	103.950
C-C	14985.539	0.324	641.213
C-O_{PEO}	33724.143	0.280	505.891
C-Li	22380.760	0.211	0.000
C-Cl	29407.119	0.327	1002.098
C- O_{LiClO4}	29415.215	0.304	420.836
C-Ti	125000.000[a]	N/A	496.000
C- O_{TiO2}	33702.400	0.280	503.040
O_{PEO}-O_{PEO}	75893.733	0.246	399.130
O_{PEO}-Li	55853.769	0.184	0.000
O_{PEO}-Cl	138350.274	0.285	790.617
O_{PEO}- O_{LiClO4}	138529.656	0.265	332.024
O_{PEO}-Ti	97622.000[a]	N/A	32.000
O_{PEO}- O_{TiO2}	75844.800	0.246	396.890
Li-Li	44186.257	0.137	0.000
Li-Cl	83642.765	0.213	0.000
Li- O_{LiClO4}	83708.296	0.198	0.000
Li-Ti	83247.274	0.145	0.000
Li- O_{TiO2}	76010.943	0.179	0.000
Cl-Cl	781407.189	0.330	1566.093
Cl- O_{LiClO4}	787164.229	0.307	657.689
Cl-Ti	748199.920	0.225	435.313
Cl- O_{TiO2}	403203.654	0.278	1044.706
O_{LiClO4}-O_{LiClO4}	793006.730	0.285	276.200
O_{LiClO4}-Ti	753476.394	0.210	182.812

Table B1 (continued)

O_{LiClO4}-O_{TiO2}	404731.035	0.258	438.730
Ti-Ti	717700.000	0.154	121.000
Ti- O_{TiO2}	394176.450	0.190	290.387
O_{TiO2}-O_{TiO2}	271700.000	0.234	696.900

[a] The value is for the parameter A'_{ij}